Metabolic engineering of yeast (*Saccharomyces cerevisiae*) with a view to optimising butanol production

A thesis submitted to The University of Manchester for the degree of Doctor of Philosophy in the Faculty of Biology Medicine and Health

2018

Olugbenga O Ogunlabi

School of Biological Sciences

Table of Contents

Word count: 31,342

List of figures

List of tables

List of abbreviations

α	Alpha
Δ	Delta (delete)
µ	Micro (prefix)
A	Adenosine
A	Absorbance
AA	Amino acids
ABE	Acetone-Butanol-Ethanol
Adhe2	butanol dehydrogenase
ATP	Adenosine triphosphate
bp	Base pair
ButR	butanol Resistant Strains
ButS	butanol Sensitive Strains
C	Carbon
Ccr	butyryl-CoA dehydrogenase
Crt	Crotonase
Da	Dalton
DEPC	Diethylpyrocarbonate
DNA	Deoxyribonucleic acid
dNTP	Deoxyribonucleotide
DTT	Dithiothreitol
EDTA	Ethylenediaminetetraacetic acid
Erg10	Thiolase enzyme
GCD1	subunit of eIF2B
GRAS	Generally regarded as safe
GTP	Guanosine triphosphate
Hbd	3-hydroxybutyryl-CoA dehydrogenase
K	Kilo (prefix)
L	Litre(s)
LB	Luria-Bertani media
m	Milli (prefix)
M	Molar
NAD	nicotinamide adenine dinucleotide
NAD(H)	nicotinamide adenine dinucleotide (reduced)
NADP	Nicotinamide adenine dinucleotide phosphate
NADP(H)	Nicotinamide adenine dinucleotide phosphate (reduced)
OD	Optical density
ORF	Open reading frame
PCR	Polymerase chain reaction
PDH	Pyruvate dehydrogenase
PEG	Polyethylene glycol
PH	a measure of acidity or alkalinity
RNA	Ribonucleic acid
rpm	Revolutions per minute
SC	Synthetic complete media (lacking glucose)
SCD	Synthetic complete dextrose

SDS	Sodium dodecyl sulphate
SDS-PAGE	Sodium Dodecyl sulphate Polyacrylamide Gel Electrophoresis
TAE	Tris acetic acid, EDTA
TAG	Triacylglycerol
TG	Triglyceride
TCA	Tricarboxylic acid
v/v	Volume per volume
w/v	Weight per volume
YP Y	east extract, peptone
YPD	Yeast extract, peptone, dextrose

Abstract

Doctor of Philosophy in the Faculty of Biology, Medicine and Health. 2018

Metabolic engineering of yeast (*S. cerevisiae*) with a view to optimising butanol production

Olugbenga O. Ogunlabi

The University of Manchester, Faculty of Biology, Medicine and Health, M13 9PT United Kingdom.

Global energetic and environmental concerns have generated interest in the biological systems for the production liquid biofuels. Butanol is one such biofuel, which can be naturally produced by some *Clostridia* species. However, possible limitations in Clostridial engineering and large-scale fermentation have led to an examination of other potential organisms that might house this pathway for butanol production. As a robust industrial host and key model organism in the study of fundamental biological processes, the yeast *Saccharomyces cerevisiae* has been used to house the Clostridial ABE-butanol pathway. However, butanol yields and titres in this yeast are relatively low. Therefore, in this thesis, three distinct strategies were carried out with the goal of optimising butanol production in the strain of yeast (previously constructed in the Ashe lab) bearing the ABE-butanol pathway:

1. Mutation of genes involved in the regulation of carbon source usage.

2. Deletion of genes where the product is involved in the consumption of cytosolic acetyl-CoA (the starting precursor for the butanol synthetic pathway).

3. Targeted mutagenesis to improve the efficiency of the thiolase enzyme, which catalyses the condensation of 2x acetyl-CoA to initiate the ABE-butanol synthesis pathway.

The results showed the first two strategies did not lead to improvements in butanol yields. However, increases of intracellular acetyl-CoA were observed in some mutant strains, even though butanol production did not increase in these strains. In order to make maximum use of the accumulating cytosolic acetyl-CoA, thiolase engineering in the butanol production yeast strain was pursued. The introduced changes caused an increase in butanol (about two fold).

Overall, this project has used a minimal engineering approach by modulation of associated pathways or optimisation of the heterologous enzyme with a view to improve butanol production in yeast. To achieve high and scalable butanol production in yeast, a robust approach involving whole synthetic biology – Design, Build Test, and Learn will need to be adopted to create a more efficient yeast-butanol system.

Declaration

No portion of the work referred to in this thesis has been submitted in support of an application for another degree or qualification of this or any other university or other institute of learning.

Copyright statement

I. The author of this thesis (including any appendices and/ or schedules to this thesis) owns certain copyright or related rights in it (the "Copyright") and s/he has given The University of Manchester certain rights to use Copyright, including for administrative purposes.

II. Copies of this thesis, either in full or in extracts and whether in hard or electronic copy, may be made only in accordance with the Copyright, Designs and Patents Act 1988 (as amended) and regulations issued under it or, where appropriate, in accordance with licensing agreements which the University has from time to time. This page must form part of any such copies made.

III. The ownership of certain Copyright, patents, designs, trademarks and other intellectual property (the "Intellectual Property") and any reproductions of copyright works in the thesis, for example graphs and tables ("Reproductions"), which may be described in this thesis, may not be owned by the author and may be owned by third parties. Such Intellectual Property and Reproductions cannot and must not be made available for use without the prior written permission of the owner(s) of the relevant Intellectual Property and/ or Reproductions.

IV. Further information on the conditions under which disclosure, publication and commercialisation of this thesis, the Copyright and any Intellectual Property and/or Reproductions described in it may take place is available in the University IP Policy (see http://documents.manchester.ac.uk/DocuInfo.aspx?DocID=24420), in any relevant Thesis restriction declarations deposited in the University Library, The University Library's regulations (see http://www.library.manchester.ac.uk/about/regulations/) and in The University's policy on Presentation of Theses

Dedication

I dedicate this work to my wife (Adenike) and to my mother (Beatrice) for their immeasurable support throughout this PhD odyssey. Leaving one's home and family to study abroad comes with a lot of sacrifice but you guys paid the most.

Acknowledgements

Special thanks to my supervisors, Professors Chris Grant and Mark Ashe for their tutorship and immense support throughout my PhD programme. Similarly, I want to thank Professors Simon Turner (my advisor) and Graham Pavit (who I like to call my unofficial supervisor) for their advice and support.

Importantly, I thank Drs Lydia Castelli (my PhD mum), Chris Keshaw, Hui Wang and Reem Swidah for putting me through things in the lab, particularly in my first year. My heartfelt thanks goes to the entire present and past members of the Ashe-Grant-Pavit lab group for all the love and support we shared during my PhD programme; I wish you all Godspeed. Special thanks also to my two jolly great friends whom I met during this PhD programme; Shawn (loyal one) and Henry (special one) for all the fun and laughter we had together during the past four years; you guys made the times go quickly.

To my darling wife (Adenike-teminikansoso), my sons (Timi and Temi), my entire family members, my friends and all my well-wishers; I thank you for all your prayers and goodwill throughout the period of this PhD programme. I could not have done it without your support and this reflects perfectly in a Yoruba adage - 'relationship is our garment for comfort and happiness'.

Most importantly, my praise is to the Lord, the Almighty, the King of creation; whose help and comfort sustained me all the way.

1. General Introduction

1.1 The Biofuel alternative to fossil fuel

Concerns about global warming (caused by excessive burning of fossil fuels) and international energy security (due to the world's diminishing crude oil reserves, the unpredictable price of crude oil and stiffening global legislations on oil production) have necessitated an international urgent search for cleaner, cheaper and universally available alternatives to petrol and other fossil fuels. In this regard, a plethora of research activities over the past few decades have centered on the exploitation of microbes for the production of biofuels from biomass resources to provide carbon neutral alternatives to fossil fuels (Buijs *et al*, 2013; Dürre, 2007; Fortman *et al*, 2008; Luque *et al*, 2008). Biomass represents a diverse source of organic materials ranging from food crops, plant lignocellulose materials, microalgae, sea weed and animal waste materials; it represents a vast source of high energy that could potentially drive and sustain global biofuel production (Kumar *et al*, 2008).

The term "biofuel" refers to fuels produced from organic materials; it includes biogas, biodiesel, ethanol, butanol and isobutanol (Nigam & Singh, 2011). Biofuels are carbon neutral fuels that do not lead to a net increase in the amount of greenhouse gases (carbon dioxide, carbon monoxide, nitrogen, sulphur-oxide and particulates) in the atmosphere; which is a major cause of global warming (Luque *et al*, 2008). Their combustion releases current carbon from plants and other autotrophs, back to the atmosphere without altering the carbon balance in any significant way. Burning fossil fuels on the other hand leads to a considerable increase in the atmospheric concentration of these green-house gases and a negative shift in geological carbon

balance since it unlocks and releases carbon which has been sequestered away, back into current geological contention thereby resulting in an undesirable increase in carbon dioxide and other greenhouse gases which ultimately result in global warming, acid rain and other forms of air pollution (Nigam & Singh, 2011). To combat the long-term risks associated with fossil fuel combustion, the use of alternative and renewable energy sources has been proposed with particular focus on the bio-conversion of the world's biomass resources for biofuel production (Fortman *et al*, 2008; Kumar *et al*, 2008).

Due to the increasing world population and the demand to satisfy the world's food needs, the sustainability of current biofuel production strategies using crop based materials represents a balance between the needs for food and fuel (Saxena *et al*, 2009). These competing demands make crop-based biofuel expensive and unsustainable; therefore, much focus is currently on the use of non-crop materials such as plant lignocellulose materials, microalgae and seaweed as feed stocks in biofuel production. This class of biomass does not compete with the world's food supply or arable land use; hence it is inexpensive and sustainable (Kumar *et al*, 2008; Luque *et al*, 2008). However, a major current challenge is to unlock the monomeric sugars present in the biomass for subsequent microbial fermentation to yield the desired products (Luque *et al*, 2008)

Microbes have become important tools within the biotechnology industry, allowing manipulation for enhanced production of a large array of desired metabolic end products (Fischer *et al*, 2008a; Hong & Nielsen, 2012; Kumar *et al*, 2008; Zheng *et al*, 2009). In recent years, there have been significant advances in microbial

biotechnology; advances in gene regulation and manipulation techniques, metabolic engineering and greater knowledge of microbial genomics have all enhanced the potential for microbial biofuels. Hence, much research is now centered on the optimization of microbial cell factories for biofuel production (Buijs *et al*, 2013; Fortman *et al*, 2008; Luque *et al*, 2008; Nigam & Singh, 2011).

1.2 Biomass

Biomass resources are organic based materials that are direct or indirect products of photosynthesis (Fig 1.1). Biomass is a neutral carbon (carbon that does not disturb the current geo-ecological balance) resource; produced by the carbon fixation activity of autotrophs for the synthesis of sugars and various other biomolecules needed for their growth and development. Autotrophs subsequently serve as food for heterotrophs (animals); therefore, biomass generally refers to all plants and animal materials (Fig 1.1) (Kumar *et al*, 2008; Nigam & Singh, 2011; Saxena *et al*, 2009). However, in biotechnology the term, biomass particularly refers to materials of plant and/or animal origin that serve as a source of raw material for the production of useful end-products (Kumar *et al*, 2008). Biomass used in the production of biofuels ranges from; oil-rich and sugar-rich crops, wood materials, agricultural plant wastes (lignocellulose biomass), municipal solid wastes and animal wastes. The estimated annual global production of these biomass sources is reported at a staggering 1.5 trillion tons (Kumar *et al*, 2008); having the potentials to supply the world's energy requirement. Figure 1.1 shows a summary of biomass-biofuel production.

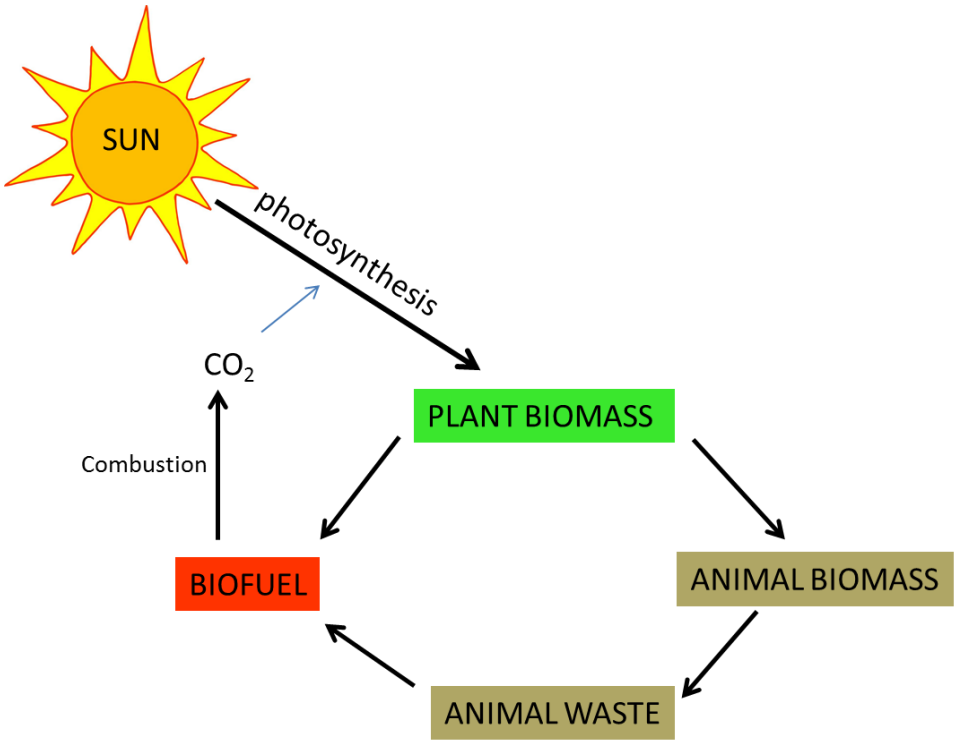

Figure1.1 General summary of biomass-biofuel production cycle

Figure shows the biomass-biofuel cycle. Plants are the primary biomass producers using energy from the sun. Carbon-dioxide produced during biofuel combustion is recycled by plants via photosynthesis and incorporated back to form biomass.

1.3 Biomass conversion

A number of methods can be used to convert biomass into useful forms of energy. Traditionally, biomass is used to produce heat by direct combustion of wood for cooking and heating. Wood materials were also used directly in combustion engines to produce electricity and for locomotive engines. However, in recent times, modern conversion methods are used to produce fuel materials (biofuel) and many useful commodity chemicals from biomass (Fortman *et al*, 2008; Luque *et al*, 2008; Saxena *et al*, 2009).

1.3.1 Chemical conversion process

This conversion process is popular for the chemical catalytic and/or non-catalytic conversion of oil-rich materials to produce bio-biodiesel (Luque *et al*, 2008). An example is the trans-esterification of triglycerides (TG) from vegetable oil using short chain alcohols (methanol and ethanol) in the presence of alkaline (NaOH and KOH) or mineral acids (sulfuric, phosphoric and hydrochloric acids) as catalysts to yield fatty acid methyl/ethyl esters (FAM/EE) (biodiesel) and glycerol as a byproduct (Fig 1.2) (Luque *et al*, 2008).

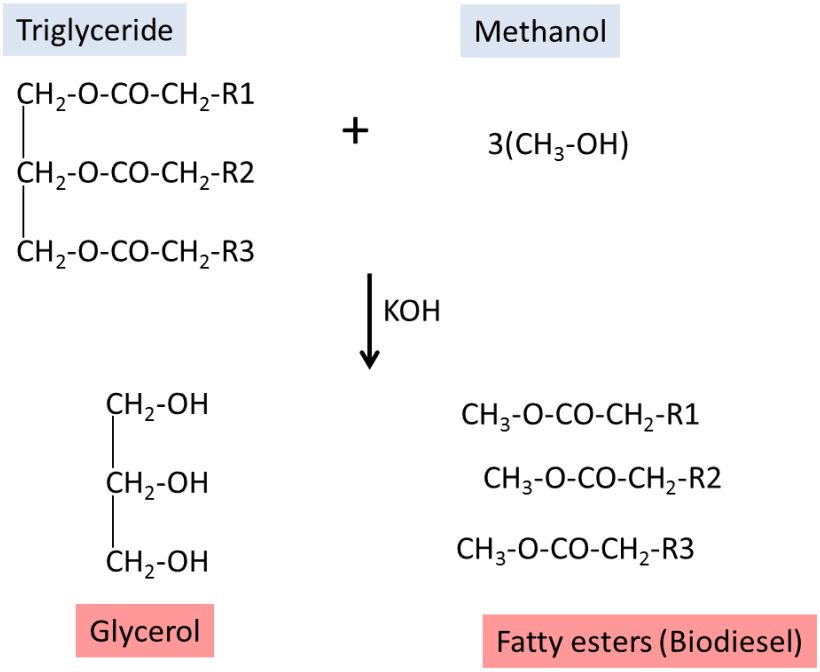

Figure 1.2 Trans-esterification reactions of fatty acids (triglycerides).

Triglyceride reacts with methanol in the presence of potassium hydroxide (KOH) to produce biodiesel (fatty esters) and glycerol by-product (Boucher *et al*, 2008; Luque *et al*, 2008).

1.3.2 Biological conversion process

Biological conversions use microbes as bio-refineries to produce biofuels from starch/sugar-rich biomass materials. This process varies and depends on the type of biofuel to be produced as well as the feedstock involved (Luque *et al*, 2008; Saxena *et al*, 2009). Examples include: enzymatic transesterification of triacylglycerols to produce fatty acid methl/ethyl esters (biodiesel), enzymatic hydrolysis and microbial fermentation of sugars to produce alcohol fuels (Fig 1.3), and bio-hydrogen production via fermentation and biophotolysis (Luque *et al*, 2008; Nigam & Singh, 2011; Saxena *et al*, 2009).

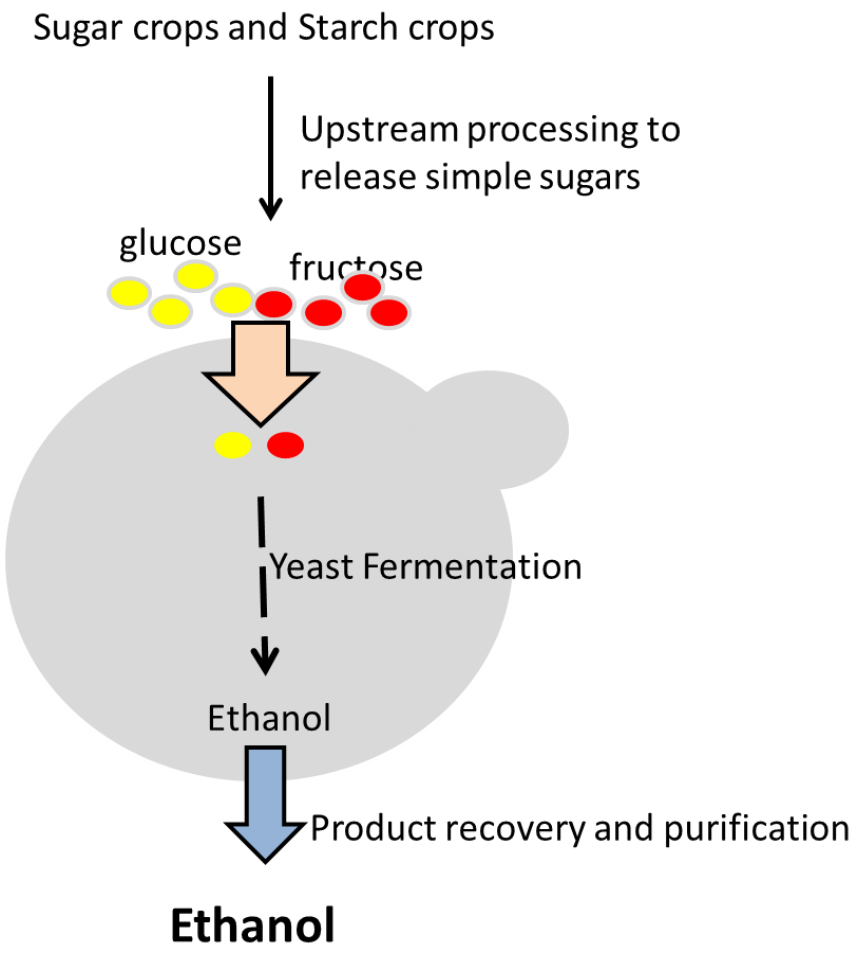

Figure 1.3 Yeast ethanol productions from sugar/starch rich crops

Sugar and starch rich crops are first hydrolysed to release their glucose and fructose which are metabolized by yeast to produce ethanol which is recovered to pure form from fermentation broth.

1.4 Biofuel development and classification

In order for biofuels to replace fossil fuels, certain key factors are essential; these include economics, sustainability, availability and environmental credibility (Fortman *et al*, 2008; Luque *et al*, 2008; Saxena *et al*, 2009). Currently, biofuel production from crop-based materials do not satisfy these essential requirements; this is because current biofuel production competes for food and for arable land; making it environmentally unfriendly since it disturbs the eco-balance and biodiversity (Nigam & Singh, 2011). Equally when lands are used for biofuel rather than food production, the use of agrochemicals such as herbicides, pesticides and fertilizers is less restricted and this might lead to environmental pollution. Hence there has been sustained interest in developing and improving biofuel production technologies using more sustainable resources and more efficient microbial bio-factories.

Biofuels can be classified in several ways based on;

1. Form/state: gas, liquid and solid

2. Source: forest, agricultural and municipal wastes

3. Complexity: primary/unprocessed and secondary/processed

4. Raw materials/technology: 1st, 2nd and 3rd generations. This classification is the current classification standard that shows advancements in biofuel technologies (Nigam & Singh, 2011).

1.4.1 1st generation biofuels

The first generation biofuels are produced from energy-rich food crops (oil-rich and sugar-rich) as feed stocks. As a result, these first generation biofuels suffer the problems of; high production cost, lack of sustainability and negative impact on the environment (Luque *et al*, 2008).

1.4.2 2nd generation biofuels

The biofuels obtained from the use of non-food dependent alternatives such as waste vegetable oils and fats, and lignocellulose biomass resources are referred to as second generation biofuels. Such biofuels are being developed to overcome the major challenges faced in the production of first generation biofuels (Luque *et al*, 2008). Plant lignocellulose biomass presents a rich source of various types of monosaccharides including glucose, galactose, xylose, arabinose, rhamnose and sugar acids; therefore, to optimize biofuel production from lignocellulose, the many types of monosaccharides present must be efficiently utilized by the microbial cell factory.

By using these renewable feedstocks, the second generation biofuel production strategies may be able to deliver sustainable, cost-effective and environmental-friendly biofuels (Kumar *et al*, 2008; Luque *et al*, 2008; Nigam & Singh, 2011; Saxena *et al*, 2009).

1.4.3 3rd generation biofuel

The use of oil rich microalgae represents a non-food alternative for the production of biofuels. Algae are known to reproduce rapidly and are excellent biomass producers, they can grow on waste water and do not compete with agricultural production systems; making their cultivation potentially eco-friendly. Algae store energy primarily in the form of oils and carbohydrates which can serve as source of animal feed and/or biofuel feedstock ("Algae for biofuel," 2014). The disadvantage of algal biofuel systems is the large amount of water and carbon-dioxide needed for their cultivation, the power required to light up and pump water through the various phases of a production system and the relative complexity of algal biology (Kenny & Flynn, 2017; Pittman *et al*, 2011).

1.5 Liquid biofuel

Growing world population has resulted in higher demand for transportation and transport fuels such as petrol and diesel (Luque *et al*, 2008) and this increasing demands comes with high environmental hazard. Biofuels such as biodiesel, ethanol and butanol represent potential replacements for petrol and diesel which are major contributors to greenhouse gases' release and global warming (Nigam & Singh, 2011).

1.5.1 Fatty acid alkyl esters (biodiesel)

Biodiesel is a non-toxic, sulfur-free biodegradable biofuel produced from plant oils and it can be blended with petroleum diesel or used pure in unmodified diesel

engines. Compared to petroleum-diesel, biodiesel has: higher lubricity, higher flash point, lower aromatic content and lower combustion emissions (Luque *et al*, 2008). Despite its sterling qualities, biodiesel still suffers from some drawbacks including; lower power (about 11% lower than petro-diesel) (Lee *et al*, 2008a), lower torque which results in low mileage and It becoming corrosive in engines when oxidized (Luque *et al*, 2008) et al.,2008). Biodiesel cannot be borne through existing pipelines and infrastructure used for petro-diesel because it has higher cloud (crystal formation) and pour (flow) points (Lee *et al*, 2008a).

1.5.2 Ethanol

Currently, ethanol dominates the biofuel market and it is the current biofuel standard (Luque *et al*, 2008). The reason for this is the ease with which it is produced to high concentrations in fermentations of *Saccharomyces cerevisiae* and the subsidies placed on bioethanol by specific governments such as Brazil and the United States. However, some of its inherent physical properties make it non-optimal as a replacement to petrol; ethanol is highly hygroscopic, has low energy density, cannot be used directly in current engines, cannot be transported using existing infrastructure, its distillation is costly and its current production competes with food (Fortman *et al*, 2008; Si *et al*, 2014a).

1.5.3 Drawbacks of the current production of ethanol and biodiesel

Current production of ethanol and biodiesel depends on limited agricultural resources; giving rise to the ‘food vs fuel’ controversy. They both have lower fuel

properties than their petroleum counterpart and both require a total overhaul of existing transportation and storage facilities.

1.5.4 Butanol

Butanols including n-butanol, 2-butanol and isobutanol are promising fuel substitutes and additives (García *et al*, 2011). 1-butanol (n-Butyl alcohol, butyl hydroxide, n-butanol) ($CH_3CH_2CH_2CH_2OH$) (MW 74.12) is a clear, colorless flammable liquid with a characteristic distinctive odour (Lee *et al*, 2008b), it is less hygroscopic than ethanol, and completely miscible with organic solvents such as glycols, other alcohols, aldehydes, ethers, and hydrocarbons (Lee *et al*, 2008b). As well as its potential value as a biofuel, butanol has a wide range of uses in the chemical and solvent industries (García *et al*, 2011; Jin *et al*, 2011; Lee *et al*, 2008b) and several bioengineering attempts have been made to produce butanol in organisms such as *E. coli* and yeast (Branduardi *et al*, 2013b; Generoso *et al*, 2015; Lee *et al*, 2012).

Interest in 1-butanol as a potential biofuel has increased due to its superior fuel characteristics compared to ethanol (Table 1.1). Butanol has an energy density (29.2 MJ/L) which is comparable to that of gasoline (32.5 MJ/L), and much higher than ethanol's 21.2 MJ/L. it safer to handle having: melting point –89.5°C, boiling point 117.2°C, flash point 36^{o}C, self-ignition temperature 340^{o}C and a relatively low heat of vaporization 0.43 MJ/kg compared to 0.92 MJ/kg for ethanol (Fortman *et al*, 2008). Furthermore, unlike ethanol which cannot be used pure in conventional motor engines, butanol can be used in its pure form or mixed with petrol at any ratio (Dürre, 2007; Fortman *et al*, 2008; Si *et al*, 2014a). Additionally, butanol is less hygroscopic

making it less corrosive than ethanol; this implies that butanol can be borne through existing steel infrastructure (pipelines and tankers) and is non-corrosive to engines (Dürre, 2007; Fortman *et al*, 2008).

Table 1.1 Fuel properties of petrol and three common alcohols (Lee *et al*, 2008b)

	Petrol	Butanol	Ethanol	Methanol
Energy density (MJ/L)	32	29.2	19.6	16
Air-fuel ratio	14.6	11.2	9	6.5
Heat of vaporization (MJ/kg)	0.36	0.43	0.92	1.2
Research octane number	91 – 99	96	129	136
Motor octane number	81 – 89	78	102	104

1.6 Butanol production

1.6.1 Chemical production of butanol

Butanol can be produced chemically from petroleum derived materials such as ethylene, propylene, carbon monoxide and hydrogen. Hydroformylation (oxo) process involves reacting propylene, carbon monoxide and hydrogen in the presence of an appropriate catalyst such as cobalt to form a product mixture of *n*-butyraldehyde and isobutyraldehyde which are subsequently hydrogenated to *n*-butanol and isobutanol, respectively (Fig1.4) (García *et al*, 2011).

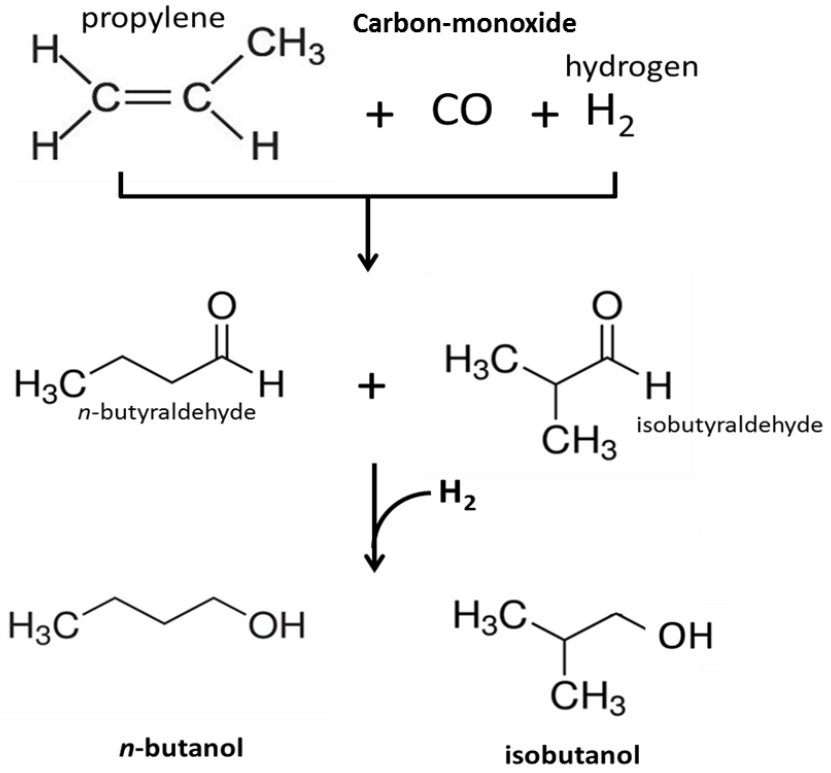

Figure 1.4 Chemical synthesis of butanol via the oxo process

Propylene reacts with carbon-monoxide and hydrogen gas to form aldehydes intermediates which are further hydrogenated to corresponding butanol isomers.

1.6.2 ABE fermentation

Louis Pasteur first reported microbial butanol production in 1861. After this, attempts were made to produce butanol for industry and were made popular by Chaim Weizmann where butanol was produced using *Clostridium acetobutylicum* via the Acetone-Butanol-Ethanol (ABE) fermentation route (Fig 1.5) (García *et al*, 2011; Lee *et al*, 2008b; Luque *et al*, 2008). The ABE fermentation of *Clostridia* occurs via the acidogenic-solventogenic pathway, which involves the production of mixed acids (acetate and butyrate during the exponential growth stage of the organism) and the eventual re-assimilation of these acids and flux of metabolic resources toward the production of acetone, butanol and ethanol when cell growth slows down (Lee *et al*., 2008). This early industrial fermentation process was important in solvent (Acetone/butanol/ethanol) production in the early 20th century and a number of improvements were made to the process to make it economically viable. By the 1950s and 1960s, the advent of cheaper petrochemical-based processes made the fermentative production of butanol economically unsustainable bringing it to gradual halt (García *et al*, 2011; Gheshlaghi *et al*, 2009). Interest in the *Clostridial* ABE fermentation pathway was rekindled in the 1970s and 1980s due to the escalating price of petroleum (Gheshlaghi *et al*, 2009; Lee *et al*, 2008b),however, the process has a number of drawbacks including; the high cost of starting raw materials, high cost of product recovery, low butanol titer and butanol intolerance (Luque *et al*, 2008). Equally the potential for bacteriophage contamination and the complex two-phase fermentation process can prove problematic.

The current appeal of sustainable biofuel production has renewed interest in butanol production via a fermentation route (Dürre, 2007) but the commercial viability of such processes demands improvements and optimization of the microbial organisms and strains used to meet reasonable metrics in terms of product titre, rate and yield (TRY) (Atsumi *et al*, 2008; Dürre, 2007; Fischer *et al*, 2008a; Lee *et al*, 2008a; Nielsen *et al*, 2013).

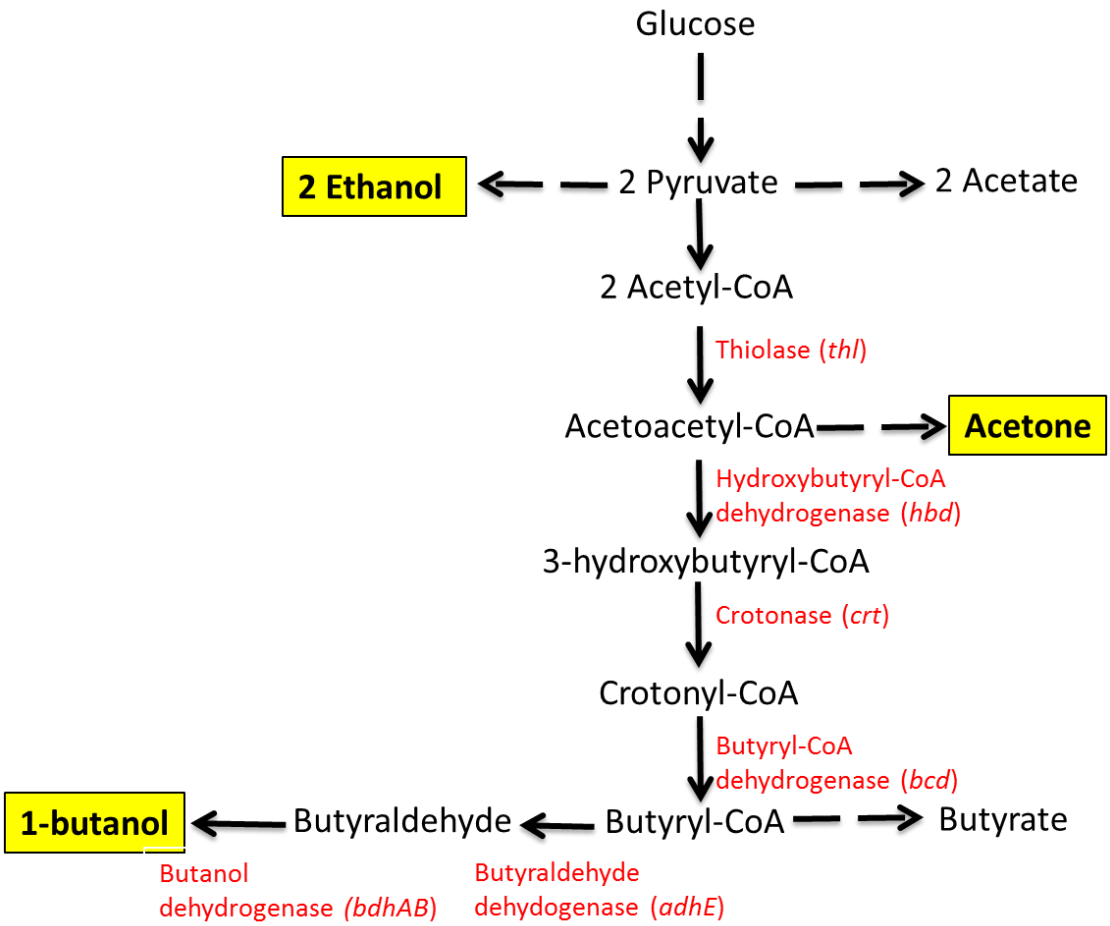

Figure 1.5 Summary of Clostridia ABE-butanol metabolic pathway.

Major enzymes leading to butanol synthesis are written in red letters with the corresponding gene in parenthesis. Acetone, butanol and ethanol are written in yellow boxes (García *et al*, 2011; Lee *et al*, 2008b).

1.7 Butanol bio-factories

Microbes have become key tools within the biotechnology industry and advancements in their genomics have enhanced their metabolic engineering for the production of various commodity chemicals; making microbial engineering the center of recent focus of efforts to optimize biofuel production (Hong & Nielsen, 2012; Kumar *et al*, 2008; Lee *et al*, 2008b; Saxena *et al*, 2009). Microbes such as; *E. coli, Saccharomyces sp.* and *Clostridia sp*. are the primary organisms used for butanol production and several recombinant strains of these organisms are being developed to allow optimal production.

1.7.1 Clostridia *sp*.

Bacterial *Clostridia* species have long been employed in several biotechnological processes including the production of cancer therapeutics, entertoxins, neurotoxins and in the conversion of renewable biomass for ABE production (Gheshlaghi *et al*, 2009). In addition to *C. acetobutylicum*, *C. aurantibutylicum, C. beijerinckii, and C. tetanomorphum,* other species of *Clostridia* are known to produce butanol as a major fermentation product but, *Clostridia acetobutylicum* is the popular industrial host for butanol production (Lee *et al*., 2008). The ABE-butanol production route suffers from several drawbacks, which make the improvement of the fermentation process difficult (Steen *et al*, 2008). The relative lack of genetic tools to manipulate *Clostridia* metabolism, slow growth, unavoidable byproducts (butyrate and acetone), intolerance to butanol (above 1-2%) are all drawbacks hindering further refinement of the ABE process (Lee *et al*, 2008b; Si *et al*,

2014a; Steen *et al*, 2008). Therefore, the production of butanol in industrially 'friendly' organisms, such as *E. coli* and *S. cerevisiae*, has become a focus of recent research efforts (Atsumi *et al*, 2008; Si *et al*, 2014a).

1.7.2 *E. coli*

Because of the difficulties in improving the Clostridial butanol platform, efforts been made to transfer the ABE-butanol synthetic pathway to non-native butanol producer organisms such as *E. coli* and *S. cerevisiae* (Atsumi, 2007; Atsumi *et al*, 2008; Fischer *et al*, 2008a; García *et al*, 2011; Steen *et al*, 2008; Swidah *et al*, 2015).

E. coli, a gram-negative bacterium, has long being exploited as a model host for many biotechnological products. It is fast growing, has a simple physiology and nutritional need, has a well characterized biology and several genetic tools are available for its manipulations. These advantages make *E. coli* an adaptable, lab friendly organism (Lamsen & Atsumi, 2012; Zheng *et al*, 2009). Though *E coli* does not produce butanol naturally, several attempts including its ectopic expression of a synthetic ABE-butanol pathway have been made for its butanol production (Atsumi, 2007; Atsumi *et al*, 2008; Bond-Watts *et al*, 2011; Nielsen *et al*, 2009; Shen *et al*, 2011).

Atsumi *et al*, (2008) expressed a heterogenous butanol pathway in *E.coli* using a two-plasmid based system resulting in a strain that produced 13.9mg/L butanol in 40 hrs under anaerobic conditions. Maximum butanol titre of 552 mg/L was obtained by their recombinant *E.coli* strain after further improvements such as; the deregulation of pyruvate dehydrogenase complex under anaerobic conditions by deletion of the gene

responsible its deactivation, the deletion of genes responsible for production of *E. coli* metabolic by-products (such as acetate, lactate, ethanol , and succinate) and using Terrific Broth (TB)-enriched/glycerol-supplemented media (Atsumi, 2007; Atsumi *et al*, 2008; Lamsen & Atsumi, 2012).

In another study, Nielsen et al., (2009) improved butanol titer in *E. coli* to 580 mg/l by co-expressing *S. cerevisiae* formate dehydrogenase (for the supply of NADH + H^+) along with the ABE-butanol pathway genes and overexpressing *E. coli* glyceraldehyde 3-phosphate dehydrogenase (to increase glycolysis flux) (Nielsen *et al*, 2009).

Similarly, Bond-Watts *et al*. (2011) achieved about 49-fold improvement in butanol production to 4.65 g/L by their recombinant *E. coli* strain (expressing a butanol synthetic pathway with genes; *phaA, phaB, crt, ccr* and *adhE2* (encoding; β-ketothiolase, acetoacetyl-CoA reductase, crotonase crotonylCoA reductase and butyraldehyde dehydrogenase respectively)) after a number of optimization strategies such as gene replacement, redox co-factor equilibrium and metabolic intermediate engineering strategies. First, *ccr* was replaced with *ter* (encoding an NADH-dependent crotonyl-CoA reductase from *Treponema denticola*), Also, *phaB* was replaced with *hbd* (encoding NADH-dependent (S)-3-hydroxybutyryl-CoA dehydrogenase from *C. acetobutylicum*), *crt* was replaced with *phaJ* (encoding an R-specific enoyl-CoA hydratase from *Aeromonas caviae*) and finally, *aceEF-lpd*, (encoding the pyruvate dehydrogenase complex) was overexpressed (Bond-Watts *et al*, 2011).

Shen *et al*. (2011) employed a number of driving force generating strategies for butanol production in a recombinant *E. coli* strain (JC166) and they reported a final

butanol titre of 30 g/L by their *E. coli* strain after optimization. The butanol synthetic pathway genes; *atoB* (*E. coli*), *adhE2*, *crt, hbd* (*C. acetobutylicum*), and *ter* (*T.denticol)* were all overexpressed in the parent strain using a two-plasmid system, they also expressed *fdh* (encoding a formate dehydrogenase from *Candida boidinii*) to reduce excess pyruvate and provide NADH equivalents needed for butanol production. The gene; *pta* (encoding a phosphate acetyltransferase) was deleted to decrease acetate formation and increase acetylCoA abundance (Shen *et al*, 2011).

Apart from *E.coli,* other bacteria including *Pseudomonas putida* and *Bacillus subtilis* have been engineered as host organism for butanol synthesis with yields of 122 mg/L and 24 mg/L butanol respectively (Nielsen *et al*, 2009).

1.7.3 Yeast (*S. cerevisiae*)

S. cerevisiae is a robust and prominent industrial host for ethanol production and the non-native production of several commodity chemicals (Gonzalez-Ramos *et al*, 2013; Hong & Nielsen, 2012; Krivoruchko *et al*, 2013; Si *et al*, 2014a); though *S. cerevisiae* is a facultative ethanol fermenter, it also produces some amount of higher alcohols including isobutanol, n-butanol and amylalcohol. *S. cerevisiae* has higher butanol tolerance than other microorganisms (above 20 g/L) and attempts at improving its butanol tolerance are being made; these advantages present *S*. *cerevisiae* as an excellent and ideal drop-in cell-factory to replace the *Clostridia* butanol biofactory. (Branduardi *et al*, 2013b; Fischer *et al*, 2008a; Gonzalez-Ramos *et al*, 2013; Hong & Nielsen, 2012; Si *et al*, 2014a; Zheng *et al*, 2009). Though many strains of *S*. *cerevisiae* are being developed for high/improved butanol production, its current

butanol production level still falls well below those of *Clostridia* and *E. coli* (Gonzalez-Ramos *et al*, 2013; Krivoruchko *et al*, 2013; Lamsen & Atsumi, 2012; Steen *et al*, 2008), but the exploitation of *S. cerevisiae* as a butanol producer has many advantages; *S. cerevisiae* is not pathogenic, it is tolerant toward many inhibitors and acidic conditions, it does not have strict nutritional and fermentation requirements, it is not affected by bacteriophage contamination as with bacteria and production set-ups will require little modification, since it is the current industrial bioethanol producer (Fischer *et al*, 2008b; Hong & Nielsen, 2012; Jin *et al*, 2011; Krivoruchko *et al*, 2013; Si *et al*, 2014a). *S. cerevisiae* is also generally regarded as safe (GRAS), therefore its industrial handling will require minimal safety precautions and poses little personnel and environmental hazard. Moreover, *S. cerevisiae's* biology is very well characterised; it is genetically tractable and amenable for a variety of genetic manipulation strategies that can be exploited to enhance its butanol production potential. Furthermore, its fermentation and downstream product recovery processing is relatively cheap and well-developed (Fischer *et al*, 2008a; Fortman *et al*, 2008).

1.7.3.1 Butanol production strategies used in yeast

Steen *et al*. (2008) first reported a plasmid based heterologous expression of the ABE-butanol pathway in yeast; they replaced some of the clostridial enzymes with isozymes from different species in order to determine the best enzyme combination. They reported 2.5 mg/L butanol produced in minimal media by yeast which over-expresses a native yeast thiolase (*ERG10*) and clostridial *hbd (*NADH-dependent

hydroxybutyryl-CoA dehydrogenase), *crt* (crotonase), *adhE2* (dual function alcohol and aldehyde dehydrogenase) and *ccr* (crotonyl-CoA reductase) (Steen *et al*, 2008).

Using strategies aimed at increasing cytosolic acetyl-CoA abundance with the heterogenous ABE-butanol pathway, 16.3 mg/L butanol was produced from yeast (Krivoruchko *et al*, 2013). They overexpressed alcohol dehydrogenase (*ADH2*), aldehyde dehydrogenase (*ALD6*), and mutated acetyl-CoA synthetase (ACS^{L641P}) genes and deleted *CIT2* (encoding peroxisomal citrate synthase) to inhibit acetyl-CoA consumption by the glyoxylate cycle.

Sakuragi *et al.* (2015) focused on eliminating competing by-products forming reactions as strategies to improve butanol production from yeast. They deleted *GPD1* and *GPD2* genes (encoding glycerol-3-phosphate dehydrogenases) to reduce both glycerol production and NADH consumption in their recombinant yeast strain (expressing the butanol pathway). Their attempt resulted in ~14 mg/L butanol production (Sakuragi *et al*, 2015).

Lian *et al.* (2014) reported improvements in butanol production from their recombinant yeast strain (expressing butanol pathway) by the deletions of *ADH1* and *ADH4* (encoding alcohol dehydrogenases) and *GPD1* and *GPD2* (encoding glycerol-3-phosphate dehydrogenases) to reduce ethanol and glycerol formation respectively (Lian *et al*, 2014).

Schadeweg & Boles (2016) reported a stepwise increase in butanol production in *S. cerevisiae* (expressing the ABE-butanol pathway) by increasing acetyl-CoA, CoA and NADH supply and also decreasing ethanol and glycerol formation. They increased

acetyl-CoA and CoA synthesis by overexpressing an ATP independent acetylating acetaldehyde dehydrogenase *adhEA267T*/E568K and pantothenate kinase *coaA* genes respectively. They also deleted alcohol dehydrogenase *ADH1*-6 and glycerol-3-phosphate dehydrogenase *GPD2* genes to inhibit ethanol and glycerol synthesis and increase redox (NADH) supply. Their strain produced a butanol titer of ~130 mg/L in minimal media (Schadeweg & Boles, 2016a). Further improvement to their strain produced a butanol titer of 860 mg/L (Schadeweg & Boles, 2016b).

1.7.3.2 Novel pathways for butanol production in yeast

Branduardi *et al*. (2013) constructed a novel pathway for butanol synthesis in yeast, involving glycine oxidase conversion of glycine into glyoxylate, malate synthase condensation of glyoxylate with butyryl-CoA to form β-ethylmalate and β-isopropylmalate dehydrogenase conversion of β-ethylmalate into α-ketovalerate, which feeds into the Ehrlich pathway for conversion to butanol. The recombinant yeast expressing *goxB* (glycine oxidase from *Bacillus subtilis*) *MLS1* and *DAL7* (malate synthase from *S. cerevisiae*) and *LEU2* (isopropylmalate dehydrogenase from *S. cerevisiae*) genes produce butanol at 92 mg/L in a medium supplemented with glycine.

Si *et al.* (2014) designed a butanol pathway around the yeast endogenous threonine catabolic pathway by overexpressing genes involved in threonine catabolism and deleting genes competing for carbon flux utilisation. They overexpressed *ILV1*/*CHA1*, *LEU1*, *LEU2* and *LEU4* encoding threonine deaminase, isopropylmalate isomerase, β-isopropylmalate dehydrogenase and α-isopropylmalate

synthase respectively and they deleted *ILV2* (encoding acetolactate synthase) and *ADH1* (encoding alcohol dehydrogenase). Their strategy resulted in butanol production of 242.8 mg/L (Si *et al*, 2014a).

Lian & Zhao (2015) engineered a reversed β-oxidation pathway in yeast cytosol for the synthesis of acetyl-CoA together with a CoA-acylating aldehyde dehydrogenase from *E. coli* (EcEutE) and butanol dehydrogenase from *C. acetobutylicum* (CaBdhB) in yeast for the production of butanol (Lian & Zhao, 2015).

Shi et al (2016) produced 835 mg/L butanol from yeast. They engineered and optimised a synergistic pathway in yeast; consisting of yeast's endogenous threonine pathway and a heterologous citramalate synthase pathway (Shi *et al*, 2016).

Attempts at yeast butanol production was also done in Chris Grant's and Mark Ashe's labs (Swidah *et al*, 2015). They constructed recombinant yeast carrying the ABE-butanol pathway and an acetyl-CoA synthesis pathway together with *adh1Δ*. This strain produces ~300 mg/L butanol. Attempts to improve the strain's butanol production are the focus of this study.

Table 1.2 Summary of some attempts at Yeast butanol production (an attempt in *E.coli* and production in *C.acetabutylicum* written for reference).

Organism	Genetic Modifications	Butanol titre	Reference
C.acetabutylicum	expression of the *adhE1*	34.2 g/L of mix ABE	(Lee *et al*, 2015)
E. coli	Overexpression of *atoB, hbd*, *crt*, *ter*, *adhE2*, *fdh* + deletion of *adhE*, *ldhA*, *frdBC*, *pta*	30 g/L	(Shen *et al*, 2011)
S. cerevisiae	*adh1Δ*,*adh3Δ*, *adh5Δ*, *adh4*Δ, *adh2*Δ, *adh6*Δ, ald6Δ, gpd2Δ + *coaA*, *adhE* $^{A267T/E568K/R577S}$, ^{Ec}fms1, ^{Sc} *ERG10,* ^{Ca} *hbd,* ^{Ca} *crt,* ^{Td} *ter,* ^{Ca} *adhE2,* ^{Ec} *eutE*	860 mg/L	(Schadeweg & Boles, 2016a; Schadeweg & Boles, 2016b)
S. cerevisiae	Overexpression of endogenous threonine catabolic pathway and synergistic CimA pathway	835 mg/L	(Shi *et al*, 2016)
S. cerevisiae	^{Sc}*ALD6-ACS2-ERG10-*^{Ca}*Hbd-Crt-*Bcd-*adhE2* + deletion of *adh1Δ*	300 mg/L	(Swidah *et al*, 2015)

Organism	Genetic Modifications	Butanol titre	Reference
S. cerevisiae	Overexpression the endogenous threonine catabolic pathway + elimination of competing pathway	242.8 mg/L	(Si *et al*, 2014b)
S. cerevisiae	A glycine to butanol novel pathway involving *goxB, MLS1, DAL7, LEU2* and PDC activities	92 mg/L	(Branduardi *et al*, 2013a)
S. cerevisiae	^{Sc}*ERG10*-^{Ca}*hbd*-^{Cb}*crt*-^{Strep}*ccr*-^{Cb}*adhe2*	2.5 mg/L	(Steen *et al*, 2008)
S. cerevisiae	*ERG10*-^{Ca}*Hbd*-^{Cb}*Crt*-Bcd-*adhE2* + deletion of *gpd1&2Δ*	14 mg/L	(Sakuragi *et al*, 2015)
S. cerevisiae	^{Ca}*Thl-Hbd,* ^{Cb}*Crt,* ^{Td}*Ter,* ^{Ec}*EutE,* ^{Ca}*Bdh,* ^{Ec}PDH, ACS^{Opt}-L	>100 mg/L	(Lian *et al*, 2014)
S. cerevisiae	*ADH2, ALD6, ACS2, adhE2,ter, crt, hbd + CIT2Δ*	16.3 mg/L	(Krivoruchko *et al*, 2013)

1.8 Glucose signaling and sensing in yeast

One of the key considerations for the biotechnological production of biofuels has to be the carbon source. Glucose (a fermentable monosaccharide) serves as the principal carbon and energy source for *S. cerevisiae* and many organisms, and yeast have evolved complex molecular regulatory mechanisms to cope with fluctuating levels of glucose in its environment (Carlson, 1998; Carlson, 1999; Gancedo, 1998; Johnston, 1999; Rolland *et al*, 2002b). Aside from its role as a nutrient, glucose also serves as a signaling molecule that regulates physiological and pathological processes making it an important biomolecule for cells (Busti *et al*, 2010; Johnston, 1999; Kim *et al*, 2013; Rolland *et al*, 2002b). Yeast; a facultative anaerobe, represses a large number of genes responsible for the expression of proteins needed for the uptake and metabolism of other non-fermentable carbon source during growth on glucose (Johnston, 1999; Kim *et al*, 2013; Rolland *et al*, 2002b). Although fermentation produces less ATP yield per unit mole of glucose than oxidative respiration, *S. cerevisiae* is able to compensate for the deficit through increased glycolytic flux (Rolland *et al*, 2002b), by enhancing glucose uptake (the first, rate-limiting step of the glucose metabolic process) through the expression of genes encoding glucose transporters and glycolytic enzymes (Kim *et al*, 2013; Özcan & Johnston, 1999). The machinery by which yeast cells sense glucose levels in the environment and tune metabolic processes to suit glucose availability involves the complex molecular crosstalk between at least three glucose sensing and signaling pathways (Fig 1.6) (Ashe *et al*, 2000; Kim *et al*, 2013; Rolland *et al*, 2002b).

1) The Rgt2p/Snf3p glucose induction pathway regulating glucose uptake

2) The Ras-cAMP pathway involved in posttranslational regulation of proteins by phosphorylation

3) The glucose repression pathway that negatively regulates the genes involved in glucose oxidation and the use of alternative sugars.

Greater understanding of how these pathways impact upon the production of biofuels such as butanol in *S. cerevisiae* will be required if yeast is to be used as a microbial platform for butanol production from sustainable feedstocks.

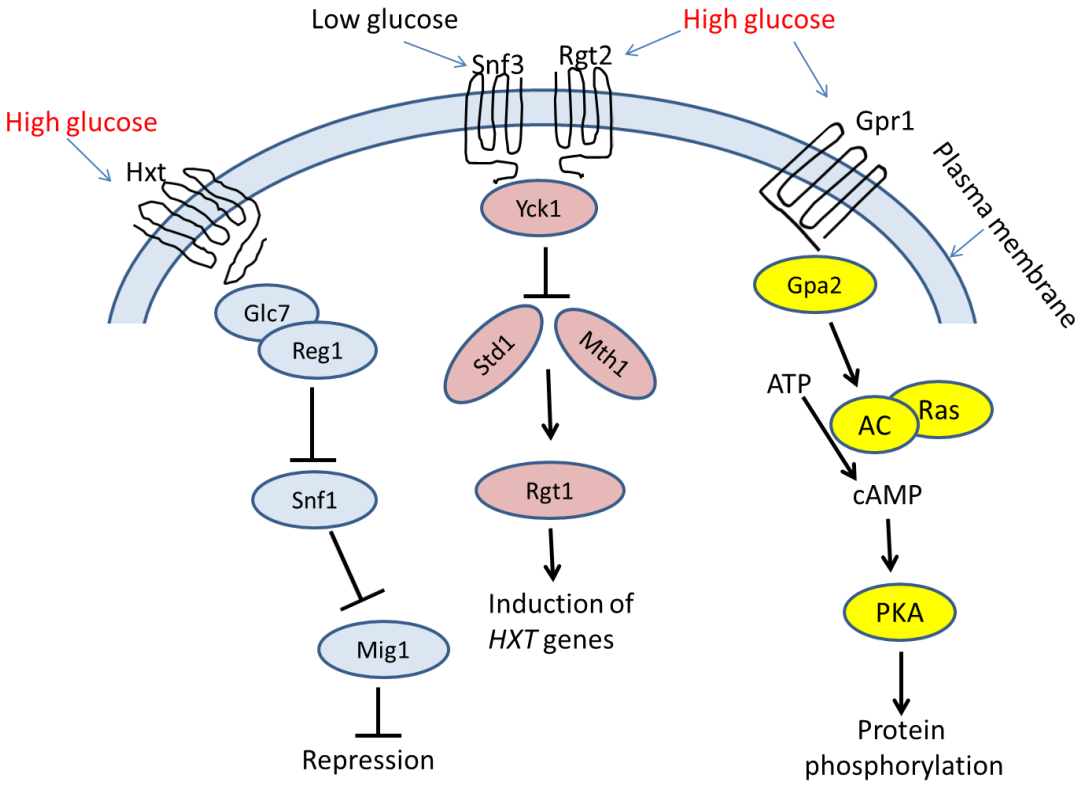

Figure 1.6 Summary of the major glucose sensing and signaling pathways in yeast.

Diagram shows the three major pathways for glucose sensing and signaling in yeast. The repression pathway is induced under high glucose; the hexose transporter (HXT) induction pathway induces different classes of hexose transporters under low and high glucose while the Ras-cAMP pathway is activated under high glucose.

1.8.1 The Rgt2p/Snf3p glucose induction pathway

S. cerevisiae possesses at least 17 members of the glucose transporter family (*HXT1* through to *HXT17*), each with slightly different expression profiles and affinities for glucose (Ko *et al*, 1993; Lagunas, 1993; Ozcan & Johnston, 1995; Özcan & Johnston, 1999). Rgt2p and Snf3p are plasma membrane glucose transporter-like proteins which act as cell surface glucose receptors that initiate signal transduction in response to glucose (Kim *et al*, 2013). Rgt2p and Snf3p differ in their affinities for glucose; Rgt2p is activated by high levels of glucose and activates the expression of low affinity glucose transporters such as Hxt1p and Hxt3p (Kim *et al*, 2013; Rolland *et al*, 2002a), whereas, Snf3p responds to low levels of glucose and activates expression of high affinity glucose transporters such as Hxt2p and Hxt4p (Kim *et al*, 2013).

1.8.2 Ras-cAMP glucose signaling pathway

In *S. cerevisiae*, cAMP signaling plays a central role in the regulation of metabolism, stress responses, growth and proliferation (Rolland *et al*, 2002a). The supply of glucose to yeast cells under derepressed conditions (such as during growth on a non-fermentable carbon source or in stationary phase), causes a transient spike in the cyclic-AMP (cAMP) level, initiating a PKA-dependent (protein kinase A) protein phosphorylation cascade which activates enzymes involved in fermentation and energy metabolism, thus offering rapid recovery from stationary phase. Yeast adenylate cyclase catalyzes the conversion of ATP to cAMP, and its activity is controlled by a G-protein coupled receptor (GPCR) system involving the G-proteins, Ras1 and Ras2. This pathway supports the glucose-dependent regulation of cAMP

levels that is critical in the modification of enzymatic activities (Hedbacker & Carlson, 2008; Rolland *et al*, 2002a; Tamaki, 2007; Thevelein & de Winde, 1999).

1.8.3 The glucose repression/ derepression pathway

Although, the cAMP dependent pathway is important in the adaptation to fluctuating carbon sources, arguably the most important response to such a change in condition is the glucose repression/ derepression pathway (Gancedo, 1998; Trumbly, 1992). Glucose repression is the down-regulation of genes responsible for respiration, gluconeogenesis and the use of alternative sugars during active growth on glucose (Ashe *et al*, 2000; Kim *et al*, 2013; Rolland *et al*, 2002a). The central components of this pathway are: Mig1p, a transcriptional repressor; Snf1p, a protein kinase (in complex with Snf4p and the three members of the Snf-interacting (Sip) family of proteins) and Glc7p, a protein phosphatase 1 (PP1) along with its regulatory/targeting subunit Reg1p (Carlson, 1998; Carlson, 1999; Gancedo, 1998; Hedbacker & Carlson, 2008; Johnston, 1999; Kim *et al*, 2013; Rolland *et al*, 2002a).

Mig1p

Mig1p is a zinc-finger-containing repressor protein that binds to the promoters of many glucose-repressible genes and represses their transcription (Rolland *et al*, 2002a). Mig1p recruits the general co-repressor proteins Ssn6p and Tup1p to elicit repression (Johnston, 1999; Rolland *et al*, 2002a). Also involved in glucose repression is Mig2; a homologue of Mig1p (Rolland *et al*, 2002a). However, molecular evidence points to Mig1p as being responsible for most of the repression of glucose-repressed

genes, making it a principal component of the glucose repression pathway (Rolland *et al*, 2002a). The function of Mig1p in glucose repression is dependent on its subcellular localization, which is regulated by the Snf1p protein kinase (De Vit *et al*, 1997; Rolland *et al*, 2002a). In the absence of glucose, Mig1p is phosphorylated by Snf1p causing it to be retained in the cytosol away from its nuclear target genes; thus relieving their repression (Johnston, 1999; Kim *et al*, 2013; Rolland *et al*, 2002a). However, in the presence of glucose, Snf1p activity is inhibited and Mig1p becomes dephosphorylated and rapidly enters the nucleus to repress transcription. Although no protein phosphatases that dephosphorylate Mig1p have been identified, one possible candidate is Reg1p–Glc7p (Johnston, 1999).

Snf1p Kinase

In *S. cerevisiae*, the Snf1p protein kinase is the catalytic subunit of a protein-serine/threonine kinase that is homologous to the mammalian AMP-dependent protein kinase (AMPK) (Hedbacker & Carlson, 2008). The Snf1p kinase exists in a heterotrimeric protein complex with the Snf4p activating subunit and members of Snf1p-interacting proteins (Sip family; Sip1p, Sip2p, Gal83p), which serve scaffolding functions (Hedbacker & Carlson, 2008; Kim *et al*, 2013). The Snf1p protein kinase is required for transcription of glucose-repressed genes in response to caloric restriction (glucose limitation) when the concentration of glucose drops below 0.2% (Carlson, 1999; Dombek *et al*, 1999; Hedbacker & Carlson, 2008). This enables yeast to switch metabolism to utilize alternate carbon (non-fermentable carbon) sources such as; sucrose, maltose, galactose, ethanol and acetate that are less preferred than glucose (Kim *et al*, 2013; Rolland *et al*, 2002a). During growth on glucose, Snf1p kinase activity

is inhibited; thus permitting Mig1p-repression of genes involved in alternative carbon source utilization, respiration, electron transport chain, gluconeogenesis, glycogenesis and stress responses (Johnston, 1999; Kim *et al*, 2013; Rolland *et al*, 2002a). However, when glucose becomes limiting, Snf1p kinase is activated and this relieves Mig1p repression; allowing the transcription of all glucose repressed genes (Johnston, 1999; Kim *et al*, 2013; Rolland *et al*, 2002a). Snf1p also regulates the activity and expression of Cat8p and Sip4p which are involved in the induction of gluconeogenic genes through carbon source-responsive promoter elements (CSRE) (Rolland *et al*, 2002a). Furthermore, Snf1p plays roles in nutrient stress responses, in growth and in the response to other environmental stresses (Busti *et al*, 2010; Celenza & Carlson, 1986; Hedbacker & Carlson, 2008; Jiang & Carlson, 1996; Kuchin *et al*, 2003). Snf1p regulates these various cellular processes through the regulation of gene transcription and by direct regulation of the activity of pathway enzymes (Hedbacker & Carlson, 2008).

Glc7p-Reg1p

Protein phosphatase type 1 (PP1) activity is essential for regulating a diverse array of processes in eukaryotic cells and its function is highly conserved across eukaryotes (Cannon, 2010; Dombek *et al*, 1999; Tu & Carlson, 1995). The *S. cerevisiae* PP1 catalytic subunit is encoded by the *GLC7* gene. Glc7p is required for the appropriate regulation of several physiological processes within the cell including the repression of many genes needed for utilization of alternative carbon sources (Dombek *et al*, 1999; Gancedo, 1998; Sanz *et al*, 2000; Tu & Carlson, 1995). The PP1 catalytic subunit has little substrate specificity (Dombek *et al*, 1999; Tu & Carlson, 1995), therefore its specificity of action is determined by its association with different

regulatory or targeting subunits (Dombek *et al*, 1999; Tu & Carlson, 1995). In *S. cerevisiae,* Reg1p is a regulatory/targeting subunit that directs the participation of the Glc7p catalytic subunit in the inhibition of Snf1p kinase activity as part of the glucose repression mechanism (Tu & Carlson, 1995). As such, it acts antagonistically to the Snf1p protein kinase in this pathway (Tu & Carlson, 1995).

The glucose repression/derepression pathway alters the entire gene expression profile of yeast in response to alterations in carbon source. The question as to whether this pathway impacts upon exogenous added pathways such as the butanol production pathway has not been addressed and serves as a focus for first part of this thesis.

1.9 Yeast acetyl-Co enzyme A (acetyl-CoA) metabolism

A metabolite that is critically important to the exogenous butanol production pathway is acetyl-CoA, as it serves as the precursor for the pathway. In yeast, acetyl-CoA metabolism is separated into four different compartments (namely, the nucleus, the mitochondria, the peroxisome and the cytosol) (Fig 1.7) and metabolism in each compartment depends on the nutrient environment of the cell (Chen *et al*, 2013; Krivoruchko *et al*, 2013). Acetyl-CoA is an important metabolite needed for several metabolic processes such as glyoxylate synthesis of succinate during growth on oleic acid or 2C and 3C molecules (including ethanol and acetate), it is needed for biosynthesis of fatty acids and sterols and it is the product of beta-oxidation reaction. Acetyl-CoA in the nucleus is the sole donor of acetyl groups for histone acetylation (Chen *et al*, 2012; Nielsen, 2014; Pietrocola *et al*, 2015). Acetyl-CoA is essential for

energy metabolism in the mitochondria where it is completely oxidized to form carbon dioxide with the generation of metabolic energy. In the cytosol, acetyl-CoA is produced via the pyruvate dehydgrogenase bypass pathway, which involves the decarboxylation of pyruvate to form acetaldehyde which is oxidized to acetate. Acetate is then converted to acetyl CoA by the addition of co-enzyme A (Lian *et al*, 2014; Shiba *et al*, 2007). A number of interesting bioproducts such as flavonoids, polyketides, polyhydroxybutyrate, sterols and, as mentioned above, butanol require acetyl-CoA as starting precursor. In yeast, organelle membranes are impermeable to acetyl-CoA, therefore it is either synthesized locally within those compartments or transported via the carnitine/acetyl-carnitine shuttle which shuttles acetyl groups between the mitochondria/ peroxisome and the cytosol (Chen *et al*, 2012). *S. cerevisiae* cannot synthesize carnitine *de novo* and must be available in the growth medium in order for this carnitine/acetyl-carnitine shuttle transport system to be functional (Chen *et al*, 2012).

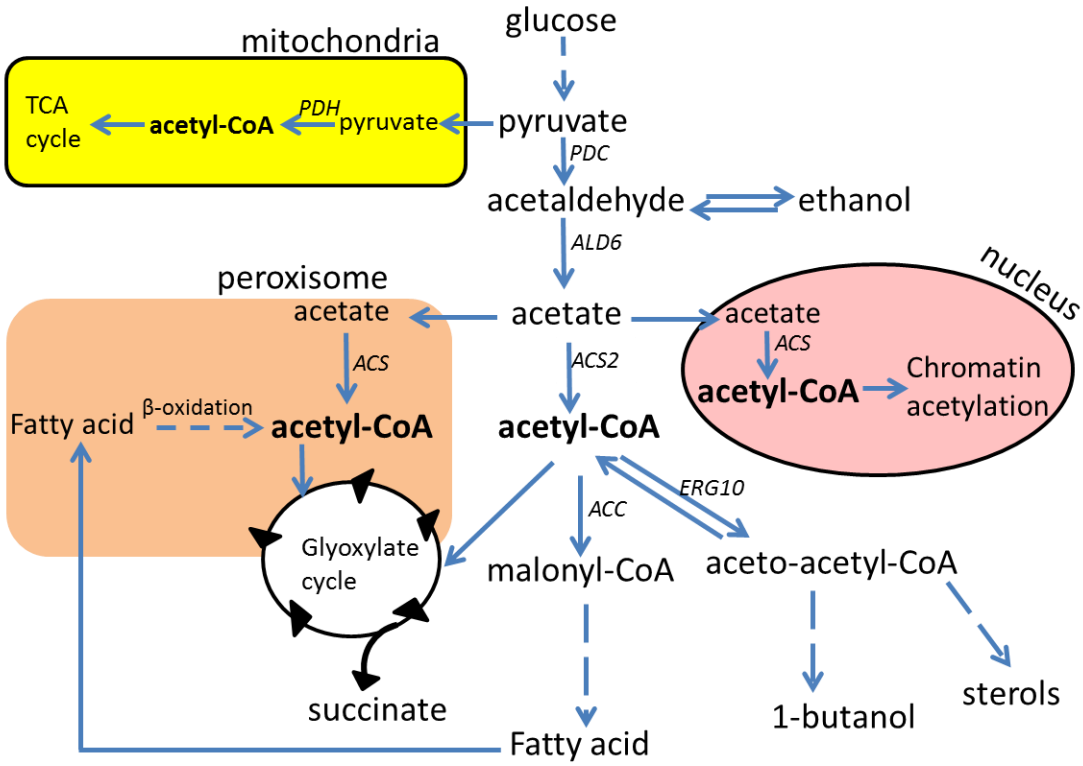

Figure 1.7 Summary of acetyl-CoA metabolism in Yeast.

Summary of acetyl-CoA metabolism in yeast showing; the nucleus, mitochondria, and peroxisome in highlight and acetyl-CoA written in bold for emphasis. Three routes for cytosolic acetyl-CoA metabolism via glyoxylate cycle, fatty acid synthesis and acetoacetyl-CoA synthesis is shown. *PDH, PDC, ALD6, ACS, ACC, ERG10* are acronyms for pyruvate dehydrogenase complex, pyruvate decarboxylase, acetaldehyde dehydrogenase, acetyl-CoA synthase, acetyl-CoA carboxylase and thiolase enzymes respectively.

1.9.1 Yeast glyoxylate cycle.

A crucial pathway involved in cytosolic acetyl-CoA metabolism is the glyoxylate cycle (Fig 1.8). The yeast glyoxylate cycle occurs part in the peroxisome and part in the cytosol and is a bypass to the mitochondrial TCA that enable cells to utilise fatty acids or C2 molecules such as ethanol or acetate as carbon energy sources (Chen *et al*, 2012; Lee *et al*, 2011). The cycle produce a net C4 -succinate from two molecules of C2-acetyl-CoA and the succinate is utilized for TCA cycle replenishing, amino acid biosynthesis and gluconeogenesis; the glyoxylate cycle therefore serves as a link between catabolism and anabolism (Kunze *et al*, 2006; Lee *et al*, 2011). In yeast, the glyoxylate shunt and the carnitine/acetyl-carnitine shuttle are the two transport systems for acetyl-CoA movement across organelles but without the supply of carnitine in the growth media, the glyoxylate cycle remains the only active transportation means for cytosolic acetyl-CoA. (Krivoruchko *et al*, 2013).

1.9.2 Summary of the glyoxylate cycle.

The glyoxylate cycle (Fig 1.8) involves the reduction of malate by malate dehydrogenase to form oxaloacetate which is condensed with acetyl-CoA to form citrate (catalyzed by citrate synthase) with release of a free Coenzyme A (CoA). Aconitase then isomerizes citrate to isocitrate and the isocitrate is split into glyoxylate and succinate by isocitrate lyase. The glyoxylate molecule is recycled by condensing with acetyl-CoA to form malate by malate synthase while the succinate is given off as the net product of the cycle.

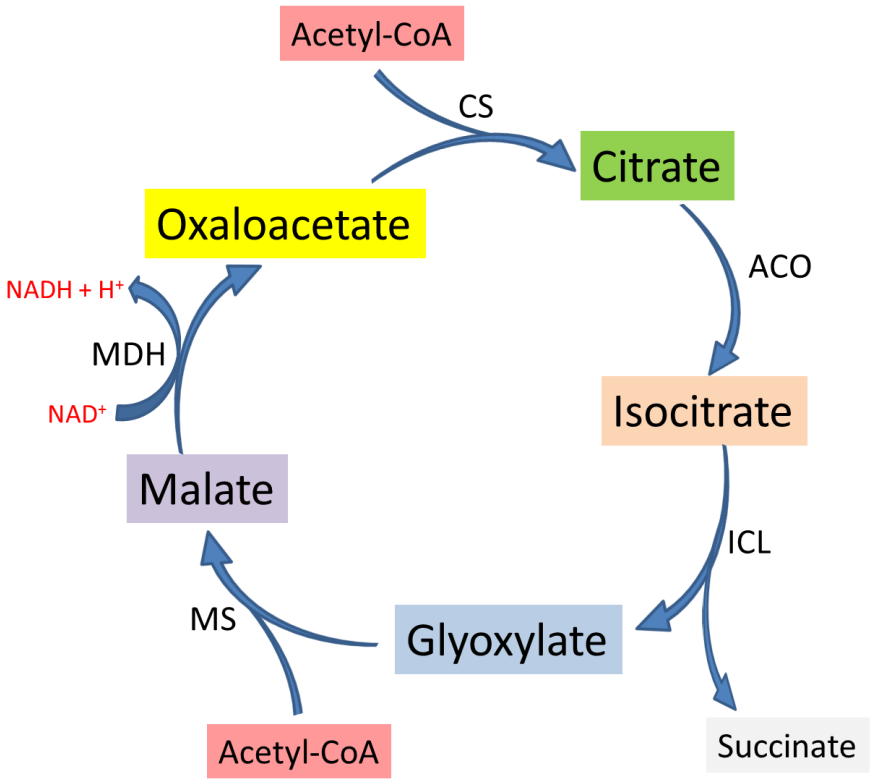

Figure 1.8 Summary of the glyoxylate cycle.

Enzymes catalyzing the pathway includes; CS (citrate synthase), ACO (aconitase), ICL (isocitrate lyase), MS (malate synthase) and MDH (malate dehydrogenase). The cycle metabolise two molecules of acetyl-CoA to give-off one molecule of succinate.

1.10 Thiolase enzyme

The first step of the ABE-butanol pathway involves the condensation of two acetyl-CoA molecules (two carbon compound) to form acetoacetyl-CoA (four carbon compound). The reaction is an example of anabolic carbon skeleton assembly reaction and it is catalyzed by thiolase enzymes. Thiolases are an abundant family of dimeric or tetrameric enzymes which are divided into two groups, biosynthetic and catabolic thiolases, each with different substrate specificity and metabolic significance. Catabolic (sometimes called degradative) thiolase II act as dimers while the biosynthetic thiolase I are tetramers (Mann & Lutke-Eversloh, 2013). The degradative thiolase (thiolase I, E.C. 2.3.1.16), referred to as 3-ketoacyl-CoA thiolase has a wide substrate range for long-chain fatty acids (C4–C16) and is involved in the β-oxidation pathway where it catalyse cleavage of 3-Ketoacyl-CoA to release acetyl-CoA. The biosynthetic enzyme (thiolase II; E.C. 2.3.1.9) known as acetyl-CoA acetyltransferase (acetoacetyl-CoA thiolase) has strict substrate specificity for C4 substrate and it catalyse the reversible Claisen condensation of two acetyl-CoA molecules to form acetoacetyl-CoA (Kim *et al*, 2015; Modis & Wierenga, 1999; Modis & Wierenga, 2000). Acetoacetyl-CoA is an important intermediate for the metabolic biosynthesis of fatty acids, ketone bodies, sterols and polyhydroxybutyrate. As stated above, it is also important for the biosynthesis of secondary metabolites such as butanol (Nielsen, 2014). The condensation reaction of biosynthetic thiolase is well regulated and it is not spontaneous *in vivo*, the reaction occurs only when there is large excess acetyl-CoA and there is prompt clearance of acetoacetyl-CoA (the reaction product) (Modis & Wierenga, 1999).

1.10.1 Thiolase sequence and structure homologies

In general, thiolases are a well-defined protein family with high sequence and structure homologies among eukaryotes and prokaryotes (Mann & Lutke-Eversloh, 2013). In *E. coli*, two forms of thiolase exist; thiolase I (encoded by *fadA*) and thiolase II (encoded by *atoB*) (Ithayaraja *et al*, 2016; Kursula *et al*, 2002). Thiolase I preferentially act on medium chain length acyl-CoA substrates (up to 16 carbons) and it is involved in fatty acid metabolism. Thiolase II is specific for acetyl-CoA and acetoacetyl-CoA, it is involved in butyric acid metabolism and it catalyzes the reverse condensation of acetyl-CoA (Kursula *et al*, 2002). In *E. coli*, thiolases are only expressed when cells perceive specific nutritional cues, such as the presence of butyrate, acetoacetate, or medium chain length fatty acids such as oleic acid (Ithayaraja *et al*, 2016; Mann & Lutke-Eversloh, 2013).

In the bacteria *Zoogloea ramigera,* the biosynthetic thiolase (PhaA) is involved in the biosynthesis of polyhydroxybutyrate and its structural studies reveal that it has a tetrameric architecture with a tetramerization motif (Modis & Wierenga, 2000). PhaA adopts a similar overall fold to the yeast peroxisomal degradative thiolase, the fold has three domains: two core domains and a loop domain. The core domains form a tightly folded, five-layered (α-β-α-β-α-β) structure and the loop domain contains a motif involved in tetramer formation (Mann & Lutke-Eversloh, 2013; Modis & Wierenga, 1999; Modis & Wierenga, 2000). Studies have shown that biosynthetic thiolases are inhibited by CoA, although little evidence for existence of allosteric domains in the thiolase protein is found; this suggests competitive end product inhibition of the enzyme (Mann & Lutke-Eversloh, 2013).

Two forms of thiolase are found in *C. acetobutylicum* which are encoded by *thlA* and *thlB* genes respectively. ThlB protein is only briefly expressed during the transition between acidogenic and solventogenic phases, probably to enhance a rapid switch to solventogenesis (Kim *et al*, 2015; Modis & Wierenga, 1999) while ThlA protein is highly expressed after acidogenesis, making it more important. The *C. acetobutylicum* thiolase shares the general quaternary architecture with the type II biosynthetic thiolase family of proteins. Its tetrameric conformation consists of two asymmetric dimers similar to other biosynthetic thiolases. Each monomer has three domains:

1. N-terminal α/β domain (N-domain, residues 1–119 and 249–269),
2. loop domain (L-domain, residues 120–248), and
3. C-terminal α/β domain (C-domain, residues 270–392).

The N- and C-domains form the typical five-layered fold (α-β-α-β-α) mentioned above, and the L-domain is involved in tetramerisation. *C. acetobutylicum* thiolase forms disulphide bonds between the two catalytic cysteine residues under oxidized conditions to serve as a form of redox switch (Kim *et al*, 2015). The *C. acetobutylicum* thiolase is reported to be very sensitive to free CoA and it is inhibited even at micromolar CoA concentrations. Other physiological inhibitors of the enzyme include butyryl-CoA and ATP (Kim *et al*, 2015).

In yeast, two thiolases; 3-ketoacyl-CoA thiolase and acetoacetyl-CoA thiolase have also been identified. These thiolases are encoded by *POT1* and *ERG10* genes and they catalyse the degradative and biosynthetic reactions respectively (Hiser *et al*, 1994;

Kornblatt & Rudney, 1971). Figure 1.9 is a representation of the structure of biosynthetic thiolase.

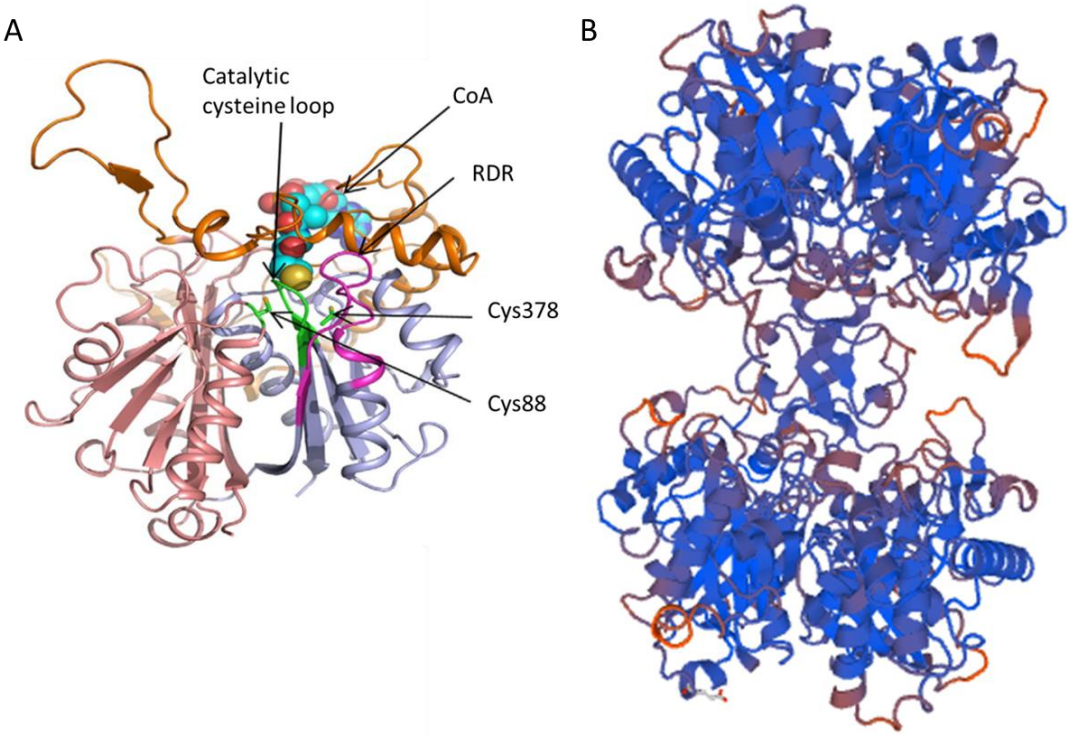

Figure 1.9 Ribbon representation of the thiolase structure

A) Ribbon model of thlA biosynthetic thiolase monomer unit; the N-, C- and L-domains are colour distinguished with salmon, light blue and orange colours, respectively (kim *et al.* 2015). The catalytic cysteine loop. regulatory determinant region (RDR),and cysteine 378 & 88 are labelled (Kim *et al*, 2015). Interaction with CoA molecule is also shown. B) Homotetrameric structure of the biosynthetic thiolase

1.10.2 Mechanism of thiolase Catalysis

Thiolase catalysis involves two cysteine residues and a histidine residue at the catalytic site. The reaction is thought to occur via a two-step ping pong mechanism for both the biosynthetic and degradative reactions (Kursula *et al*, 2002; Merilainen *et al*, 2009; Modis & Wierenga, 1999; Modis & Wierenga, 2000). In the first step of the biosynthetic reaction, a cysteine residue is activated by the catalytic histidine residue and it nucleophilically attacks the acetyl-CoA substrate. This leads to the formation of a covalent acetyl-CoA-enzyme intermediate, whereupon a second cysteine residue stabilizes the reaction by transferring a proton to CoASH with the formation of the acetyl-enzyme intermediate (Fig 1.9). In the second step, acetyl-CoA reacts with the acetyl–enzyme intermediate in a claisen condensation mechanism to release acetoacetyl-CoA product from the enzyme (Merilainen *et al*, 2009; Modis & Wierenga, 1999).

The thiolase step represents a key initiating step in the ABE-butanol pathway and in the butanol production strain, the establish this pathway in yeast rely on the yeast Erg10 enzyme, this step represents an obvious point at which optimization strategies can be targeted

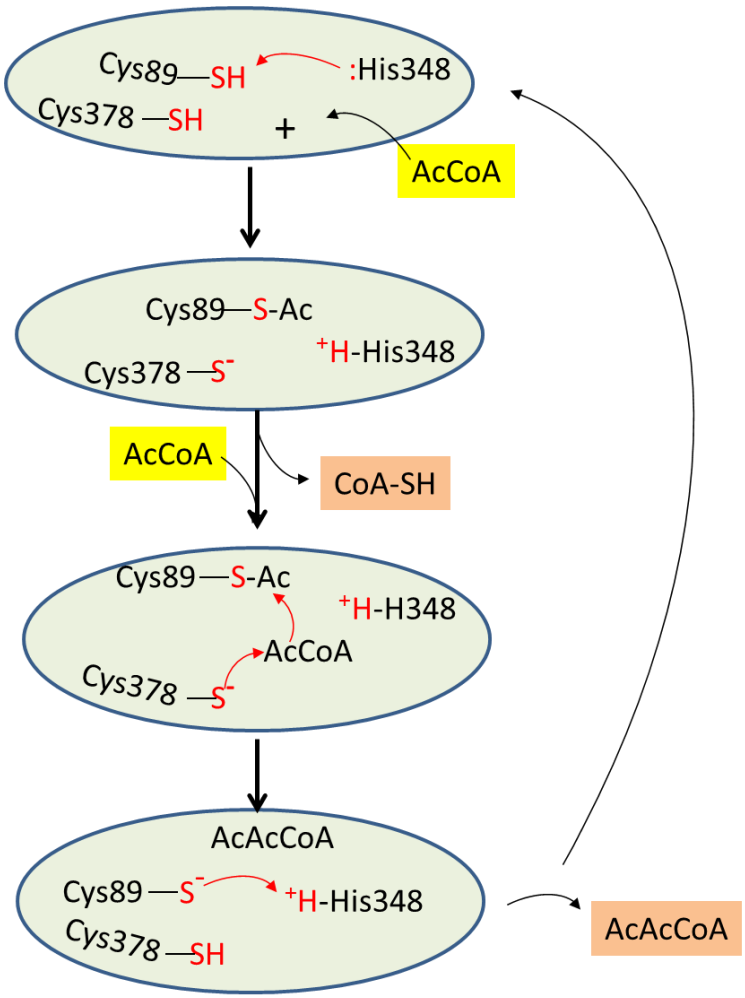

Figure 1.10 Reaction mechanism of biosynthetic thiolase II

Summary of steps involved in the two-step ping-pong Claisen condensation of two acetyl-CoA (AcCoA) to form acetoacetyl-CoA (AcAc-CoA). An acetyl-enzyme complex is formed through Cys89 (activated by His348), and then a second AcCoA molecule (activated by Cys378) condenses with the acetyl-enzyme complex with the release of acetoacetylCoA in a Claisen condensation manner.

1.11 Research background

Yeast *Saccharomyces cerevisiae* has many advantages as a cell factory for bio-butanol production (Buijs *et al*, 2013; Gonzalez-Ramos *et al*, 2013; Hong & Nielsen, 2012; Si *et al*, 2014a). Previously, several studies have described metabolic engineering approaches to insert the ABE-butanol pathway into yeast with varying levels of success; butanol production levels of 242.8 mg/L was achieved by Si *et al*., (2013); (Krivoruchko *et al*, 2013) reported a 16.3mg/L level, while a 2.5mg/L titer was reported by (Steen *et al*, 2008). Collaborative work, in the Chris Grant and Mark Ashe labs, developed a strain of yeast (BPS strain) that produces a titer of ~300mg/L butanol in rich media (Swidah *et al*, 2015). This strain contains five genes (5g) encoding the enzymes of the ABE-butanol production pathway (Swidah *et al*, 2015) (Fig 1.10). These genes include; four Clostridial genes (*crt, hbd, bcd* & *AdhE2*) and one *Saccharomyces cerevisiae* gene (*ERG10*). These genes were all inserted into the genome under the control of the *TDH3* promoter using various selectable markers. Additionally, the strain is deleted for the *ADH1* gene, that encodes the main cytosolic yeast alcohol dehydrogenase, as well as carrying overexpressed versions of the *ALD6* and *ACS2* genes, that encode an aldehyde dehydrogenase and acetyl-CoA synthase respectively (Swidah *et al*, 2015). However, the level of butanol produced by the strain is still well below the level of ethanol produced by yeast cells and is well below a level that would be commercially competitive with petrol based fuels.

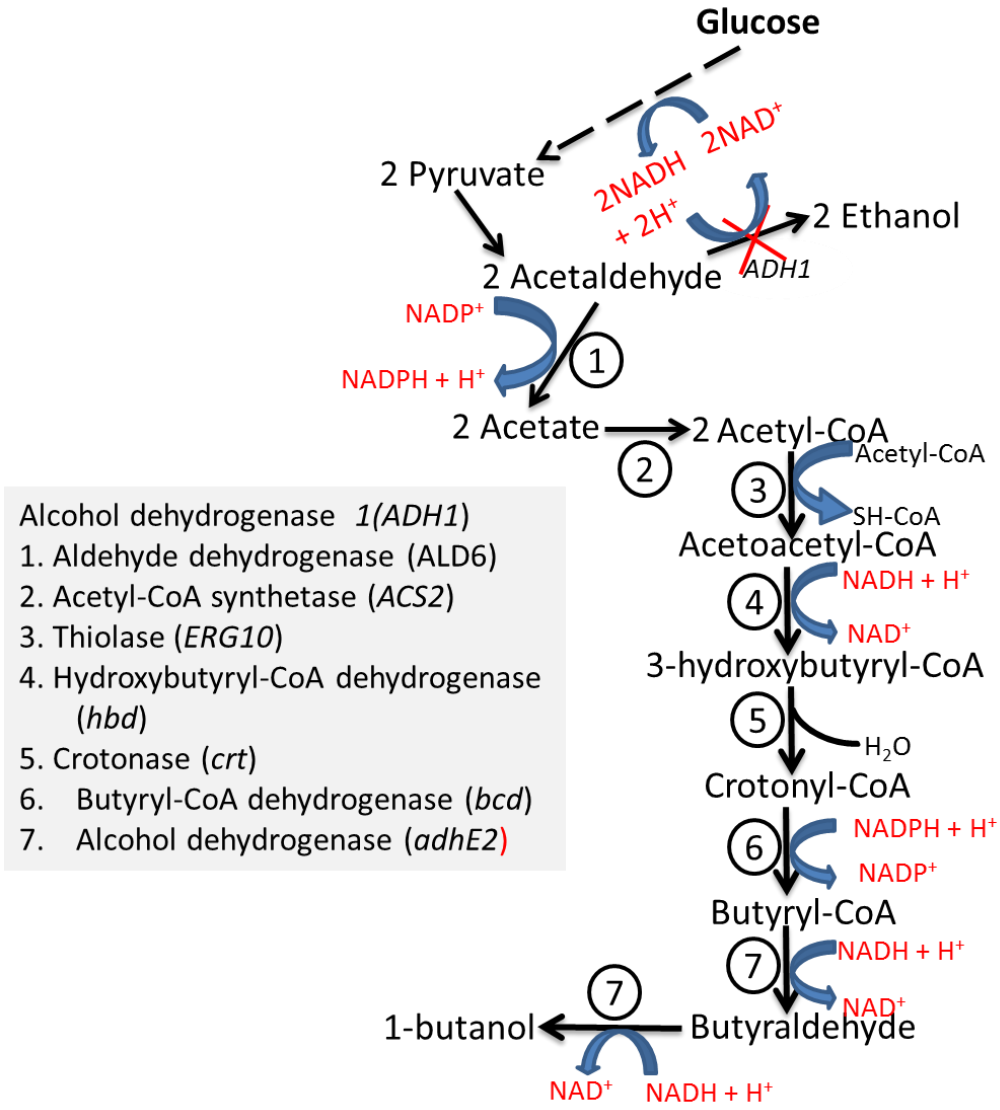

Figure 1.11 Summary of the pathway for butanol synthesis in the BPS strain.

The strain has; *ADH1* gene deleted, five heterologous genes for butanol synthesis over-expressed and two yeast genes for acetyl-CoA synthesis equally overexpressed. All overexpressed enzymes and their corresponding genes (in parenthesis) are numbered.

1.12 Aims and objectives of research

The primary goal of my PhD research is to improve the level of butanol production in the BPS yeast strain. In order to achieve this, I have taken three different strategies with distinct aims. The first aim was to disable the glucose repression pathway with a view to dysregulating glucose repression so as to allow a number of discrete outcomes. It was considered that dysregulated glucose repression might increase butanol production, improve yeast's tolerance to butanol and allow growth on less preferred carbon sources. To dysregulate glucose repression, a strategy was undertaken to delete the *REG1* gene in the butanol producing strain of *S. cerevisiae* and selected control yeast strains. As a control, a *SNF1* deletion mutation that would elicit the opposite effect, constitutive glucose repression, was also constructed in the same set of strains.

A second aim encompassed the hypothesis that increasing the level of the cytosolic substrate of the butanol production pathway, acetyl CoA, would improve butanol yields. A strategy was therefore devised to manipulate specific glyoxylate cycle steps in the butanol production and control strains that would be expected to increase cytosolic acetyl CoA. More specifically, strains deleted in the *MLS1* and *CIT2* genes encoding acetyl CoA entry points in the glyoxylate pathway were generated.

A third aim was to improve the efficiency of the synthetically added butanol production pathway in the strains. The initiating step in the butanol pathway is the thiolase step where two acetyl-CoA molecules undergo a Claisen condensation reaction to produce acetoacetyl-CoA. The enzyme that had been over-expressed in the butanol production strains that the lab had previously produced was the yeast Erg10

thiolase. Therefore, in an effort to improve the efficiency of this step, a strategy was devised to replace the yeast Erg10 thiolase in the butanol biosynthetic pathway with other forms of the enzyme; the natural *C. acetobutylicum* thiolase, two mutant form of the *C. acetobutylicum* enzyme or the natural *Z. ramigera* thiolase. These thiolase genes and mutants were selected based upon various previously described properties such as affinity for acetyl-CoA and the thermodynamic properties of the enzymes.

All three strategies involved complex genetic manipulations of yeast strains that were generated and validated; the resulting strains were tested for their impact on butanol and other metabolite yields.

2. Materials and methods

2.1 Growth media

2.1.1 Yeast rich media

Yeast extract peptone medium (YP) (1% w/v yeast extract, 2% w/v Bacto-peptone, 0.015% w/v Tryptophan) containing 2% w/v glucose (YPD) was used for routine culture and maintenance of *S. cerevisiae* strains (Guthrie and Fink, 1991). YPS, YPX YPE, YPG, YPA media contain 2% w/v of sucrose, xylose, ethanol, glycerol, or acetate respectively in place of glucose. Solid media are prepared by adding 2% (w/v) bacto-agar (Melford) in growth media.

2.1.2 Yeast minimal media

Synthetic complete (SC) medium (0.17% w/v yeast nitrogen base, 0.5% w/v ammonium sulfate and 1% w/v amino acid mix) containing 2% w/v of desired sugar/carbon energy source was also used for yeast cell culture. SC media containing antibiotics are prepared using 0.1% w/v L-glutamic acid monosodium salt instead of ammonium sulphate.

2.1.3 Bacteria growth media

Luria broth (LB) (1% w/v tryptone, 0.5% w/v yeast extract and 1% w/v NaCl) was used for routine bacteria culturing. LB solid media was made by adding 2% w/v bacto-agar in the growth media.

2.2 Growth conditions

2.2.1 Yeast growth condition

Routine yeast cell culturing was performed at 30^{o}C with 180 rpm shaking for liquid media culturing. Growth of yeast cell culture was assessed by measuring the optical density (OD) of the culture at 600nm (OD_{600}). Cultures are diluted up to 10 fold with sterile distilled water (SDW) to obtain OD_{600} value that is near 0.6 units for better accuracy. Growth media containing 300 µg/ml Kanamycin (G418) sulphate (Melford), 100 µg/ml cloNat (BioWerner), 300 µg/ml hygromycin B (Invitrogen) and 10 µg/ml phleomycin (Apollo scientific Ltd) were used for selection of *kanMX, natNT2*, *hphNT1* and *ble* resistance respectively. YPS media containing 0.2% w/v 2-deoxyglucose (Sigma) was used for the selection of *reg1Δ* mutants and YPD containing antimycin A (20 µg/ml) (Sigma-Aldrich) was used for selecting *snf1Δ* mutants.

2.2.3 Bacteria growth conditions

Growth of bacteria (*Escherichia coli*) strains was performed at 37°C with 180 rpm shaking for culturing in liquid media. Media containing appropriate antibiotics was used for plasmid selection. Bacteria growth media containing 50 µg/ml Kanamycin (G418) sulphate and 150 µg/ml Ampicillin or carbencillin disodium (Sigma-Aldrich) was used for selection of *KanR* and *Amp* plasmid resistance respectively. 5-Bromo-4-chloro-3-indolyl b-D-galactopyranoside (X-gal) and Isopropyl β-D-1-thiogalactopyranoside (IPTG) were used at 40 µg/ml and 0.1 mM concentrations respectively.

2.2.2 Spot test growth assays

Yeast growth assay on solid media was performed using overnight cultures. Cells were grown overnight, washed and re-suspended in sterile distilled water (SDW) to an OD_{600} unit of 1. Three tenfold serial dilutions were prepared (OD_{600} of 0.1, 0.01 and 0.001), and 3 µl of each dilution was spotted on agar media and incubated at 30°C.

2.3 DNA manipulation and analysis

2.3.1 Yeast genomic DNA extraction

Yeast cells were harvested from 5 ml of overnight culture at 5000 rpm for 5 min, washed with 1 ml of buffer EB (1 M sorbitol, 1 mM EDTA, 30 mM DTT) and suspended in 500 µl of 1 mg lyticase (Sigma-Aldrich)/ml buffer EB before incubation at 37^{O}C for excess of 1 hr. The mixture was vigorously vortexed after addition of 55 µl of stop solution (containing; 3 M NaCl, 20 mM EDTA, 100 mM Tris pH 8.0) and 30 µl of 20% w/v SDS. 500 µl of phenol-chloroform solution (pH 8.0) was added, vortexed and then centrifuged at 13,000 rpm for 2 min. The aqueous upper layer was collected and the phenol/chloroform cleaning repeated. The aqueous layer was again extraction with 400 µl chloroform solution and DNA was pelleted at 13,000 rpm for 10 min after addition of 1 ml of ethanol solution (absolute). The DNA pellet was then washed with 70% v/v ethanol, dried at 50^{O}C, suspended in 20 µl SDW and stored at -20^{O}C.

2.3.2 Bacteria plasmid preparation

Bacteria cells were cultured on selection media (solid), colonies were then grown overnight in 5 ml liquid LB media at 37^{o}C (containing selection antibiotics). Cells were harvested by centrifugation at 5000 rpm for 5 min and plasmid DNA was extracted using the Qiagen mini-prep kit according to the manufacturers' recommended protocol. A ten- fold dilution of the plasmid DNA extract was made for quantification on a Thermo Scientific NanoDrop spectrophotometer and stored at -20^{o}C.

2.3.3 DNA amplification by polymerase chain reaction (PCR)

PCR amplification was performed in a Biometra® T3000 thermocycler using; the Expand high fidelity PCR system (Roche), Ranger enzyme system (Bioline) or HotstarTaq enzyme system. Reactions were carried in capped 200 µl tubes following recommended reaction recipes by the manufacturers. PCR conditions were usually optimized for individual reactions in order to obtain PCR product. A regular PCR condition includes the following steps:

Initial denaturation at 95 – 98^{o}C for 3 minutes

Denaturatuion at 95^{o}C for 15 – 30 seconds

Annealing at 55 – 68^{o}C for 30 seconds

Extension at 72^{o}C for 45 seconds/kbp product size

Final extension at 72^{o}C for 60 seconds

Final hold at 4^{o}C

2.3.4 Quantification of DNA samples

DNA concentration was evaluated using NanoDrop® 8000 spectrophotometer (Thermo Scientific). 2 µl of DNA solution was spotted onto the machine sensor (after initial blanking using SDW) and the DNA concentration recorded at 260 nm (UV wavelength).

2.3.5 Agarose gel electrophoresis

DNA was separated based on molecular size using agarose gel electrophoresis. DNA samples were run through agarose gel (0.8 – 1 % w/v) containing 5 µg/ml SYBR® safe DNA stain (Invitrogen) in 1 X Tris-acetate-EDTA (TAE) buffer (40 mM Tris base, 20 mM acetic acid, 1 mM EDTA, pH 8.0). 5 µl (25% w/v) loading dye (10 mM Ficoll, EDTA pH 8.0 , 2.5 mg/ml Orange G (Sigma-Aldrich)) was mixed with 10 µl DNA samples before loading into the gel. A DNA molecular weight marker (1kb hyperladder®) was loaded into the gel to assess the size of the sample bands. Gels are run at 100V for up to 45 min and DNA visualized using a 365nm Transilluminator (Bio-Rad) and the computer software Quantity One (Bio-Rad).

2.3.6 Restriction of plasmid DNA

Plasmid DNA was digested using appropriate restriction enzymes. 20 µl restriction reactions contained; 0.5 - 1 µg plasmid DNA, 1 µl restriction enzyme, 2 µl recommended buffer and distilled water (to 20 µl). Reactions were performed in

capped 200 µl tubes and incubated at recommended temperatures for 90 min. Generally, reactions were terminated by incubation at 65^{o}C for 20 min.

2.3.7 DNA ligation

Plasmid vector and insert DNA fragments with complementary overhangs were joined together using T4 DNA Ligase (NEB®) enzyme system. Ligation reaction contains; 1 µl T4 DNA ligase enzyme, 2 µl 10X T4 DNA Ligase Buffer, vector DNA, insert DNA and nuclease-free water to 20 µl. Reaction was incubated at 16^{o}C for 60 min and terminated at 65^{o}C for 10 min.

2.3.8 Purification of DNA

(I) DNA used for transformation

For difficult transformations, the PCR product (transformation cassette) was seperated by electrophoresis at 100 V for 40 min through 80 % agarose gel, the DNA band corresponding to size of the transformation cassette was cut from the gel and extracted using the Zymoclean Gel DNA recovery kit according to the manufacturers recommended protocol. The DNA extract was concentrated as previously described (Dowhan, 2008); an equal volume of phenol-chloroform was added to the DNA solution in a 1.5ml microcentrifuge tube, vortexed for about 10 sec and centrifuged for 1 minute at maximum speed. The upper phase was removed into fresh tubes and 1⁄10 volume of 3 M sodium acetate, pH 5.2 and 2.5 X volume of 100% ethanol added to

precipitate the DNA. The precipitating sample was placed in the -20^{o}C freezer for 1 hr before pelleting the DNA at 13,000 rpm for 10 min. DNA pellet was washed with 1 ml of 70% ethanol, dried at 50^{o}C for 1 min on a heat block or air dried for about 5 min and then resuspended in 10 µl of SDW at 50^{o}C for 5 min or overnight at -20^{o}C.

(II) DNA used for Ligation reaction

Linearized plasmid vectors and insert DNA fragments were separated as described above by electrophoresis. The DNA bands that correspond to the size of vector or insert DNA were cut from the gel, tied into dialysis tubes which were then filled with 1 ml TAE buffer. DNA was allowed to separate from the cut agarose gel piece into the buffer by electrophoresis at 100 V for 5–10 min. The DNA solution was transferred into clean eppendoff tubes and was concentrated as described (Dowhan, 2008).

2.4 Yeast transformation

Yeast was transformed using the high efficiency Lithium acetate method (Gietz & Woods, 2002). Yeast cells were cultivated in 50 ml YPD and grown at 30^{o}C to OD_{600} ≈1.0. Cells were harvested by centrifugation at 5000 rpm for 5 min in a Sigma 4K15 centrifuge and after washing in 25 ml SDW, resuspended in 1 ml of 100 mM lithium acetate. Cells were then pelleted by centrifugation at 13000 rpm for 15 seconds in a microcentrifuge and resuspended in 200 µl of 100 mM lithium acetate. To 50 µl aliquots of the 100 mM lithium acetate cell suspension, the following solution was added; 240 µl polyethylene glycol (PEG) (50% w/v), 36 µl of 1 M lithium acetate, 12.5 µl of Salmon sperm DNA (5 mg/ml) and 10 µl PCR product or SDW (negative control). Prior to use, the Salmon sperm DNA was boiled for 5 min and immediately chilled on

ice. The transformation mix was vigorously vortexed, incubated at 30^{o}C for 1 hr at 180 rpm and heat shocked at 42^{o}C for 25 min. After pelleting at 8000 rpm for 15 sec cells were washed in 1 ml SDW, resuspended in 1 ml YPD and incubated overnight at room temperature. The overnight culture was pelleted, washed in 1 ml SDW and re-suspended to a final volume of 200 µl in SDW after which, 100 µl aliquot was spread and incubated at 30^{o}C on selection media to select successfully transformed cells.

2.5 Molecular cloning

Plasmid vectors were cloned in competent *Escherichia coli* DH5α (Invitrogen) using standard protocols. To 50 µl aliquot *E. coli* cells (thawed on ice) was added 2 µl β-mercapto-ethanol, the mixture was incubated on ice for 10 min (flicking tube every 2 min) before 2 µl of plasmid DNA was added. The transformation mixture was then incubated on ice for 30 min then heat shocked at 42^{o}C for 30 second, incubated again on ice for 2 min after which 1 ml pre-warmed LB media was added. This was then incubated at 37^{o}C for 1 hr at 180 rpm, after which 50 µl aliquot was spread onto selective LB agar plate (supplemented with: 50 µg/ml Kanamycin sulphate or 150 µg/ml carbencillin/ampicillin disodium for selection of *KanMX* or *Amp* resistannce respectively) and incubated overnight at 37^{o}C.

2.6 *Cre*-recombinase mediated excision

The *Cre*-recombinase excision of *loxP* site from the genome of *loxP-natNt2-loxP* mutants (to allow the removal of *natNT2-loxP*) was done using plasmid pSH65 (Carter

& Delneri, 2010; Gueldener *et al*, 2002). Yeast was transformed with 0.5-1 µg pSH65 plasmid DNA according to the lithium acetate transformation protocol (Gietz and Woods, 2002). Potential transformants were selected on phleomycin and were incubated overnight in 5 ml YPR (raffinose) media. Cells were harvested at 3000 rpm for 5 min, washed in SDW and resuspended in 5 ml galactose minimal media (SCG) to OD_{600} unit of 0.3. The culture was incubated for 3 hours at 30^{o}C 180rpm after which it was diluted 10, 100 and 1000 fold respectively. 100 µl of each dilution was spread out on YPD-agar and incubated for 24 hours at 30^{o}C. Plate with the fewest colonies was replicated on YPD and YPD-cloNat to select strains that have lost the cloNat marker (*natNT2* gene).

2.7 Sub-cloning into pGEM-T Easy® vector

PCR amplified DNA fragments (thiolase gene modules used in this study) were first cleaned to remove oligonucleotides using QIAquick Nucleotide removal kit. Then, adenosine (A) tails were joined to the ends of the DNA fragment; 10 µl ligation reactions contain: 2 µl DNA, 1 µl (5 units) Taq DNA polymerase, 2 µl reaction buffer, 1 µl $MgCl_2$ (25mM) and 0.2 mM dATP. Reaction was incubated at 70^{o}C for 30 min in a thermocycler. The A-tailed DNA fragment was finally sub-cloned into pGEM-T Easy vector using the pGEM®-T Easy Vector system (Promega) according to manufacturer's recommended protocol; 10 µl reaction contain 5 µl ligation buffer, 1 µl pGEM-T Easy vector, 1 µl T4 DNA ligase, 2 µl A-tailed DNA fragment and 10 µl SDW. Reaction was incubated at room temperature for 2 hr after which ligates were transformed into competent *E. coli* cells. Transformed cells (white colonies) were selected on LB/IPTG/X-gal/carbencillin plates (see section 2.2.3).

2.8 Site-directed mutagenesis

Alterations in DNA sequence were made using the QuikChange lightning site-directed mutagenesis kit. For each DNA substitution, a pair of primers (forward and reverse) was designed with the substituted DNA sequence placed at the middle of the primers. Reactions were performed according to manufacturer's recommended protocol; 50 µl reaction contain 1 µl of QuikChange Lightning Enzyme, 5 µl reaction buffer (10X), 1.5 µl Quik solution reagent, 1 µl dNTP mix, 1.5 µl each of primers and 1 µl DNA template (10 - 100 ng). Reaction mix was incubated in a thermocycler according to recommended cycling parameters. 2 µl of *Dpn*I restriction enzyme was added after the reaction (to digest the parent plasmid DNA) and incubated for 10 mins at 37^{o}C. Finally, the altered plasmid DNA (*Dpn*I-treated) was cloned into competent *E. coli* cells and verified by DNA sequencing analysis after its extraction.

2.9 Yeast ribosomal extraction

Yeast cells were cultivated in YPD to an OD_{600} of 0.6. 50 ml of the culture was harvested at 5000 rpm for 3 min and resuspended in 50 ml of medium with or without glucose (YP or YPD) or in YPD with different butanol concentrations. After incubation for 10 min at 30^{o}C, the culture was immediately added to pre-chilled tubes containing 500µl of 10mg/ml cycloheximide (Calbiochem) and incubated on ice for 30 min. Cells were pelleted at 5,000 rpm for 5 min and washed in 25 ml lysis buffer (20 mM Hepes pH 7.4, 2 mM magnesium acetate, 100 mM potassium acetate, 100 µg/ml

cycloheximide, 0.5 mM DTT). Cells were again pelleted at 5,000 rpm for 5 min and resuspended in 800 µl lysis buffer and transferred into 1.5 ml microcentrifuge tubes. Cells were finally pelleted at 13,000 rpm for 1 min, resuspended in 200 µl lysis buffer and lysed with 200 µl of pre-chilled acid-washed glass beads (Sigma-Aldrich) by vortexing 6 X 20 seconds with a cooling interval of 40 seconds in iced water. Lysate was cleared briefly at 10,000 rpm for 1 min, followed by a 10 min centrifugation at 13,000 rpm to give the final lysate which was immediately snap-frozen in liquid nitrogen before being stored at -80^{0}C prior to use.

2.10 Preparation of linear sucrose density gradients

Sucrose solutions ranging between 15-50% were prepared with 60% sucrose solution (in 0.01% Diethyl pyrocarbonate [DEPC] treated deionized sterile water) and 10X polysome buffer (100 mM Tris acetate pH7.4, 700 mM ammonium acetate, 40 mM magnesium acetate) as detailed in table 2.1. Solutions were then dispensed into SW41 polyallomer centrifuge tubes (Beckman Coulter) in 2.25 ml aliquots, starting with 50% and ending with 15% to generate gradients. Layers were frozen in liquid nitrogen before dispensing the next layer. Gradients were stored at -80^{0}C and defrosted overnight at 4^{0}C prior to use.

Table 2.1 Preparation of sucrose density gradient

	% sucrose solution				
Components	**50%**	**42%**	**33%**	**24%**	**15%**
10X Polysome buffer (ml)	11.25	11.25	11.25	11.25	11.25
60%Sucrose solution (ml)	93.75	78.75	62.5	45	28.125
DEPC water (ml)	7.5	22.5	38.75	56.25	73.125

2.10.1 Analysis of yeast ribosomal distribution

The A_{260} (absorbance 260 nm) of samples was measured using a Thermo scientific NanoDrop 8000 Spectrophotometer, and 2.5 A_{260} units were layered onto a 15–50% linear sucrose gradient as previously described (Luthe, 1983). The gradient was centrifuged in a SW41 rotor (Beckman) for 2.5 hr at 40,000 rpm, 4^{o}C in Optima XE-90 ultracentrifuge (Beckman Coulter) after which the gradient was pumped through a flow-through UV spectrophotometer (ISCO, Model UA-6) using a peristaltic pump (ISCO) and the absorbance at 245 nm was continuously measured to generate the ribosomal distribution trace.

2.11 Protein analysis

2.11.1 Yeast total protein extraction

Yeast was cultured in 50 ml YPD to an OD_{600} of between 0.5–1.0. Cells were harvested at 3000 rpm for 5 min, resuspended in 1 ml lysis buffer (140 mM NaCl, 1 mM

$MgCl_2$, 0.5% NP40, 0.5 mM DTT and 1 tablet each of protease and phosphatase inhibitor cocktail [Roche]) and incubated on ice for 5 min. Cells were pelleted at 10,000 rpm for 1 min in fast prep tubes, resuspended in 100 µl of cold lysis buffer, and lysed in the presence of 2 volumes of glass beads (Sigma-Aldrich) by vortexing 4 times in FastPrep-24 (MP) at top speed with 40 seconds cooling intervals in ice. The tube was pierced using hot needle, placed on Eppendorf tubes and spin at 1500 rpm to remove the lysates. Lysates were cleared at 10,000 rpm for 15 min, placed in fresh Eppendorf tubes and 1 volume of loading buffer (10% v/v glycerol, 5% v/v β-mercaptoethanol, 3% w/v SDS, 62.5 mM Tris pH6.8, bromophenol blue) was added to an equal volume of protein sample and boiled for 5min before separation by electrophoresis or storage at -20^{o}C.

2.11.2 Preparation of yeast soluble and aggregated proteins

Cells were cultured in 50 ml YPD to OD_{600} unit of 0.6. 20 OD_{600} unit of the culture was harvested at 4000 rpm for 5 min, washed with 1 ml pre-chilled aggregate lysis buffer (ALB) (50 mM potassium phosphate buffer pH 7.0, 1 mM EDTA, 5% glycerol, 1 mM Phenylmethylsulfonyl fluoride (PMSF) and resuspended in 300 µl of ALB. 100 µl of 10 mg/ml lyticase (in ALB) was then added to the cell suspension and incubated at 30^{o}C for 45 min. Cells were lysed by sonication for 8 X 5 seconds while kept on ice after which cell debris was removed at 3000 rpm for 15 min and the lysate was transferred to new eppendorf tube. The lysate was centrifuged at 13,000 rpm for 20 min to pellet the aggregated protein fraction and the soluble protein fraction was carefully removed by aspiration into new tubes while the pelleted aggregated protein was resuspended in

400 µl of ALB. Samples were mixed with 1/10 and 1/4 volumes of NuPage® antioxidant and NuPage®protein loading buffer (Invitrogen) respectively then boiled for 5 min at 95^{o}C before separation by electrophoresis or storage at -20^{o}C

2.11.3 Protein quantification using Bradford method.

Protein concentration was determined according to the method of Bradford (Bradford, 1976). Protein standard curve was prepared with serial concentrations (0 – 1.4 µg/ml) of Bovine Gamma Globulin (Sigma-Aldrich). 200 µl of Bradford reagent (Bio-Rad) was added to 800 µl of protein standard solution; mixture was thoroughly mixed and left at room temperature for 5 min to develop colour. The absorbance was then read at 595nm (OD_{595}) and the mean from three repeats were plotted against their protein concentration on a linear scale. Yeast protein extract was diluted 100 fold in ddH_2O, 10 µl of the dilution was further diluted 80-fold to 800 µl with ddH_2O and 200 µl Bradford reagent was added, mixed thoroughly and allowed to develop colour for 5 min. The absorbance at OD_{595} was read and the mean absorbance value of three repeats was used to calculate the protein concentration of each sample from the slope of the protein standard plot.

2.11.4 SDS-PAGE

Proteins were separated by electrophoresis through a 10% polyacrylamide precast gel (Novex) with protein running buffer (76.8 mM glycine, 0.1% w/v SDS, 10 mM Tris pH 8.3).. 20 µl of prepared sample was loaded carefully on top of the gel and

run at constant voltage of 200 V for 1 hr or until the dye front reaches the bottom of the gel.

2.11.5 Western blot analysis

SDS-PAGE resolving gel was carefully removed and immersed in 1 X transfer buffer (192 mM glycine, 0.1% w/v SDS, 25 mM Tris in 20% v/v methanol). Also, sponges, Whatman® blotting papers (Sigma-Aldrich) and Hybond-ECL Nitrocellulose blotting membrane (Sigma-Aldrich) were all soaked in 1 X transfer buffer prior to being used. When Polyvinylidene difluoride (PVDF) transfer membrane (ThermoScientific) was used in place of Nitrocellulose membrane, it was activated for 5 min in methanol before use. The blotting set up was arranged to allow electro-blotting transfer of proteins from the gel onto the nitrocellulose membrane. Electrophoresis was performed at 35 V in 1 X transfer buffer for 1 hr after which the nitrocellulose membrane was removed and stained with Ponceau S (Sigma-Aldrich) solution (0.1% w/v Ponceau S in 5% v/v acetic acid) to check for protein transfer. The blotting membrane was washed several times with 1 X PBST buffer (washing buffer) (230.8 mM NaCl, 0.1% v/v Tween20 10 mM sodium phosphate buffer pH7.4) to clear the Ponceau stain.

2.11.6 Immuno-detection of epitope tagged proteins.

The blotting membrane was soaked in blocking solution (5% w/v skimmed milk solution in 1 X PBST) while rocking for 1 hr at room temperature or overnight at $4^{O}C$. The membrane was then transferred into primary antibody solution (1:10000 primary antibody (anti-FLAG M2 (Sigma-Aldrich®) or anti-Myc (abcam®), 5% w/v skimmed milk

in 1 X PBST) with gentle rocking for 1 hr after which membrane was washed three times by rocking for 5 min in 1 X PBST before being transferred into a IRDye secondary antibody solution (LI-COR) (1:5000 secondary antibody, 5% w/v skimmed milk in 1 X PBST) for 1 hr with gentle rocking. The membrane was washed and detected using the Odyssey Fc dual-imaging system (LI-COR).

2.12 Yeast metabolite extraction

Yeast cells were cultured for 4 days under similar conditions for n-butanol production. 8 ml of culture was added to 40 ml pre-chilled (-80^{o}C) 100% methanol in 50 ml falcon tube and harvested at 3000 rpm for 10 min at -20^{o}C in an Eppendorf® 5804R cold centrifuge. 2 ml boiling 70% ethanol was added to the cell pellet and boiled at 95^{o}C in a water-bath for 5 min. The boiled mixture was transferred into clean 1.5 ml Eppendoff tube and cleared by centrifugation at 13,000 rpm at -10^{o}C for 10 min. The supernatant was transferred to new 1.5 ml eppendoff tube, vacuum dried in a SpeedVac® concentrator (Thermo Scientific) (set at medium drying rate without heat). Pellet was resuspended to 200 µl using deionized water and stored at -20^{o}C (Gonzalez *et al*, 1997; Lian *et al*, 2014)

2.13 Establishment of acetyl-CoA assay

The Acetyl-CoA concentration in yeast metabolite extract was measured using acetyl-CoA assay Kit (Sigma-Aldrich®). The assay involves a coupled enzyme reaction which results in a fluorometric product with excitation and emission wavelengths of

λ_{ex}= 535 nm and λ_{em}=587 nm respectively. Acetyl CoA is reacted and the product formed interacts with a fluorescent probe to generate fluorescence. Acetyl-CoA standard curve (Fig 4.12) is generated using standard solutions of acetyl-CoA prepared from a stock solution from the kit. The reaction is done in Corning™96-Well Clear Bottom Black plate (Fischer Scientific) and fluorescence is read using BioTek synergy HT plate reader operated with Gen5® software. The concentration of acetyl-CoA is calculated based on the following formula:

$C_A = (S_A / S_V)$ x 809.6 g/mole

C_A is concentration of acetyl-CoA

S_A is amount of acetyl-CoA in sample (obtained from standard curve)

S_V is sample volume used for the assay

Acety-CoA molecular weight (809.6 g/mole).

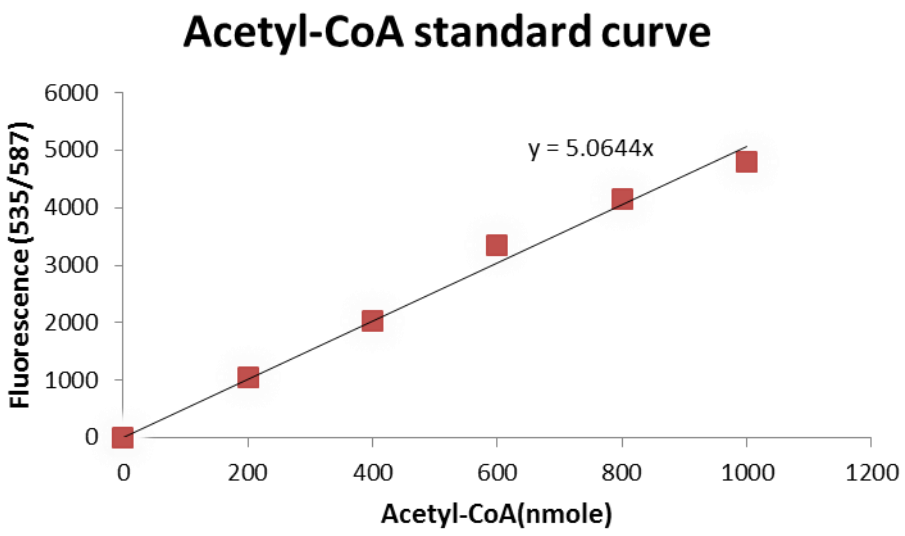

Figure 2.1 Acetyl-CoA standard curve.

2.14 Propidium iodide staining and flow cytometry analysis

10ml of culture was harvested and cellular viability was determined using propidium iodide-Flow cytometry method (PI–FCM) (Ocampo & Barrientos, 2011). Propidium iodide is a membrane non-permeable substance; it does not get incorporated into healthy living cells. Harvested cells were suspended in 10 ml phosphate-buffered saline (PBS) at 10^6 cell/ml and were incubated for 30 min at 30^{o}C in the presence of 2 mM PI (Molecular Probes, USA) (Ocampo & Barrientos, 2011). Flow cytometry analysis was performed on a Becton Dickinson (BD) LSRFortessaTM cell analyser. Excitation was performed using a yellow/green laser at 561 nm; emission was detected using a 20 nm bandpass filter centered at 660 nm (Becton Dickinson, NJ, USA). Triplicate samples of ten thousand cells for each yeast population were analysed.

2.15 Semi-anaerobic Fermentation

Yeast cells were grown (30^{o}C 180 rpm) in 5 ml YPD (in 20 ml Universal tube) for about 48 hr to final OD_{600} unit of 2.5 - 3.5. 45 ml of freshly prepared YPD was dispensed into 50 ml glass bottles which were sealed with rubber and metal capping and then autoclaved. The sealed bottles were inoculated with the yeast pre-cultures to a starting OD_{600} of 0.1 (using sterile needle and syringe) and incubated for 18 days at 30^{o}C. Aliquots were taken from the culture at periodic day intervals to measure cell density and alcohol production. 2.5 ml aliquot was taken using sterile needle (0.8 mm X 40 mm) and syringe; part of it was filtered through a 0.22µm syringe filter (Merck Millipore) into 2 ml glass bottles (which were sealed and stored at -20^{o}C until analysed

on the GC-FID for alcohol quantification) while cell density at OD_{600} was measured with the remaining.

2.16 Alcohol quantification using GC-FID

The ethanol and butanol in the prepared samples were detected with a GC-FID (gas chromatograph flame ionisation detector) machine (Agilent Technologies) using a DB-WAX capillary column (30 m, 0.25 mm (internal diameter), 0.250 µm film thickness) (Agilent Technologies). Samples (0.6 µl aliquots) were injected in the split mode (split ration 6:1) with oven temperature set at 230 °C using helium as a carrier gas at a flow rate of 20 ml/min. The column temperature was maintained isothermally at 40 °C for 1 min, raised to 140 °C (15 °C/min), then raised to 220 °C (50°C/min) and maintained isothermally for 10 min. The FID temperature is set at 250^{o}C, hydrogen (H_2) flow rate 30.0 ml/min and air flow rate 300 ml/min. Standard solution containing; 1% v/v ethanol, 100 ppm v/v isobuanol, 100 ppm v/v n-butanol, 1% glycerol, and 1% acetaldehyde was prepared with pure deionized water (ddH_2O) and was used as reference for the calibration of alcohol concentrations in the sample. The standard and samples were run on the GC-FID and data was calibrated using the Chemstation® data analyse software. The concentrations of alcohol in the samples were calculated as; area of sample per area of standard, multiplied by concentration of standard. The mean and standard deviation values from five biological repeats were considered.

Table 2.2 Details of restriction enzymes used in this study

Enzyme	Optimal temperature	Reaction time	BSA
*BamH*I	37°C	60 min	yes
*Mnl*I	37°C	60 min	yes
XhoI	37°C	60 min	yes

Table 2.3 Details of oligonucleotides used in this study.

Primer	Purpose	Sequence 5' to 3'	Reference
DREG1F	Deletion of *REG1* gene	ATAATATCCTTGAAGATTATAAATCCTAAAGCA AGCATATTGACGAAGACGAGATAAGAAAAATC CAAAACGTACGCTGCAGGTCGAC	This study
DREG1R	Deletion of *REG1* gene	TAAAGACGGCACTGATCCACACTACCTGGATTT TTATTTTCTCTTCATGTTGACTTCAAAATTCTTTC TTCACTATAGGGAGACCGGCAG	This study
VREG1 F	Verification of *REG1* upstream site	CACCACCTCCTGAAAGAGAAC	This study
VREG1R	Verification of *REG1* downstream site	CGACTATGGAAGCTCAAGAAG	This study
VNATint.F	Verification of *natNT2* internal site	GGTCAGGTTGCTTTCTCAGG	This study
VNATint.R	Verification of *natNT2* internal site	GTACGAGACGACCACGAA	This study
DSNF1F	Deletion of *SNF1* gene	TAATCATAGCGAAAGAAATAGAAGTTTTTTTTT GTAACAAGTTTTGCTACACTCCCTTAATAAAGT CAACCGTACGCTGCAGGTCGAC	This study
DSNF1R	Deletion of *SNF1* gene	AAGATGTTGCAAATACGTTACGATACATAAAAA AAAGGGAACTTCCATATCATTCTTTTACGTTCCA CCACACTATAGGGAGACCGGCAG	This study
VSNF1F	Verification of *SNF1* upstream site	GTACTGTAGGCTTGTTACCAG	This study

Primer	Purpose	Sequence 5' to 3'	Reference
VSNF1R	Verification of *SNF1* downstream site	GCCACTAGTAGTACTCATCTC	This study
DMLS1F	Deletion of *MLS1* gene	AGTACCTAAGAATAACGACTATTGTTTTGAACT AAACAAAGTAGTAAAAGCACATAAAAGAATTA AGAAACGTACGCTGCAGGTCGAC	This study
DMLS1R	Deletion of *MLS1* gene	GGATTCCGATACATAATCATATAGGCATGAATA TATTTTTATATATGTGTACACTGGGGCAAGGGA GACACTATAGGGAGACCGGCAG	This study
VMLS1F	Verification of *MLS1* upstream site	GCGAAGGA TCGATGACCC TT	This study
VMLS1R	Verification of *MLS1* downstream site	CAA TGGTTGATGC CTTCGCCG	This study
DCIT2F	Deletion of *CIT2* gene	GAACAATATCAACACATATCATAACAGGTTCTC AAAACTTTTTGTTTTAATAATACTAGTAACAAG AAAACGTACGCTGCAGGTCGAC	This study
DCIT2R	Deletion of *CIT2* gene	TAAATAAGTGCTAAATACTAAATGGTCATGAG GAAAGAAAAATATGCAGAGGGGTGTAAAAGT AGGATGTAATCCAACACTATAGGGAGACCGGC AG	This study
VCIT2F	Verification of *CIT2* upstream site	GTAGCTAGACGTCTATCAGG	This study
VCIT2R	Verification of *CIT2* downstream site	GTTATCGCGTGATAGCTTCCGC	This study
VCHX XIV F	Verification of chromosome XIV upstream (727312)	GATTAATCTGATATCAAGTTA	This study
VCHX XIV R	Verification of chromosome XIV downstream (727705)	GGATAAATGAGATGCTACCCT	This study
thiolase-F	Amplification of thiolase integration cassettes from pYM30(thiolase) vector	TCTTGGTTATGCGTTATTTAAATCCTCATCTGCC GCTGCTTAAAAAAAGCAGCTAAAGTGTTGCGT AGGCA	This study
thiolase-R	Amplification of thiolase integration cassettes from pYM30(thiolase) vector	GAAAGAATTAAATATTCACTAGGCTGCGATAC GATAGACAAACGAAGTGATTGAAACCCGAATT AACGGA ATCGATGAATTCGAGCTCGTT	This study
VthlA F	Internal verification of *thlA* thiolase downstream	GAACTAGGTGTTAAACCCTTGGCCAAAATT GTTTCATATGGTTCTGC	This study
VthlA R	Internal verification of *thlA* upstream	AGCTGGATTTTGACCTAAACCTGCTTGCAG AACATTTCCCAGAAT	This study

Primer	Purpose	Sequence 5' to 3'	Reference
VphaA F	Internal verification of *phaA* downstream	CGT AGA GGA ATC CAA CCG CTA GGC AGG ATT GTA TCA TGG GCT ACT GTA GGA GTT GAT CCT AAG	This study
VphaA R	Internal verification of *phaA* upstream	AGG ATT TTG ACC TTC GCC GGC GGG CAG CAC TTG CCC TAG AAT GAC	This study
GCD1F	Amplification of *GCD1*	TGCTGACCAAAAG	Mark Ashe
GCD1R	Amplification of *GCD1*	AGCATTCAAGTT	Mark Ashe
QtoV F	Site mutagenesis Q(Gln) to V(Val)	CT TCT TTT AAA GCA GGA TTG CCA **GTA** GAG ATA CCC GCT ATG ACG ATT	This study
QtoV R	Site mutagenesis Q(Gln) to V(Val)	AAT CGT CAT AGC GGG TAT CTC TAC TGG CAA TCC TGC TTT AAA AGA AG	This study
YtoN F	Site mutagenesis Y(Tyr) to N(Asn)	GAT GGT CTA TGG GAT GCA TTC **AAT** GAC TAC CAT ATG GGT ATT ACA G	This study
YtoN R	Site mutagenesis Y(Tyr) to N(Asn)	CTG TAA TAC CCA TAT GGT AGT CAT TGA ATG CAT CCC ATA GAC CAT C	This study
KtoA F	Site mutagenesis K(Lys) to A(Ala)	T TCT GCT GGG GTC GAC CCT **GCA** ATC ATG GGT TAC GGG CCT TT	This study
KtoA F	Site mutagenesis K(Lys) to A(Ala)	GAA AGG CCC GTA ACC CAT GAT TGC AGG GTC GAC CCC AGC AGA A	This study
RtoG F	Site mutagenesis R(Arg) to G(Gly)	AAC AAT GCT AGA TGG GGC TAC **GGT** ATG GGT AAC GCC AAA TTC GTT G	This study
RtoG R	Site mutagenesis R(Arg) to G(Gly)	CAA CGA ATT TGG CGT TAC CCA TAC CGT AGC CCC ATC TAG CAT TGT T	This study
HtoN F	Site mutagenesis H(His) to N(Asn)	A TGG GAT GCA TTC AAT GAC TAC **AAT** ATG GGT ATT ACA GCC GAG AAT	This study
HtoN R	Site mutagenesis H(His) to N(Asn)	ATT CTC GGC TGT AAT ACC CAT ATT GTA GTC ATT GAA TGC ATC CCA T	This study
GtoV F	Site mutagenesis G(Gly) to V(Val)	ACG GAT GAG CAT CCT AGA TTT **GTA** TCC ACC ATC GAA GGA TTG GC	This study
GtoV R	Site mutagenesis G(Gly) to V(Val)	GCC AAT CCT TCG ATG GTG GAT ACA AAT CTA GGA TGC TCA TCC GT	This study
phaASeq1	DNA sequencing of *phaA* gene	GTC ATT CTA GGG CAA GTG CTG CCC GCC GGC GAA GGT CAA AAT CCT	This study
phaASeq2	DNA sequencing of *phaA* gene	CGT AGA GGA ATC CAA CCG CTA GGC AGG ATT GTA TCA TGG GCT ACT GTA GGA GTT GAT CCT AAG	This study

Primer	Purpose	Sequence 5' to 3'	Reference
thlASeq1	DNA sequencing of *thlA* gene	CAACCTCAATGGAGTGATGCAACCTGCCTGGA GTAAATGATGAC	This study
thlASeq2	DNA sequencing of *thlA* gene	ATT CTG GGA AAT GTT CTG CAA GCA GGT TTA GGT CAA AAT CCA GCT	This study
thlASeq3	DNA sequencing of *thlA* gene	GAA CTA GGT GTT AAA CCC TTG GCC AAA ATT GTT TCA TAT GGT TCT GC	This study

Table 2.4 Details of *S. cerevisiae* strains used in this study

Strain	Abbreviation	Genotype	Reference
yMK23	W303-1A	MATa ade2-1 his3-11,15 leu2-3,112 trp1-1 ura3-1 can1-100 GCD1-P180	Mark Ashe
yMK2076	5g	Derived from yMK23 CHRXVI881267:TDH3p-HBD-flag2-LEU2 CHRXVI776494:TDH3p-ADHE2-flag2-URA3 CHRXIV727312:TDH3p-ERG10-flag2-KanMX4 CHRXIII481412:TDH3p-CCR-flag2-HIS3 CHRVIII529857:TDH3p-CRT-flag2-TRP1	Mark Ashe
yMK2235	*adh1*Δ	MATa adh1::ADE2 ade2-1 his3-11,15 leu2-3,112 trp1-1 ura3-1 can1-100 GCD1-P180	Mark Ashe
yMK2227	BPS	Derived from yMK2076 adh1:ADE2 ALD6 ACS2-Hygromicine	Mark Ashe
yMK2266	W303-1A *reg1*Δ	Derived from yMK23 reg1:: loxP-natNT2-loxP	This study
yMK2267	5g *reg1*Δ	Derived from yMK2076 reg1: loxP-natNT2-loxP	This study
yMK2268	adh1Δ reg1Δ	Derived from yMK2235 reg1:: loxP-natNT2-loxP	This study
yMK2269	BPS *reg1*Δ	Derived from yMK2227	This study

Strain	Abbreviation	Genotype	Reference
		reg1:: loxP-natNT2-loxP	
yMK2779	W303-1A snf1Δ	Derived from yMK23 snf1:: loxP-natNT2-loxP	This study
yMK2780	5g *snf1Δ*	Derived from yMK2076 snf1:: loxP-natNT2-loxP	This study
yMK2781	*adh1Δ snf1Δ*	Derived from yMK2235 snf1:: loxP-natNT2-loxP	This study
yMK2782	BPS *snf1Δ*	Derived from yMK2227 snf1:: loxP-natNT2-loxP	This study
yMK3024	W303-1A *mls1Δ*	Derived from yMK23 mls1:: loxP-natNT2-loxP	This study
yMK3025	5g *mls1Δ*	Derived from yMK2076 mls1::natNT2	This study
yMK3026	*adh1Δ mls1Δ*	Derived from yMK2235 mls1:: loxP-natNT2-loxP	This study
yMK3027	BPS *mls1Δ*	Derived from yMK2227 mls1:: loxP-natNT2-loxP	This study
yMK3028	W303-1A *cit2Δ*	Derived from yMK23 cit2:: loxP-natNT2-loxP	This study
yMK3029	5g *cit2Δ*	Derived from yMK2076 cit2:: loxP-natNT2-loxP	This study
yMK3030	*adh1Δ cit2Δ*	Derived from yMK2235 cit2:: loxP-natNT2-loxP	This study
yMK3031	BPS *cit2Δ*	Derived from yMK2227 cit2::loxP-natNT2-loxP	This study
yMK3032	W303-1A *cit2Δ natNT2Δ*	Derived from W303-1A cit2Δ cit2Δ::loxP	This study

Strain	Abbreviation	Genotype	Reference
yMK3033	5g *cit2Δ natNT2Δ*	Derived from 5g cit2Δ cit2Δ::loxP	This study
yMK3034	*adh1Δ cit2Δ natNT2Δ*	Derived from adh1Δ cit2Δ cit2Δ::loxP	This study
yMK3035	BPS *cit2Δ natNT2Δ*	Derived from BPS cit2Δ cit2Δ::loxP	This study
yMK3036	W303-1A *mls1Δ cit2Δ*	Derived from W303-1A mls1Δ cit2::loxP-natNT2-loxP	This study
yMK3037	5g *mls1Δ cit2Δ*	Derived from 5g mls1Δ cit2::loxP-natNT2-loxP	This study
yMK3038	*adh1Δ mls1Δ cit2Δ*	Derived from adh1Δ mls1Δ cit2::loxP-natNT2-loxP	This study
yMK3039	BPS *mls1Δ cit2Δ*	Derived from BPS mls1Δ cit2::loxP-natNT2-loxP	This study
yMK2759	BPS*	Derived from BPS (TDH3p-ERG10-flag2-KanMX4)Δ	Mark Ashe collection
yMK3040	BPS* *thlA*	Derived from BPS* CHRXIV727312:TDH3p-thlA-myc-KanMX4	This study
yMK3048	BPS* $thlA^{red}$	Derived from BPS* CHRXIV727312:TDH3p-$thlA^{red}$-myc-KanMX4	This study
yMK3049	BPS* $thlA^{CoA}$	Derived from BPS* CHRXIV727312:TDH3p-$thlA^{CoA}$-myc-KanMX4	This study
yMK3050	BPS* *phaA*	Derived from BPS* CHRXIV727312:TDH3p-phaA-myc-KanMX4	This study

Table 2.5 Details of plasmids used in this study

Plasmid	Main features	Bacteria source	Reference
pZC2	*loxp-natNT2-loxp*	BMK757	(Carter & Delneri, 2010)
pYM30	pAgTEF-*KanMX*-tAgTEF	BMK585	Mark Ashe
pYM30-thlA	thlA gene module upstream of KanMX cassette	BMK865	This study
pYM30-thlA^{red}	thlA^{red} gene module upstream of KanMX cassette	BMK866	This study
pYM30-thlA^{CoA}	thlA^{CoA} gene module upstream of KanMX cassette	BMK867	This study
pYM30-phaA	phaA gene module upstream of KanMX cassette	BMK868	This study
pSH-Cre-*ble^{r}*	Cre recombinase enzyme BMK721	BMK721	Mark Ashe
pMK-phaA	phaA thiolase gene module	BMK869	This study
pGEMT ®Easy	3' thymine (T) overhangs. T7 and SP6 RNA polymerase promoters flanking a multiple cloning region within lacZ coding region	N/A	Promega®
pG-thlA^{red}	thlA^{red} gene module subcloned in pGEMT® Easy	BMK870	This study
pG-thlA	Derived from pG-thlA^{red} via site-directed mutagenesis (3 x nucleotide substitution)	BMK871	This study
pG-thlA^{CoA}	Derived from pG-thlA via site-directed mutagenesis (3 x nucleotide substitution)	BMK872	This study

3. Modulation of the glucose repression pathway in yeast (*Saccharomyces Cerevisiae*) with a view to improving butanol production.

3.1 Introduction

In this chapter, two key deletions were made in the glucose repression pathway (Fig 3.1) to establish whether alterations of the glucose repression pathway will result in recalibration of metabolic resources and increase the level of butanol that yeast produce. The starting aim was to delete the *REG1* gene and to study whether in the butanol production strain of *S. cerevisae* this deletion would optimise the use of all glucose repressed genes, direct metabolic resources to increase butanol production, improve butanol tolerance and possibly expand the portfolio of carbon sources that the yeast will be capable of growing on. Follow on from the deletion of *REG1* gene, *SNF1* gene was deleted to provide a control for the *REG1* deletion and as a strategy to cause the strain to utilise the reductive heterogenous butanol synthesis pathway route for redox balance in the absence of mitochondrial resources under *ADH1* gene deletion.

In *S. cerevisiae*, the Snf1p protein kinase is required for transcription of glucose-repressed genes in response to glucose limitation when the concentration of glucose drops below 0.2% (Carlson, 1999; Dombek *et al*, 1999; Hedbacker & Carlson, 2008); this enables yeast to switch metabolism to utilise alternate carbon sources that are less preferred than glucose (Kim *et al*, 2013; Rolland *et al*, 2002b). Snf1p also positively regulates the induction of gluconeogenesis and play roles in nutrient and

environmental stress responses (Busti *et al*, 2010; Celenza & Carlson, 1986; Hedbacker & Carlson, 2008; Jiang & Carlson, 1996; Kuchin *et al*, 2003).

During growth on glucose, Reg1p inhibits Snf1p kinase activity therefore acting in antagonism to Snf1p protein kinase in the glucose repression pathway (De Vit *et al*, 1997; Dombek *et al*, 1999; Mark & Marian, 1992; Sanz *et al*, 2000; Tu & Carlson, 1995).

The initial aim can be broken down into a number of discrete goals

- Singly deletions of *REG1* and *SNF1* genes in appropriate butanol production and control strains
- Validation of each mutation genotypically, phenotypically and physiologically
- Evaluation of butanol production in the resulting strains,
- Interpret the data and design follow on strategies

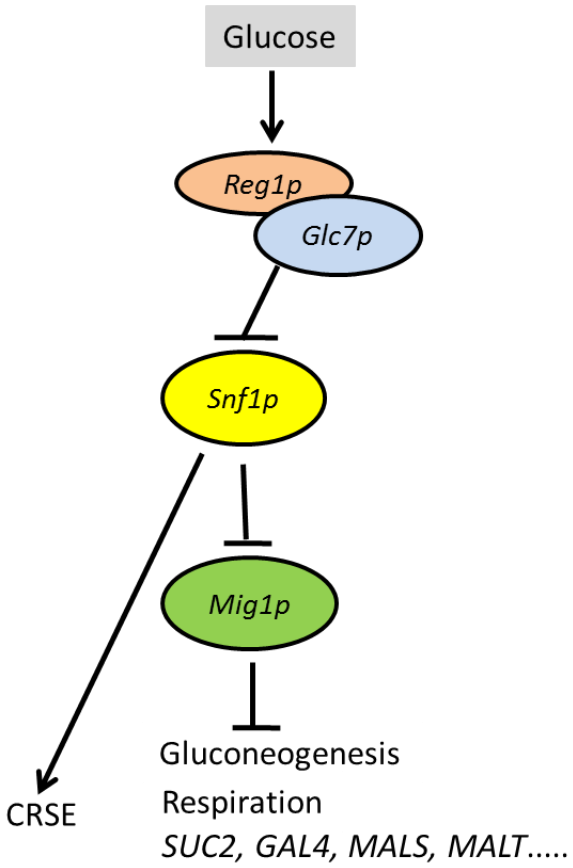

Figure 3.1 Summary of the glucose repression pathway in yeast.

Figure shows the central component of yeast's glucose repression pathway; Reg1p/Glc7p, Snf1p and Mig1p. Arrows represent activation while blunt ended lines signify inhibition. CRSE, SUC2, GAL4, MALS and MALT are acronyms for carbon source responsive promoter (Ashe *et al*, 2000; Rolland *et al*, 2002b).

3.2 Validation of starting strains

It was important to validate our starting strains before proceeding with further experimentation:

1. The butanol production strain (BPS): yMK2227 (adh1Δ.ACS2 ALD6 + 5g); this strain has *ADH1* deleted, *ACS2* and *ALD6* overexpressed and the five genes (5g) of the ABE-butanol pathway incorporated in its genome.

2. Control strains: the following three yeast strains were selected as control strains

- W303-1A (yMK23): This is the wild type parent lab strain.
- 5g (yMK2076): This strain has the five genes of the ABE pathway incorporated in the genome
- *adh1Δ* (yMK2235): This strain has *ADH1* gene deleted

3.2.1 Confirmation of *GCD1-P180* genotype in the starting strains

The four starting strains used in this study are derived from a butanol resistant (ButR) background strain carrying a point mutation within the *GCD1* locus (which encodes the ϒ subunit of the eIF2B) (translation initiation factor) (Ashe *et al*, 2001). The ButR strain contains *GCD1-P180,* as opposed to *GCD1-S180* in the butanol sensitive strain (*ButS*) (Ashe *et al*, 2001). PCR amplification of genomic DNA using a pair of *GCD1*-specific primers generates a 1200 bp product which gives different *Mnl*I restriction patterns for the ButR and ButS *GCD1* alleles respectively. The *GCD1*

fragment was amplified by PCR from the four starting parent strains to confirm their ButR status. The PCR product obtained was digested with the *Mnl*I restriction enzyme, before separation by electrophoresis through a 1% agarose gel. The restriction digest pattern obtained for the four strains have a distinctive ~400bp fragment, which is indicative of ButR allele relative to the ~550bp fragment for ButS allele (Fig 3.2).

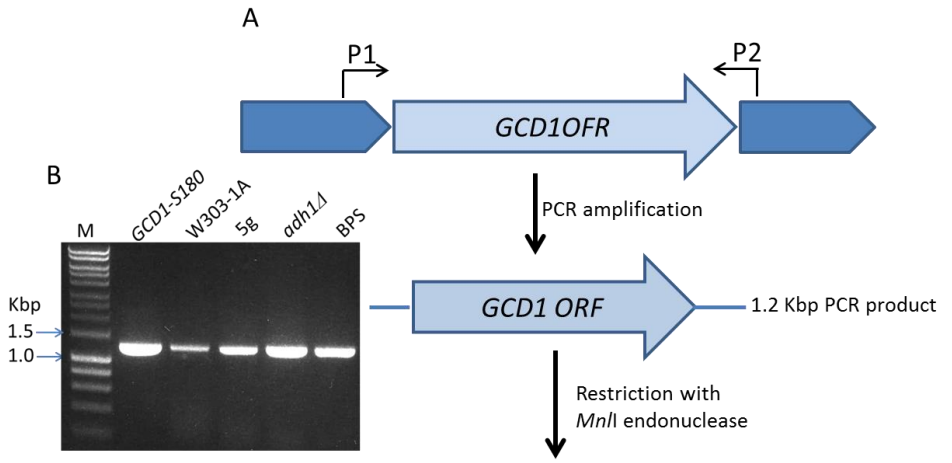

C

GCD1-S180	***GCD1-P180***
66	66
-	164
175	175
191	191
199	199
-	**391**
555	-

Expected restriction pattern for *GCD1-S180* and *GCD1-P180*.

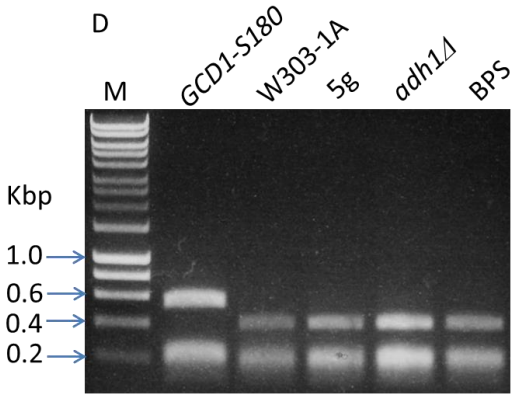

Figure 3.2 Verification of GCD1 allele in strains.

Figure shows; (A) strategy for the PCR amplification of *GCD1* fragment from genomic DNA using primers that surround the *GCD1* locus. (B) Image of agarose gel showing the size of the *GCD1* PCR product after electrophoresis. C) Table of expected *Mnl*I digestion fragments for the *GCD1-S180* and *GCD1-P180* alleles respective. (D) Image of agarose gel showing sizes of the M*nl*I digestion fragments of the *GCD1* PCR products after electrophoresis.

3.2.2 Analysis of phenotypic markers

To validate the various phenotypic markers for the four strains, the strains were grown on selection SC minimal media bearing appropriate markers for the selection of their respective genotype. The presence of integrated *ACS2 ALD6* and *ERG10* was verified by growth on hygromycin B and G418 sulphate, respectively, while *CCR, CRT, HBD, ADHE2* and *adh1Δ* phenotypes were verified by growth on minimal media lacking amino acids: his (histidine), trp (tryptophan), leu (leucine) and nucleobases ura (uracil) and ade (adenine) respectively in the growth media. The result confirmed that the strains were all of the expected genotype; the 5g and BPS strains grow on the 5g selection media, the *adh1Δ* and BPS strains grow on the *adh1Δ* selection media, and only the BPS strain grow on the BPS selection media (Fig 3.3).

A

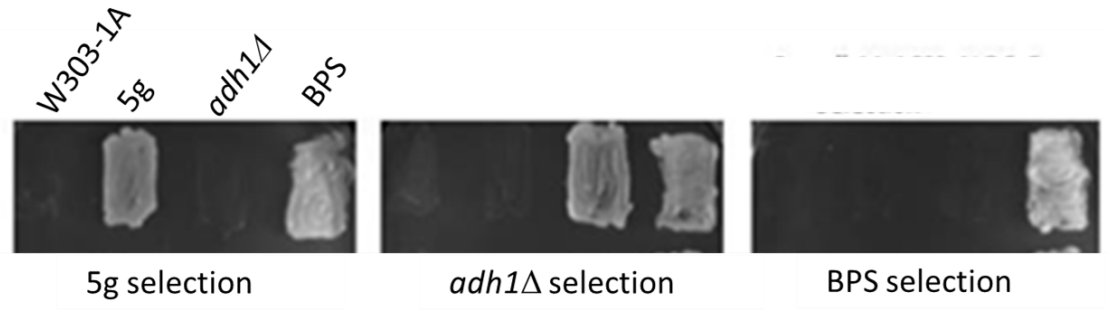

B

Strains	Genotypic markers	Selection media
W303-1A	*ade2-1 his3-11,15 leu2-3,112 trp1-1 ura3-1*	SCD complete media supplemented with five amino acids (**ade, his, leu, trp, and ura**)
5g	Derived from W303-1A *CHRXVI881267:TDH3p-HBD-flag2-**LEU2*** *CHRXVI776494:TDH3p-ADHE2-flag2-**URA3*** *CHRXIV727312:TDH3p-ERG10-flag2-**KanMX4*** *CHRXIII481412:TDH3p-CCR-flag2-**HIS3*** *CHRVIII529857:TDH3p-CRT-flag2-**TRP1***	SD minimal media supplemented with **ade** amino acid and **G418 sulphate**
adh1Δ	Derived from W303-1A ***adh1::ADE2***	SD minimal media supplemented with four amino acids (**his, leu, ura and trp**)
BPS	Derived from 5g ***adh1:ADE2*** ***ALD6 ACS2-Hygromicine***	SD minimal media supplanted with **G418 and Hygromycine B**

Figure 3.3 Verification of phenotypic markers in the four starting strains

Figure shows; (A) Photographic images of 5g, *adh1Δ* and BPS selection medium showing growth of the four strains. B) Table of the genotypic markers for each strain and the corresponding selection media.

3.3 Construction of *reg1*Δ and *snf1*Δ mutant strains.

3.3.1 Amplification of deletion cassettes by PCR

The *reg1::natNT2* and *snf1::natNT2* deletions were individually constructed in all four strains according to the strategy outlined in Fig 3.4A. Firstly, gene-deletion cassettes were amplified by PCR from the plasmid pZC2 using gene-specific primers (either for *reg1Δ* or *snf1Δ*). The plasmid pZC2 contains a nourseothricin sulphate (cloNat) resistance gene (*natNT2*) surrounded by *loxP* sequences, which after genomic integration allow removal of the marker with *Cre* recombinase where necessary (Carter & Delneri, 2010). The success of the PCR amplifications was verified by electrophoresis on a 1% agarose gel as described in the Materials and Methods. The size of DNA band obtained for each cassette matched the calculated size of the respective *REG1*-deletion cassette (1760 bp) and *SNF1*-deletion cassette (1760 bp) (Fig 3.4B).

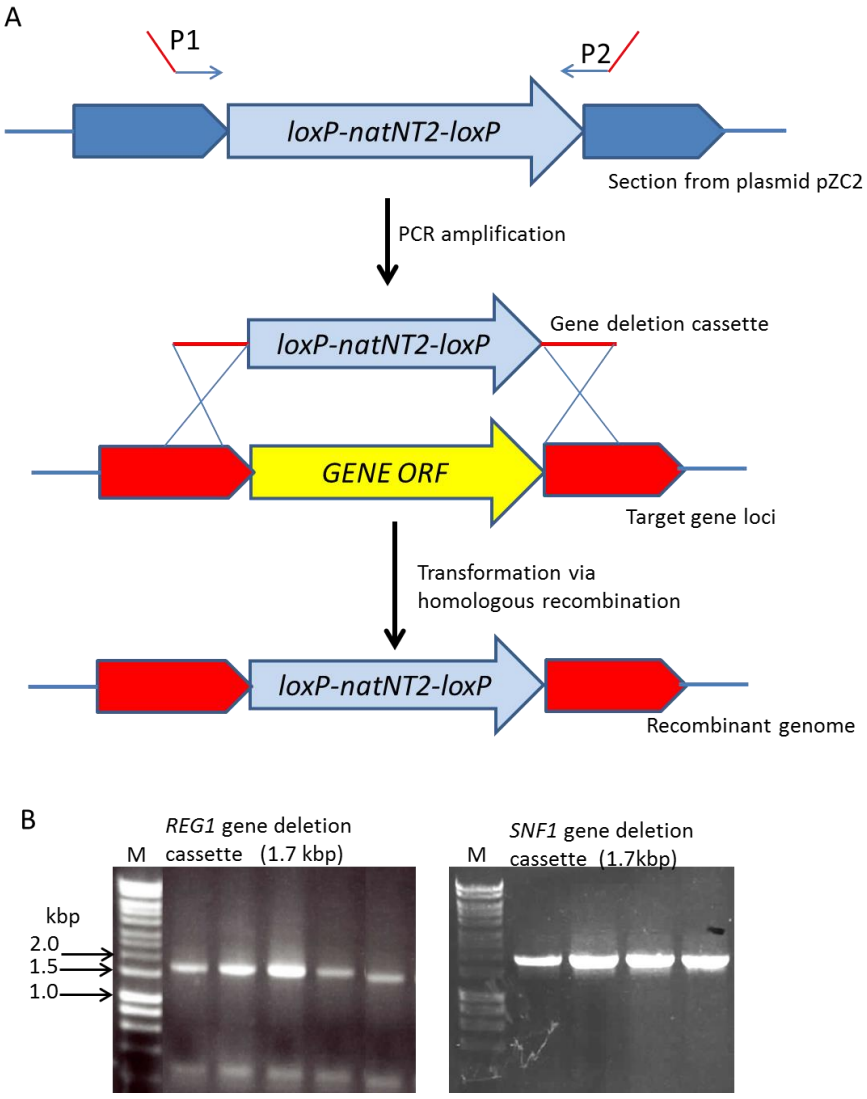

Figure 3.4 Strategy for yeast gene deletion using loxP-natNT2-loxP cassette.

(A) PCR based strategy for the amplification of *loxP-natNT2-loxP* gene deletion cassette from plasmid pZC2 using gene specific primers (P1 and P2). (B) Image of agarose gels showing bands corresponding to the expected sizes of the *REG1* and *SNF1* gene deletion cassettes after their separation by electrophoresis. Lanes on the gels represents the PCR products for each deletion cassette.

3.3.2 Targeted gene deletion and verification

Targeted deletion of the *REG1* and *SNF1* genomic loci was performed with each respective deletion cassette using the Lithium acetate high efficiency transformation protocol (Gietz & Woods, 2002). Nourseothricin (cloNat) resistant transformants were selected on 100 μg/ml cloNat plates. Validation of the successful deletion of either the *REG1 or SNF1* genomic locus in the four yeast strains was confirmed by PCR analysis on genomic DNA prepared from potential transformants. Three sets of PCR amplifications were conducted (amplification of regions that are upstream, downstream and across the *REG1* or *SNF1* loci) using primers specific for each verification site (Fig 3.5A). The sizes of these PCR products were verified by gel electrophoresis and they matched the calculated expected sizes (Fig 3.5B). Therefore, at the genomic level it would appear that the *REG1* and *SNF1* genes have been successfully deleted.

A

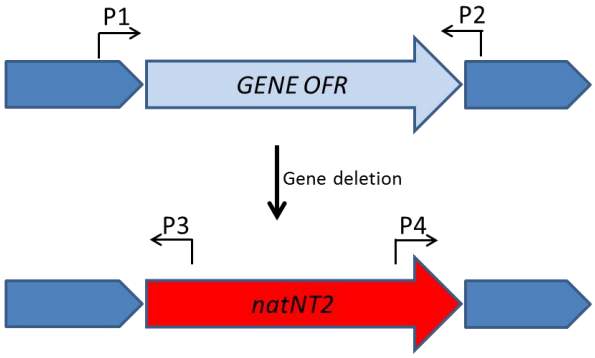

Verification PCR amplification reactions

	Primer sets	Expected product sizes (Kbp)			
		REG1	*reg1Δ*	*SNF1*	*snf1Δ*
1.	P1/P2 =	3.0	2.0	2.4	2.0
2.	P1/P3 =	Nil	1.0	Nil	1.0
3.	P4/P2 =	Nil	0.5	Nil	0.5

B

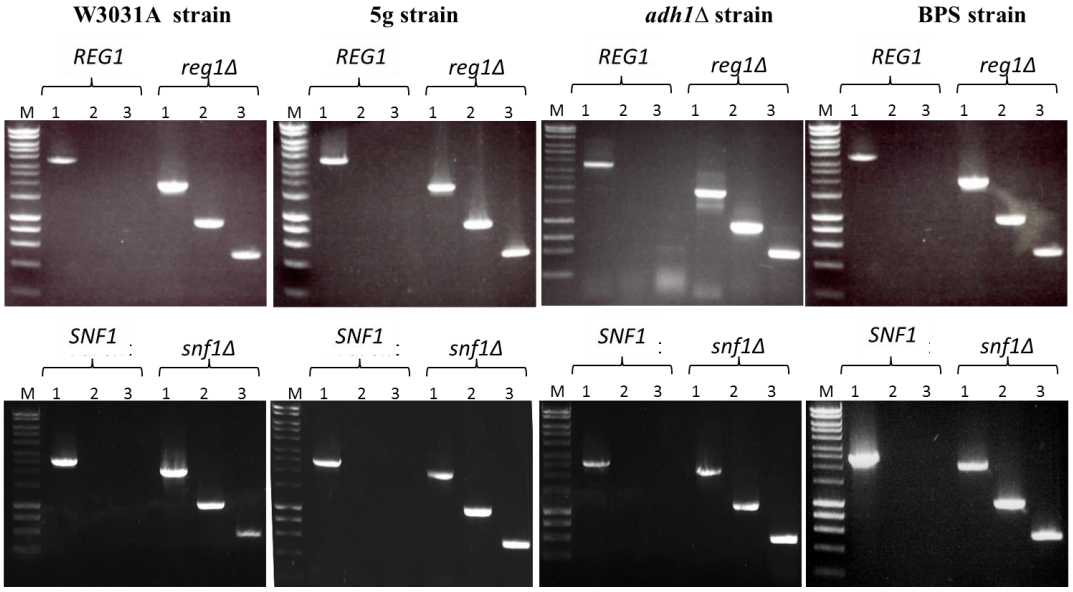

Figure 3.5 Verification of the reg1Δ and snf1Δ deletions by PCR amplification.

Figure shows: (A) PCR verification strategy using primers that surround the *REG1* or *SNF1* loci and within the *natNT2* gene respectively. (B) Table of verification PCR reactions and the expected product sizes (c) Image of agarose gels showing the size of the various verification PCR products in the four strains.

3.4 Validation and phenotypic characterisation of *reg1Δ* strains

To validate the *reg1::natNT2* strains phenotypically, the strains were first grown on cloNat containing media as the *natNT2* gene should confer resistance to cloNat (nourseothricin sulfate) (Fig 3.6). Secondly, a strategy was used to validate that in the *reg1Δ* strains, glucose repressed genes such as SUC2 is constitutively derepressed. The *SUC2* gene encoding the invertase enzyme needed for sucrose metabolism is glucose repressed and this repression is mimicked by 2-deoxyglucose (a non-metabolisable analogue of glucose). In the presence of 2-deoxyglucose, wild-type *REG1* strains cannot express invertase for sucrose utilization, therefore, wild type strains will not grow on media with sucrose as the carbon source in the presence of 2-deoxyglucose (YPS-2DG media) (Fig 3.6). However, deletion of *REG1* subverts the glucose repression pathway enabling *reg1Δ* mutants to constitutively express invertase and metabolise sucrose even in the presence of 2-deoxyglucose. The results (Fig 3.6) confirm that the strains phenotypically reproduce the expected results for *REG1* deletion mutants and combined with the genotyping results, they provide strong evidence that deletion of *REG1* has been successful in all cases.

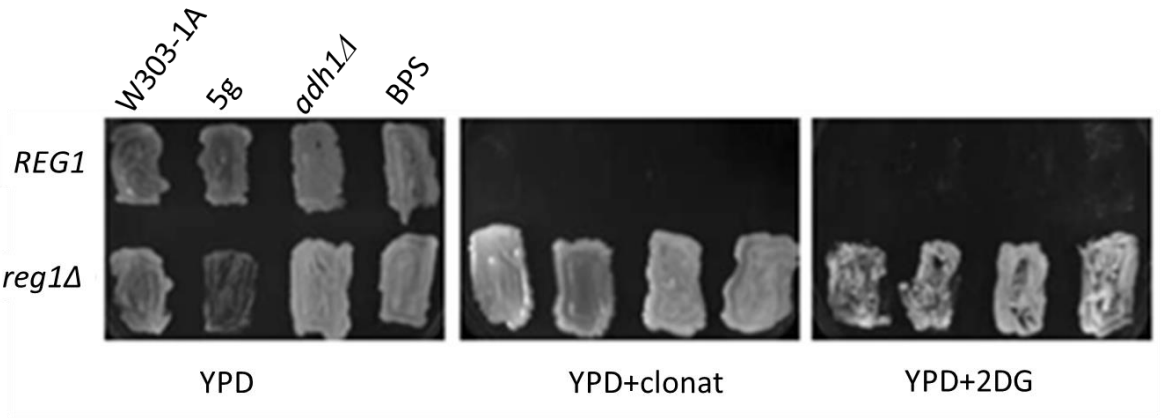

Figure 3.6 Phenotypic verification of reg1Δ strains.

Photographic images of YPD, YPD+cloNat and YPD+2DG growth media respectively showing the growth of *REG1* parent strains and their corresponding *reg1Δ* mutants.

3.5 Validation and phenotypic characterisation of *snf1Δ* strains

To validate *snf1Δ* strains phenotypically, strains are generally grown on sucrose as the sole carbon source. The *snf1Δ* phenotype was originally identified as a sucrose non-fermenting phenotype. So a wild type (*SNF1*) strain can utilise sucrose under fermentative conditions because when glucose is limiting Snf1p kinase leads to derepression of genes for sucrose utilisation. The deletion of *SNF1* means that the genes for sucrose utilisation are constitutively repressed and so the strain should be incapable of growth on sucrose. In practice under aerobic conditions, mitochondrial respiration allows some growth in *snf1Δ* strains on sucrose. Therefore, it is common practice to include antimycin A in the media to prevent mitochondrial respiration. Overall, wild type SNF1 strains should grow on sucrose media with antimycin A, whereas *snf1Δ* strains should not (Momcilovic *et al*, 2006). The four genotypically verified *snf1Δ* strain constructs were tested using this strategy (Fig 3.7), and all four grew on rich media but not on YPS+antimycin A media. This result shows that the *snf1Δ* strains exhibited phenotypes consistent with the deletion of *SNF1*.

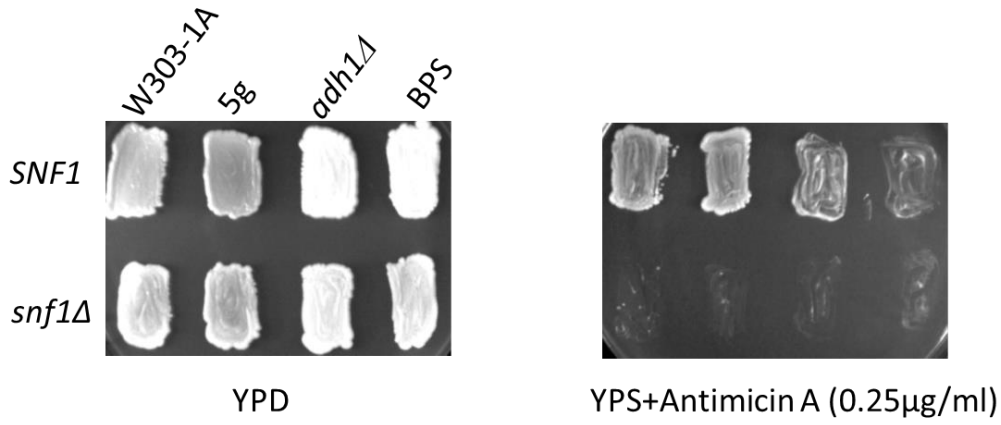

Figure 3.7 Phenotypic verification of *snf1Δ* on antimycin A.

Photographic images of YPD and YPS+antimycin media showing the growth of *SNF1* strains and their corresponding *snf1Δ* mutant strains.

3.6 Expression and Immunoblotting of FLAG-Tagged Proteins

Because both the *REG1* and *SNF1* genes are involved in the regulation of gene expression, it is important to test whether their deletions affect the expression of any of the heterologous ABE pathway genes. All the ABE pathway genes as well as the overexpressed *ALD6* and *ACS2* genes carry C-terminal Flag epitope tags. Therefore, to determine if the deletion of *REG1* or *SNF1* has any impact on the expression of these genes; immunological detection by western blotting using anti-Flag antibodies was conducted The result of the western blot analysis shows that all the seven heterologous genes (*ACS2 ALD6, ERG10, CCR, CRT, HBD and ADHE2*) were similarly expressed in the parents and mutant (*reg1Δ and snf1Δ)* constructs (Fig 3.8).

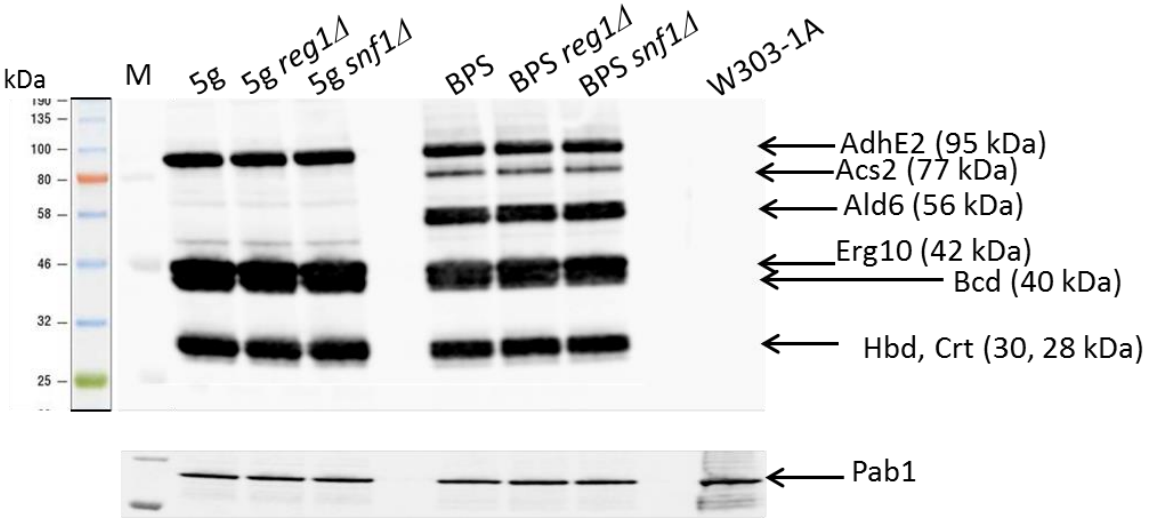

Figure 3.8 Immuno-detection of FLAG-tagged proteins.

Figure shows the image of nitrocellulose paper blot probed with anti-flag antibodies. The bands corresponding to the sizes of Flag-tagged proteins in the 5g and BPS strains and their corresponding *reg1Δ* and *snf1Δ* mutants are labeled. The size of each protein is written and a protein marker label is added. Pab1 protein is used as a loading control.

3.7 Analysis of translational activity in reg1Δ mutants

It has previously been shown that *reg1Δ* strains are resistant to the inhibition of translation initiation caused by glucose depletion (Ashe *et al*, 2000). Therefore, translational activity was examined in the *reg1Δ* mutant strains using polysome analysis. Polysomes are actively translating ribosomes and can be separated and characterised using sucrose density gradients. Cells were grown in YPD media and then washed for 10 min in YP (lacking glucose) after which ribosomal extracts were separated by sedimentation in sucrose gradients. Normally, in wild-type strains growing 'happily' under glucose abundance, there is normal distribution of polysomes on multiple ribosomes (Fig 3.9A). However, when the cells are growing under glucose restriction, translation becomes inhibited and there is redistribution of polysomes into a single ribosomal peak (Fig 3.9B). In the *REG1* parent strains, glucose depletion caused a redistribution of polysomes into a single ribosomal 80S peak, indicative of inhibition of translation initiation (Fig 3.10). However, the *reg1Δ* strains were unaffected by glucose removal and had a normal ribosomal distribution profile following glucose starvation (Fig 3.10). The result indicates that *reg1Δ* strains are resistant to inhibition of translation initiation caused by glucose restriction as shown previously (Ashe *et al*, 2000) and this is not affected by the presence of the ABE pathway or other genetic alterations in the strains constructed here.

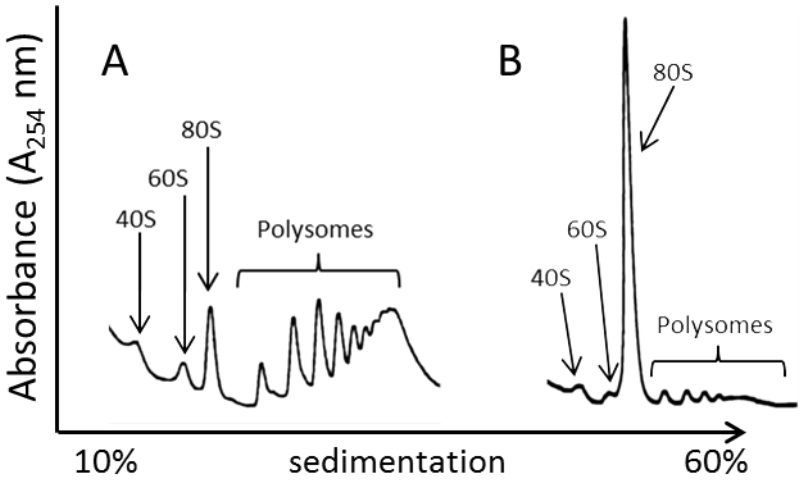

Figure 3.9 Ribosomal distribution profiles for active and inhibited wild-type cells

Figure shows (A) the ribosomal distribution profile of cells under glucose abundance (actively translating cells) and (B) the ribosomal distribution profile of cells during glucose restriction (translation inhibition). The x-axis shows the direction of ribosomal sedimentation in sucrose gradient and y-axis indicates the absorbance wavelenght.

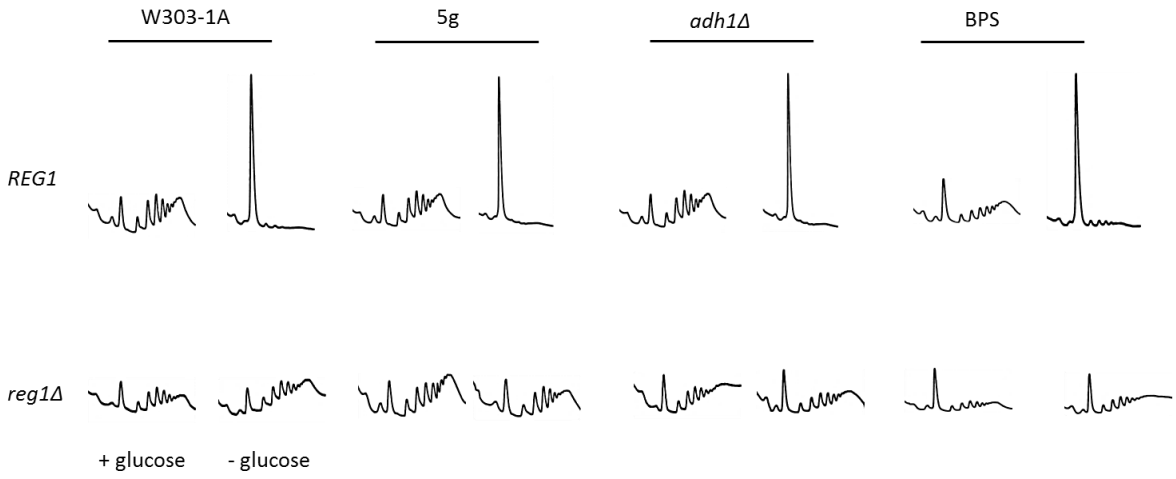

Figure 3.10 Comparison of polysome profile for *REG1* parent and their corresponding
reg1Δ mutants under glucose (+) and glucose limiting (-) conditions**.**

Images are the polysome distribution profile trace for strains under both glucose and glucose limiting conditions for 10 min.

3.8 Assessment of butanol tolerance in reg1Δ strains

Up to a third of yeast genes are altered in expression levels after changes to the carbon (glucose) environment and many of these include genes involved in yeast stress responses (Busti *et al*, 2010). Therefore, disabling the glucose repression pathway may alter tolerance to butanol stress. This hypothesis was tested by assessing the sensitivity of the *reg1Δ* constructs to butanol stress at the level of translation since one of the earliest responses to stress in yeast is the rapid inhibition of translation (Simpson & Ashe, 2012). Cells were grown in YPD media and then exposed to 1%, and 1.25% butanol (in YPD) for 10 min, followed by polysome analysis. The W303-1A and W303-1A *reg1Δ* strains are largely resistant to 1% butanol, while in both strains, treatment with 1.25% butanol causes a redistribution of ribosomes from polysomes into the 80S monosomal fraction (Fig 3.12). This redistribution of ribosomes is characteristic of an inhibition of protein synthesis at the translation initiation step (Ashe *et al*, 2000). The 5g strain which bears the 5 enzymes of the ABE pathway, exhibits a similar profile of butanol sensitivity to the W303-1A strain. In contrast when *REG1* is deleted in the 5g background the strain now exhibits butanol sensitivity at the 1% concentration (Fig 10B). Perhaps the most surprising profile was observed for the *adh1Δ* and the matched *adh1Δ reg1Δ* strain. Here the *adh1Δ* strain is more sensitive to 1% butanol than a wild type strain, yet the *reg1Δ adh1Δ* strain is more resistant than the wild type (Fig 3.12). Finally, for the BPS and matched BPS *reg1Δ* strains the polysome profiles and level of sensitivity to butanol is similar to the wild type and its matched *reg1Δ mutant* just with a slightly higher level of inhibition observed at 1% butanol (Fig 3.12).

Overall, the results show that the deletion of *REG1* had strain-specific effects on butanol sensitivity at the translational level. For instance in the 5g strain, *REG1* deletion sensitises cells to butanol, whereas in the context of the *adh1Δ* background, a *reg1Δ* mutant is more resistant to butanol. It is unclear why these differences are observed, however it is known that the glucose repression pathway is responsible for the transcriptional regulation of a very large number of genes (Carlson, 1999; Johnston, 1999; Rolland *et al*, 2002b). Therefore, mutants such as *reg1Δ* where this transcriptional repression is debilitated could have a huge range of pleiotropic effects especially in combination with other genetic alterations such as *ADH1* deletion and or heterogenous genes expression. Disabling *REG1*-mediated glucose repression might have rescued some of the effects of *adh1Δ,* including; oxidative stress as a result of a shift in the cellular redox balance towards a decrease in NAD^+/NADH ratio and acetaldehyde accumulation (Marisco *et al*, 2011). Perhaps *reg1Δ* might have activated the strain's stress response machinery thereby conferring more resistance to butanol in the *adh1Δ reg1Δ* strain.

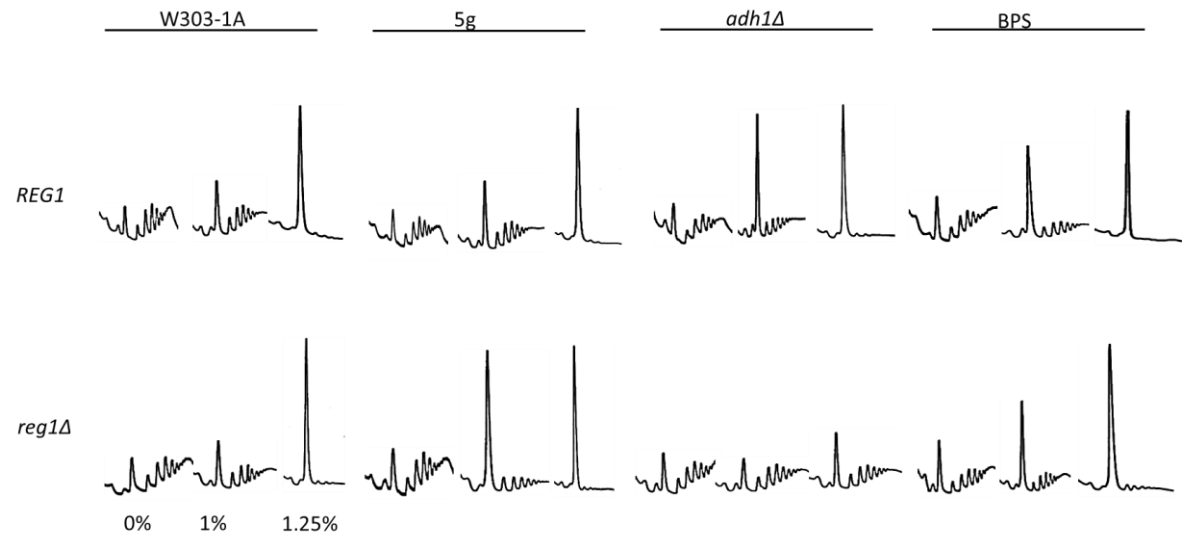

Figure 3.11 Comparison of polysome distribution profile for REG1 parent and their corresponding reg1Δ mutants under butanol treatment.

Images of the polysome distribution profile trace for strains after 0%, 1% and 1.25 % (v/v) butanol treatment for 10 min.

3.9 Growth analysis on alternative carbon

One of the aims of this project is to increase the range of carbon sources on which the strains can grow. Glucose negatively regulates a number of genes responsible for the diauxic shift and growth of yeast on non-fermentable carbon sources (Carlson, 1999; Johnston, 1999). Modulating the glucose repression pathway may therefore allow yeast strains to grow on non-fermentable carbon sources. To test this, a serial dilution analysis with the *reg1Δ* and *snf1Δ* strains was conducted on some selected carbon sources. For our result; W303 *snf1Δ* and 5g *snf1Δ* strains did not grow on any of the selected carbon, the *adh1Δ snf1Δ* and BPS *snf1Δ* shows slight growth on sucrose, xylose and glycerol and this is comparable with their growth on YP, this suggest a residual growth effect of the YP media rather than the presence of the carbon source added. The growth profile for the *reg1Δ* strains is similar to that of the parents on the growth medium tested. Overall, deletion of *REG1* in the strains did not have significant effect on their growth on all the four alternative carbons tested.

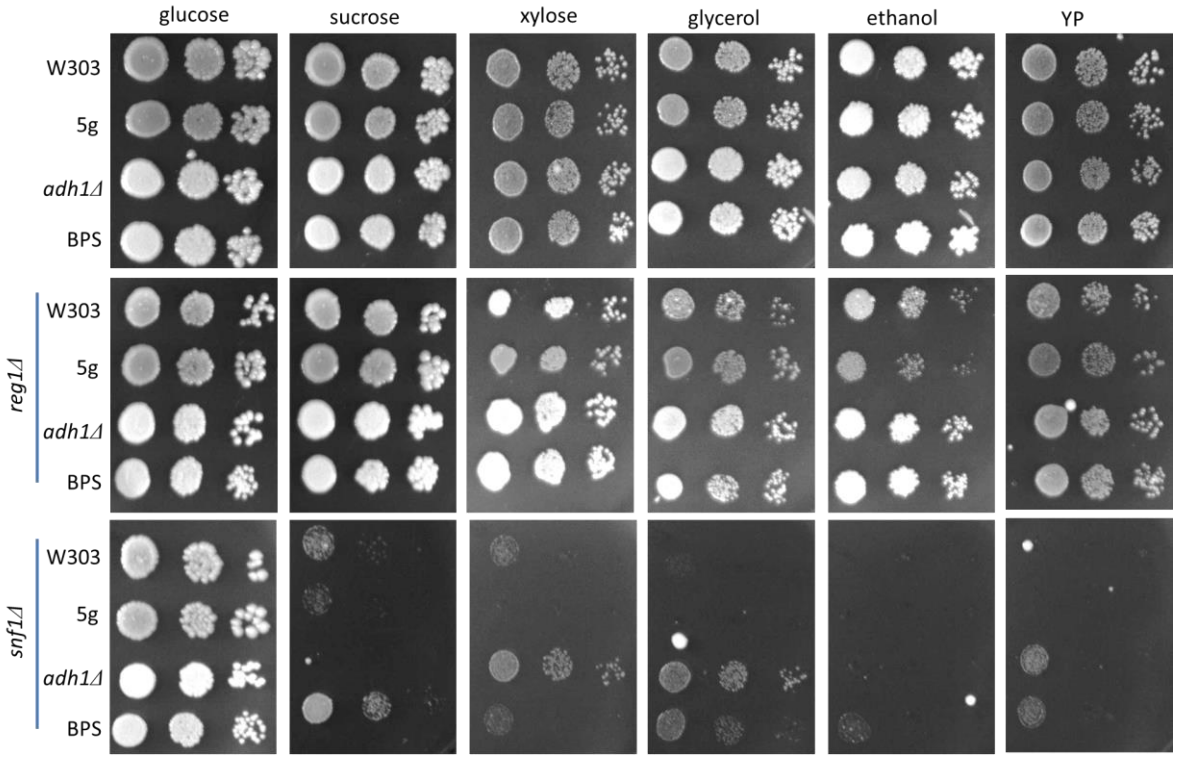

Figure 3.12 Comparison of the growth of strains on alternative carbon sources

Images of the growth spot analysis of the parent strains, *reg1Δ* and *snf1Δ* mutant strains on glucose, sucrose, glycerol, xylose and ethanol containing media, strains were also grown on YP (blank) to serve as control. Image represents their growth after three days.

3.10 Fermentation experiment

Having validated the deletions of *REG1* and *SNF1* in the butanol producing strain and the three control strains of *S. cerevisiae*, fermentation studies were undertaken to investigate yields of butanol. Cells were grown under semi-anaerobic conditions in 50 ml sealed glass bottles for up to 18 days at 30^{o}C. Results of five biological repeats are presented.

3.10.1 Fermentation with W303-1A and 5g background strains

The results show that deletion of *REG1* or *SNF1* gene in the W303-1A and 5g strains decreased the growth rate and final cell yield (final OD_{600}) compared to the respective parent strains (this indicates poor growth) (Fig 3.13A and 3.13B). For the W303 *reg1Δ*, initial growth is delayed compared to the parent. This delay is however not observed in the 5g *reg1Δ*; this may be due to the effect of AdhE2p overexpression (providing additional alcohol dehydrogenase function for ethanol synthesis and NAD^{+} regeneration) in the 5g strain. In both W303-1A and 5g strain backgrounds; *snf1Δ* caused a large decrease in the level of growth compared to the respective parent strains (Fig 3.13A and 3.13B). In terms of ethanol yield, the results show that ethanol production initially lags behind for both the W303 *reg1Δ* and W303 *snf1Δ* compared to the parent however; peak ethanol yield is relatively similar across all strains (Fig 3.13A). Similarly, for the 5g *snf1Δ* strain; ethanol production initially lags behind compared to the parent. However, for the 5g *reg1Δ* strain, the ethanol profile is comparable to the parent (Fig 3.13B). When the ethanol yield is normalised to the OD_{600} value (Fig 3.13C), the result shows that *snf1Δ* cells have a higher ethanol/OD_{600}

yield compared to the respective parent strains. Though there is decrease in growth of the *reg1Δ* and *snf1Δ* mutant compared to the parent (in both W303-1A and 5g strains), the results show similar ethanol yield across the respective strain's panel. The relatively similar ethanol yield for the *snf1Δ* strains (despite decreases in their growth rate) compared to the parent strain is probably due to constitutive expressions of glycolytic enzymes and inhibition of diauxic shift which may lead to more efficient ethanol fermentation and inhibition of ethanol uptake/utilization by the cells. For the *reg1Δ* strains, the expression of other *ADH* genes may lend power towards ethanol production despite the reduced growth of the strains. While alterations in growth and ethanol production were observed, critically butanol was not detected for any of the strains

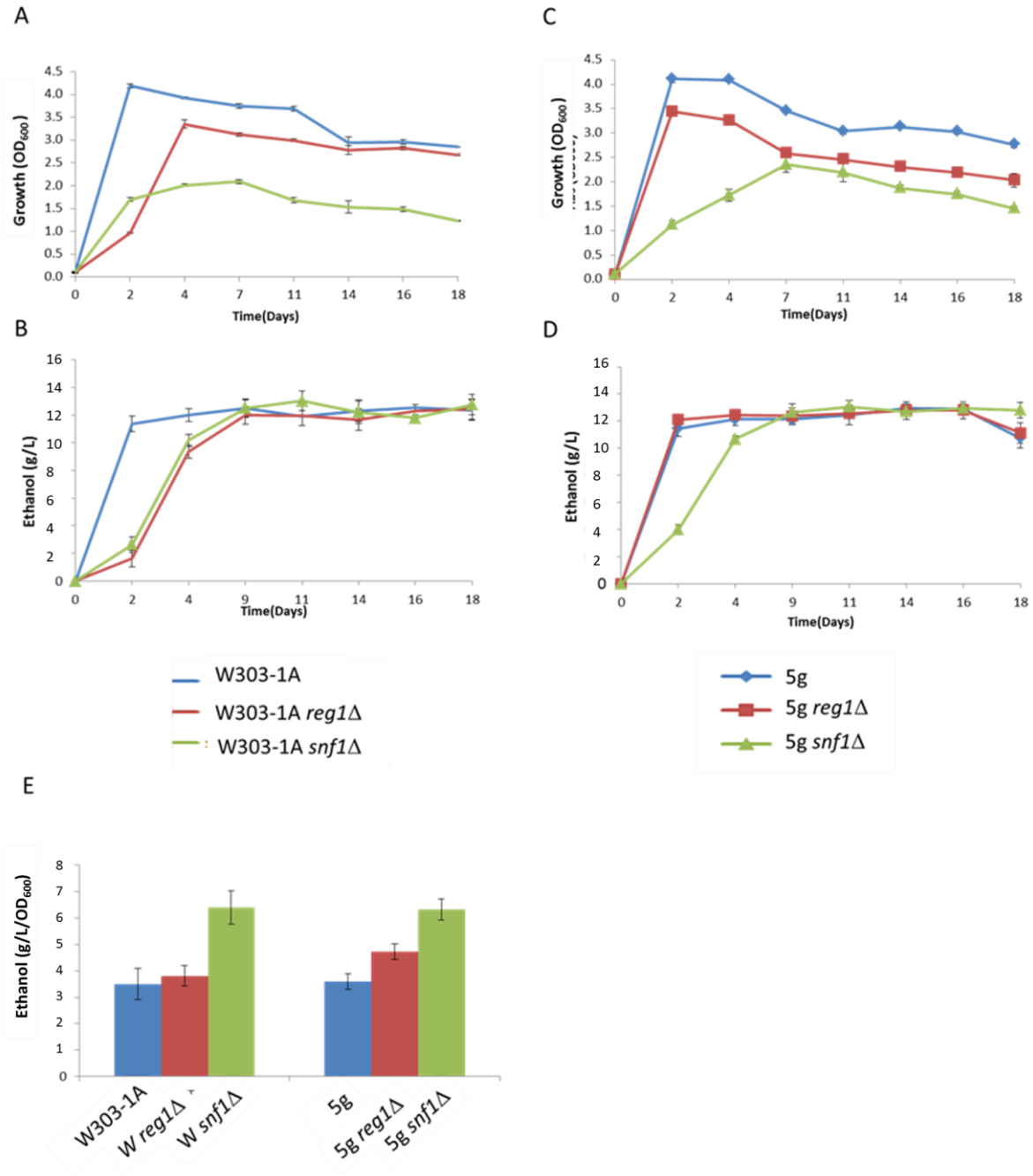

Figure 3.13 Fermentation yield in W303-1A and 5g background strains

Figure showing growth (A and C) and ethanol (B and D) levels in W303-1A and 5g strain series during fermentation. (E) is graph showing ethanol yield per cell density for days 4-16 by the strains. Data represent the mean value of three biological repeats with standard error bars. The 'W' in W *reg1Δ* and W *snf1Δ* is abbreviations for W303-1A.

3.10.2 Fermentation with *adh1Δ* background strains

The growth profiles of the *adh1Δ reg1Δ* and *adh1Δ snf1Δ* strains are similar to the parent strain (Fig 3.14A). The ethanol profile for the *adh1Δ reg1Δ* is similar to the parent strain, while *adh1Δ snf1Δ* has a higher ethanol yield compared to the parent strain (Fig 3.14B). As reported, the *adh1Δ* strains produce some butanol even without an heterologous butanol pathway (Branduardi *et al*, 2013b). The *adh1Δ reg1Δ* strain has peak butanol level that is comparable to the parent but butanol level is lower in the *adh1Δ snf1Δ* strain compared to the parent (Fig 3.14C). The higher ethanol yield for the *adh1Δ snf1Δ* strain may be due to the activation of other *ADH* genes; since *SNF1* is known to negatively control *ADH1* (alcohol dehydrogenase 1) and *GCN4* (an activator of amino acid biosynthesis genes) (Shirra *et al*, 2008). There is higher ethanol per cell density (OD_{600}) yield and lower butanol per cell density yields respectively in the *adh1Δ snf1Δ* strains compared to the parent strain (Fig 3.14D); as stated earlier, *SNF1* deletion may enhance ethanol synthesis for redox balance in the strain. Overall, the result suggests that the ethanol and butanol yield for the *adh1Δ reg1Δ* strains is growth dependent while in the *adh1Δ snf1Δ* strain, they are dependent on some metabolic recalibrations.

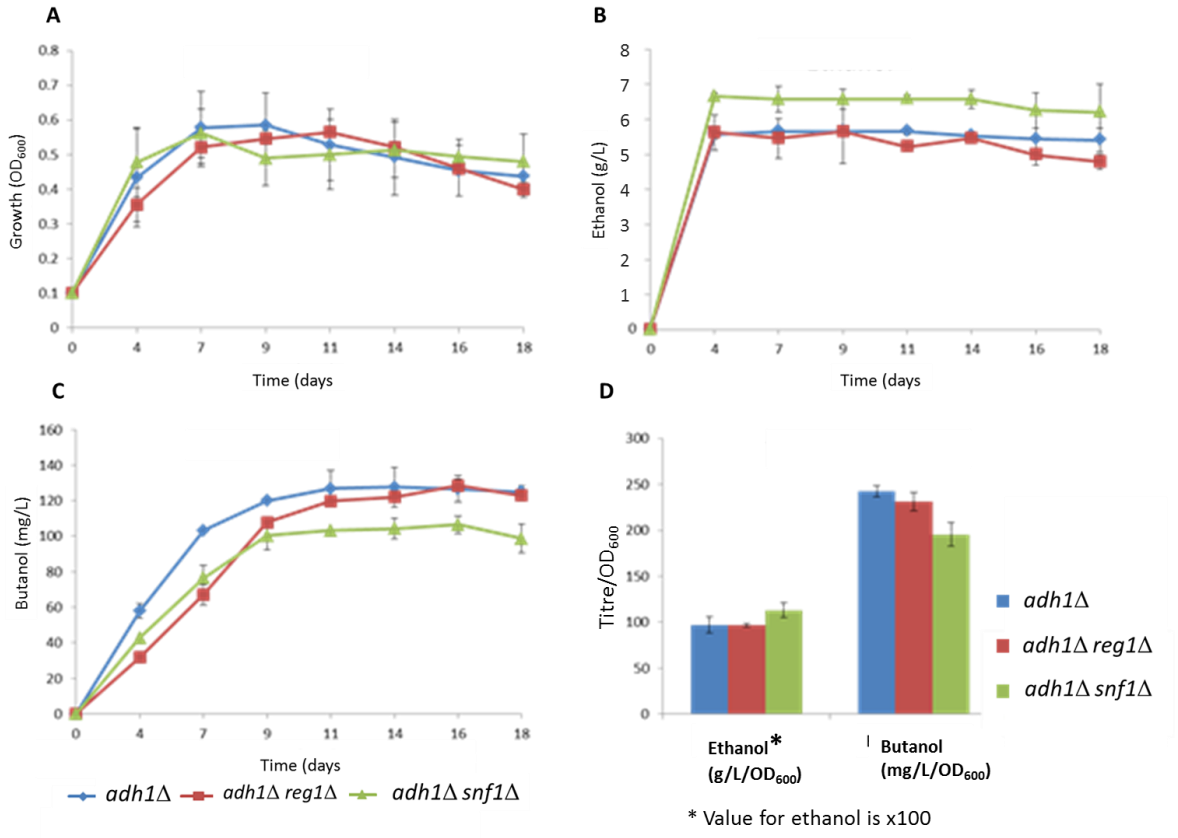

Figure 3.14 Fermentation yield in *adh1Δ* background strains.

Figure show (A) growth (cell density), (B) ethanol and (C) butanol levels in the *adh1Δ, adh1Δ reg1Δ* and *adh1Δ snf1Δ* strains during fermentation. (D) is the graph for amount of ethanol and butanol per cell density (OD_{600}) on peak day 14. Data represent the mean of three biological replicates with standard error bars.

3.10.3 Fermentation with BPS background strains

The presented results show that the BPS *reg1Δ* and BPS *snf1Δ* strains grow poorly compared to the parent BPS strain and the level of both ethanol and butanol is equally reduced for the strains (Fig 3.15). Surprisingly, the BPS *reg1Δ* and BPS *snf1Δ* strains grow poorly compared to the *adh1Δ reg1Δ* and *adh1Δ snf1Δ* strains (Fig 3.15A & 3.14A); this may be due to the expression of the heterologous ABE-butanol pathway genes and ACS2 *ALD6* (imposing unclassified genetic interactions and burdens) in the BPS strain background. The dip in ethanol and butanol yield for BPS *reg1Δ* and BPS *snf1Δ* strains compared to the parent may be growth related (Fig 3.15B&C). However, the yield of ethanol and butanol per cell density (OD_{600}) show decreases for the BPS *reg1Δ* and BPS *snf1Δ* deletion strains (Fig 3.15D); suggesting the involvement of more factors than growth. Probably, decrease in growth also result in some recalibration of metabolism in these strains.

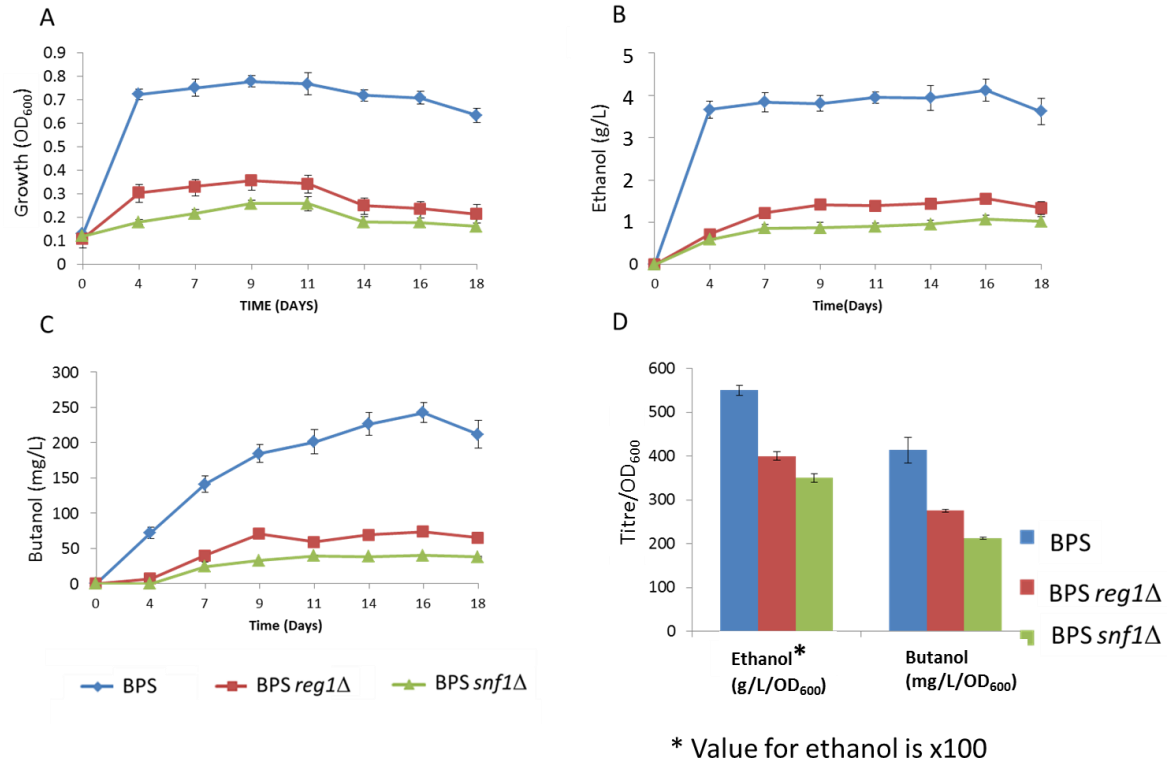

Figure 3.15 Fermentation yield in BPS background strains

Figure shows the growth (A), ethanol (B) and butanol (C) levels for BPS, *reg1Δ.BPS* and *snf1Δ.BPS* strains during fermentation. (D) is graph showing the amount of ethanol and butanol per cell density (OD_{600}) at day 14. The data represent the mean of three biological repeats with standard error bars.

Table 3.1 compares the peak fermentation yield across the strains. The W303 and 5g strains did not produce any butanol even with *REG1* or *SNF1* deletions. Ethanol titre/OD_{600} in the W303 *snf1Δ* and 5g *snf1Δ* is higher compared to their respective reference parent strains. Surprisingly, the Ethanol titre/OD_{600} value for the *adh1Δ* and BPS background strains were much higher than in W303 strain suggesting that the strains actually produce more ethanol relative to the wild type W303. This result poses a concern especially in the BPS strain where ethanol contamination is undesirable. *REG1* and *SNF1* deletions reduced butanol in both the *adh1Δ* and BPS strains

Table 3.1 Summary of peak growth, ethanol and butanol across the *reg1Δ* and *snf1Δ* strains

strain	Max growth (OD_{600} unit)	Ethanol titre (g/L)	Ethanol titre/OD_{600} (g/L/OD_{600})	Butanol Titre (g/L)	Butanol titre/OD_{600} (g/L/OD_{600})
W303 1A	4.2 ± 0.4	12.5 ± 0.2	2.98	-	-
W303 *reg1Δ*	3.36 ± 0.4	12.0 ± 0.3	3.57	-	-
W303 *snf1Δ*	2.1 ± 0.1	13.0 ± 0.3	6.19	-	-
5g	4.11 ± 0.5	12.9 ± 0.3	3.14	-	-
5g *reg1Δ*	3.44 ± 0.4	12.8 ± 0.3	3.30	-	-
5g *snf1Δ*	2.36 ± 0.2	13.0 ± 0.3	5.51	-	-
adh1Δ	0.59 ± 0.01	5.7 ± 0.1	9.66	127.6 ± 10	215.2
adh1 *reg1Δ*	0.66 ± 0.02	5.6 ± 0.1	8.50	122.0 ± 15	184.8
adh1 *snf1*	0.66 ±0.02	6.7 ± 0.1	10.15	106.5 ± 10	161.4
BPS	0.69 ± 0.03	4.1 ± 0.04	5.94	233 ± 18	337.7
BPS *reg1Δ*	0.34 ± 0.01*	1.6 ± 0.01*	4.71	74 ± 10*	217.6
BPS *snf1Δ*	0.26 ± 0.01*	1.1 ± 0.03*	4.23	40 ± 10*	153.8

Standard errors of three biological replicates is indicates as (±). Student's t-test analysis was used for statistical analysis of the data of the BPS background strains in triplicates. Asterix sign (*) indicates a result that was significantly different compared to the reference BPS strain ($p < 0.05$).

3.11 Viability of strains

Given that deletion of *REG1* or *SNF1* genes did not improve butanol production, we examined cell viability of the four starting parent strains under these experimental conditions to ensure that there was no loss of robustness. Since the *adh1Δ* strains grow poorer compared to the *ADH1*-active counterparts it is necessary to ascertain particularly, the viability of the BPS strain under the condition for butanol production. The strains were cultured for 4 days under semi-anaerobic condition and for the control; W303-1A strain was grown to exponential phase after which the culture was heated at 95^{o}C for 10 mins (to kill the cells). Cell viability was then determined using propidium iodide-flow cytometry method (PI–FCM) (Ocampo & Barrientos, 2011). The result in Fig 3.16 shows that; ~80%, 75%, 90% and 75% of cells were alive in the W303-1A, 5g, *adh1Δ* and BPS strains respectively. The *adh1Δ* strain has more living cells compared to the W303-1A which may be due to a decrease rate of cell senescence in the *adh1Δ* strain. The lower amount of living cells for the 5g and BPS strains may be due to the extra physiological burden of expressing the heterologous genes in these strains. Overall, the result suggests that the viability across all the strains is reasonably comparable and unlikely to explain the reduction in cell number under the fermentation conditions.

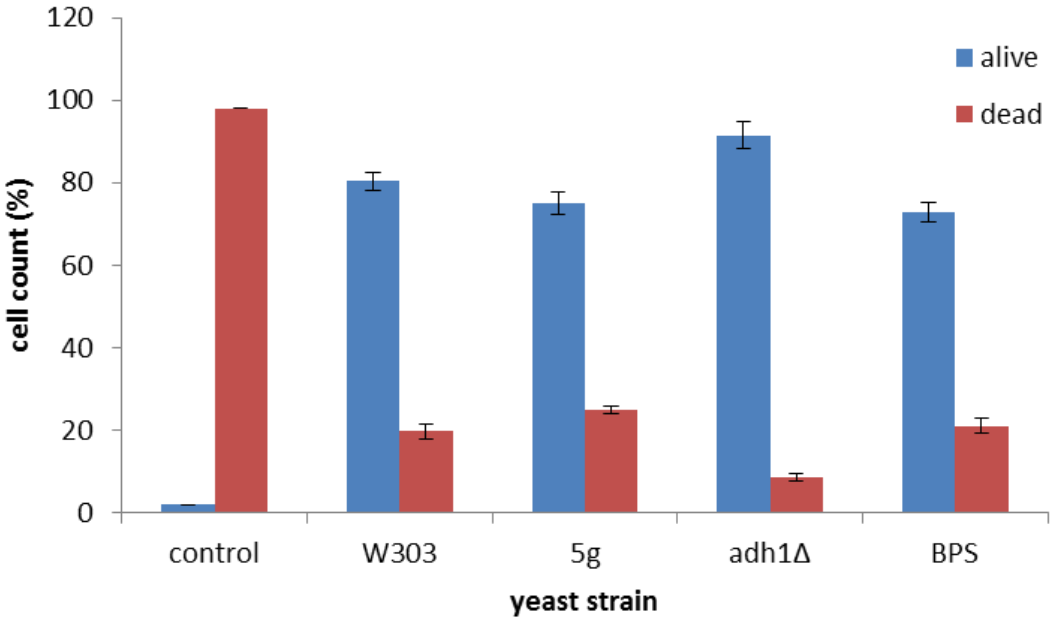

Figure 3.16 Viability of strains.

Graph shows the percentages of live and dead cells in the strains after fermentation for four days.. The Data represents the mean of three biological replicates with standard error bars.

3.12 Intracellular accumulation of butanol

The transport of butanol out of the cell may not be as efficient as that of ethanol and these may lead to intracellular accumulation of butanol causing cellular inhibitions. To test this assumption, we examined whether more butanol accumulates within cells than is obtained in the extracellular media. The BPS strain was grown for 11 day under semi-anaerobic condition and was treated with digitonin (10 µg/ml) for 6 hr and 12 hr respectively to disrupt cell membrane permeability (Kroschwald et al., 2015). Result shows that the 6 hr digitonin treated culture did not show any increase in butanol compared to the untreated sample (Fig 3.17). The 12 hr treated culture produced 'noisy' trace on the GC machine (uncharacterized high molecular weight materials indicative of proteins and cell debris) which contaminated the GC DB-wax column (data not shown). This result is suggestive that butanol did not accumulate within the BPS strain, however, it is important to emphasise that we do not have any control to confirm that digitonin has effectively disrupted cell permeability.

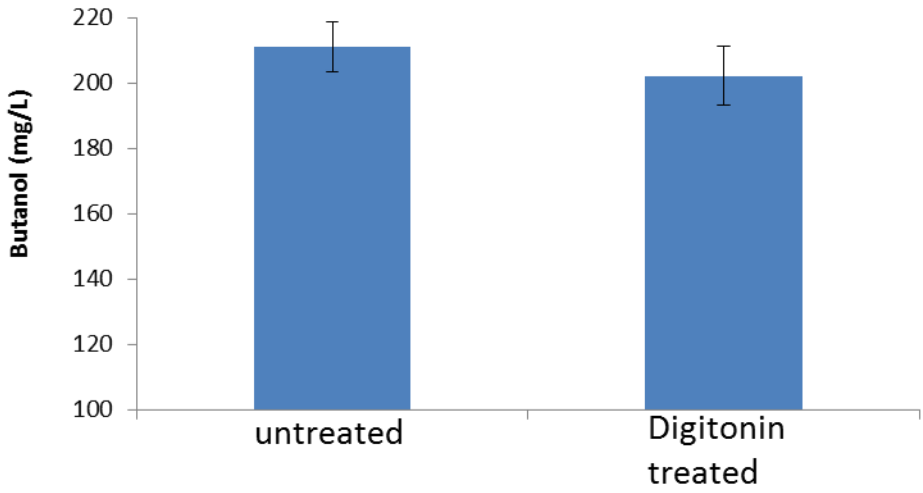

Figure 3.17 Comparison of butanol levels in Digitonin treated and untreated BPS cells

Graph shows the concentration of butanol in BPS strain for digitonin treated and untreated cells. Data represents the mean of three biological replicate with standard error bars.

3.13 Discussion

The deletion of the *REG1* and *SNF1* genes (encoding two regulator proteins in the glucose repression pathway; the Reg1p and Snf1p proteins; key players in the glucose repression and derepression mechanisms respectively) were singly constructed in the four selected yeast strains used in this study. We hypothesized that these alterations might lead to two outcomes. Firstly, disabling the glucose repression pathway (*REG1* deletion) would enable the yeast to constitutively express many glucose repressed genes for the utilisation of non-fermentable sugars, which might improve the level of carbon available for fermentation to butanol. Alternatively, in a constitutive glucose repression strain (*SNF1* deletion) glycolytic flux might be channelled more towards the synthetic butanol pathway. Overall deletion of the two genes did not improve butanol production. Particularly, in the butanol production strain, the deletions led to a decrease in butanol. Since glucose sensing, signalling and its subsequent metabolic control depends on a crosstalk across several pathways, by modulating one aspects of this complex circuitry (the glucose repression pathway), it might be difficult to characterise an empirical outcome for such modulations especially in the background of the butanol production strain which carries other genetic alterations that affect glucose metabolism. Perhaps, detailed genetic analysis may provide a clearer picture and a detailed understanding of the interaction that these modulations have with other cellular mechanisms and the impact on cell functions such as fermentation

3.14 Conclusion

The results in this chapter show that modulation of the glucose repression pathway (deleting *REG1* and *SNF1)* has strain specific effect across the four strains; however, it did not improve butanol production. Since *REG1* and *SNF1* are global metabolic regulators that affect yeast's cellular functions, it may be difficult to track the plethoric change that results from the deletion of these genes or to fully explain the reason for some of the effects observed.

Going forward, a more direct approach at improving butanol production could be to channel metabolite towards the butanol pathway. Increasing acetyl-CoA availability for the acetyl-CoA dependent heterogenous butanol pathway seems a practical approach at optimising the pathway's yield. Others have reported successful increase in butanol yield by increasing acetyl-CoA level in microbial systems (Krivoruchko *et al*, 2013; Lian *et al*, 2014; Schadeweg & Boles, 2016b; Shen *et al*, 2011). In the next chapter of this research, I seek to exploit the obstruction of the glyoxylate cycle with a view to prevent the drain of cytosolic acetyl-CoA and increase its availability for butanol production. Hopefully, this 'block' strategy will increase acetyl-CoA available for butanol synthesis and improve production in the *BPS* strain.

4. Disabling yeast glyoxylate cycle with a view to improving butanol production

4.1 Introduction

Acetyl-coenzyme A (Acetyl-CoA) is a central metabolic intermediate; a product of several catabolic reactions, as well as the starting precursor of many anabolic processes (Chen *et al*, 2013; Krivoruchko *et al*, 2013; Pietrocola *et al*, 2015). The abundance of acetyl-CoA can be used to report on the energetics of the cell and it determines the balance between anabolism and catabolism (Pietrocola *et al*, 2015). Acetyl-CoA modulates the activities of enzymes, transcription factors and chromatin by affecting their acetylation profile (Cai *et al*, 2011). It also acts through allosteric means to regulate the activities of some enzymes (including pyruvate dehydrogenase, pyruvate decarboxylase, pyruvate carboxylase (Pietrocola *et al*, 2015), thiolase (Modis & Wierenga, 1999), carnitine palmitoyltransferase I, acetyl-CoA carboxylase, and some transcription factors (HNF4-α and PPARα) (Leonardi & Jackowski, 2013). Acetyl-CoA also regulates some important physiological processes including energy metabolism, cell growth, cell proliferation and autophagy/apoptosis (Cai et al, 2011; Pietrocola et al, 2015). Acetyl-CoA is made up of an acetyl group joined by a thioester bond to Coenzyme A (Fig 4.1). Acetyl-CoA in the cell acts as the carrier of 'high energy' acetate, and the high energy nature of the thioester bond in the molecule facilitates transfer of the activated carbon (acetyl moiety) to acceptor molecules leading to C-C bond formation (Pietrocola *et al*, 2015).

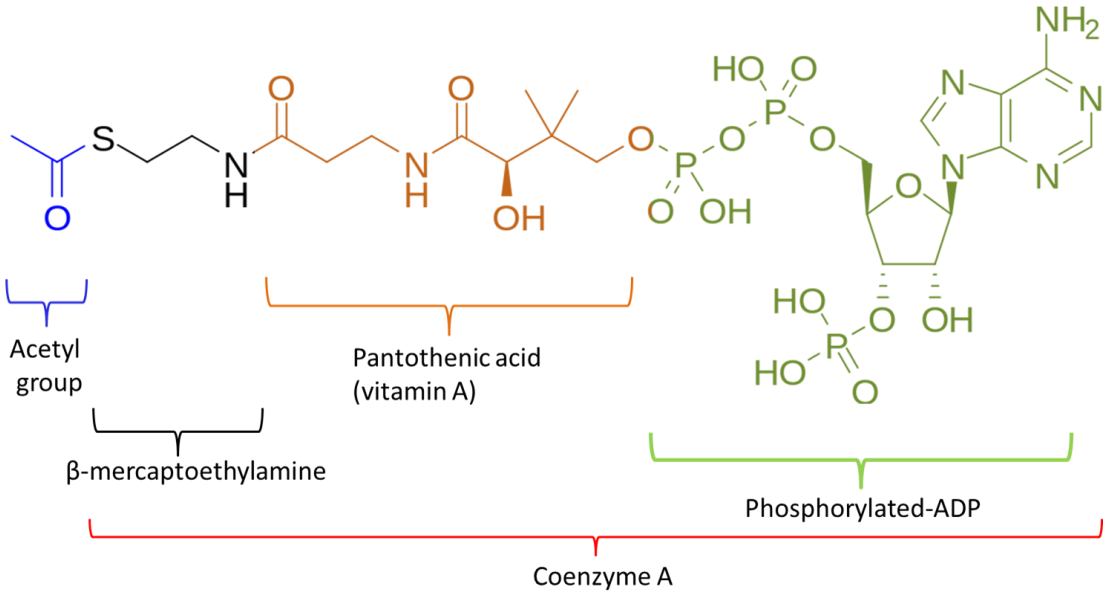

Figure 4.1 Structure of acetyl-CoA molecule.

Figure is molecular structure of acetyl-CoA ($C_{23}H_{38}N_7O_{17}P_3S$) showing its component parts.

4.2 Acetyl-CoA is a central metabolic precursor

In yeast, the metabolism of acetyl-CoA is highly compartmentalized, occurring in four separate organelles (nuclei, peroxisomes, mitochondria and cytoplasm) (Schadeweg & Boles, 2016a). Acetyl-CoA is the precursor 'fuel' for the mitochondrial TCA cycle, it is the building block for cytosolic synthesis of fatty acids, it is the acetyl donor for protein acetylation in the nucleus and also the end product of fatty acid β-oxidation in the peroxisome. Biosynthesis of desirable commodity chemicals such as fatty acids, higher alcohols, polyhydroxyalkanoates, polyphenols, polyketides and isoprenoids in microbial hosts have been designed around intracellular acetyl-CoA metabolism (Fig 4.2) (Chen *et al*, 2013; Krivoruchko *et al*, 2013). However, the production of these acetyl-CoA dependent commodities in yeast still lags behind compared to their production in other host microbes such *E.coli* (Krivoruchko *et al*, 2013; Schadeweg & Boles, 2016b)*;* this is probably due to the complexity of central carbon and acetyl-CoA metabolism in yeast (Krivoruchko *et al*, 2013; Matsuda *et al*, 2011). In order for these heterologous pathways to achieve high product yield in yeast, factors such as; precursor and cofactor synthesis, redox and metabolic flux balance and robust cell growth/fitness must be maintained (Matsuda *et al*, 2011). Aside from the challenges of heterologous gene expression, the overexpression of heterologous pathways may also lead to a metabolic drain on the cell. The nature of yeast central metabolism (restriction in its metabolic flux distribution) may hinder metabolic supplies to the pathways, making it difficult for the cell to fine-tune its metabolism so as to accommodate any drain in its central metabolic network (Krivoruchko *et al*, 2013; Matsuda *et al*, 2011). The successful biosynthesis of higher alcohols in yeast, especially butanol, therefore requires a number of metabolic strategies aimed at increasing

intracellular acetyl-CoA abundance, synthesis/supply of reducing equivalent and maintenance of a cell's physiological fitness among other things (Krivoruchko *et al*, 2013; Nielsen, 2014).

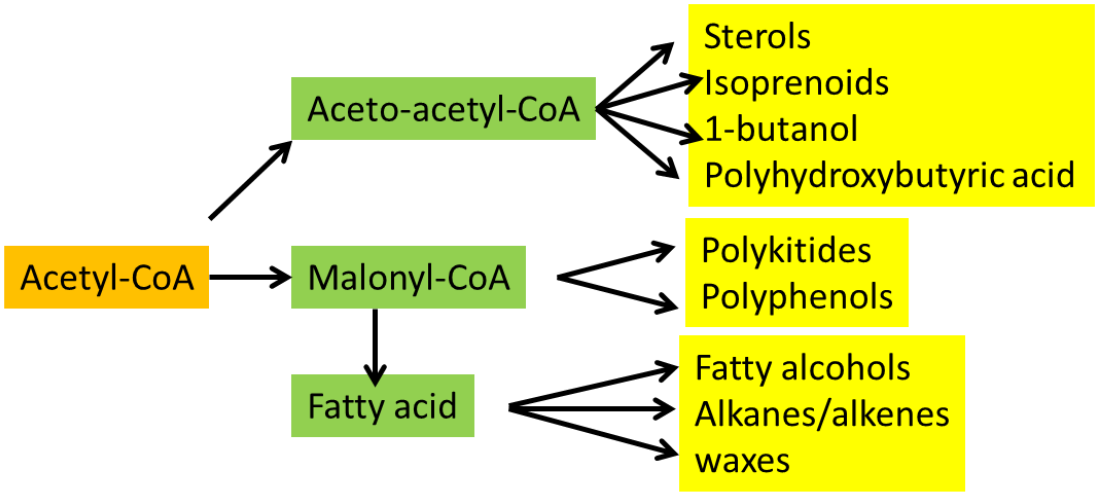

Figure 4.2 Summary of acetyl-coA derivable metabolic products.

Figure is a summary of derivable products from acetyl-CoA. (Chen *et al*, 2013; Krivoruchko *et al*, 2013; Nielsen, 2014).

4.3 The glyoxylate cycle

Acetyl-CoA is consumed through the glyoxylate cycle to produce four-carbon carboxylic acids for mitochondrial anaplerosis, protein synthesis and gluconeogenesis (Chen *et al*, 2012). Each of citrate synthase and malate synthase catalyse steps in the glyoxylate cycle that utilise acetyl-CoA respectively. The glyoxylate cycle is tightly regulated in most organisms and has been shown to be active even during fermentation in yeast (Krivoruchko *et al*, 2013; Regenberg *et al*, 2006). Krivoruchko *et al*, (2013) reported a strategy to optimize butanol production by inhibiting the glyoxylate cycle in their recombinant yeast, which expresses the ABE-butanol pathway via episomal plasmids. They reported improvements in butanol production that correlate with increases in cytosolic acetyl-CoA to a maximum butanol titre of 16.3 mg/L. Butanol titre of ~300 mg/L was reported for the BPS yeast strain currently used in this study (Swidah *et al*, 2015); this strain has synthetic genes for butanol production incorporated into the genome thereby eliminating the possibilities of gene/plasmid loss and the strain has *ADH1* deleted to inhibit ethanol synthesis.

This current study, aims to further improve butanol production in the above strain by limiting the flux of acetyl-CoA through the glyoxylate cycle. The butanol synthetic pathway depends on cytosolic acetyl-CoA; therefore disabling acetyl-CoA consuming pathways, such as the glyoxylate cycle, may increase acetyl-CoA abundance for butanol synthesis. Particularly, in the background of an *adh1Δ* it is expected that such strategy will further narrow the channels for central carbon metabolism and drive metabolites towards the butanol pathway.

4.4 Obstruction of acetyl-CoA entry steps of the glyoxylate cycle

CIT2 and *MLS1* code for citrate synthase 2 (Cit2p) and malate synthase 1 (Mls1p) respectively: these steps in the glyoxylate cycle represent the points where acetyl-CoA can be incorporated. Therefore, the strategy in this chapter was to delete these genes both singly and in combination to generate *cit2Δ*, *mls1Δ* and *cit2Δ mls1Δ* mutants in the BPS and the three control strains (W303-1A lab wild type strain, 5g strain expressing the five butanol synthetic genes and the *adh1Δ* mutant strain).

4.4.1 Construction of cit2Δ mutant strains

CIT2 encodes a peroxisomal citrate synthase (Lewin *et al*, 1990) which catalyses the condensation of acetyl-coA with oxaloacetate to produce citrate. *CIT2* was deleted in all four strains using a *loxP-natNT2-loxP* deletion cassette. The deletion cassette was amplified by PCR from the plasmid *pZC2* (Carter & Delneri, 2010) using *CIT2* deletion primers. The amplified deletion cassette has the cloNat resistance gene surrounded by *loxP* sequences and 70 bp targeting sequences with homology to the 5' and 3' untranslated regions of *CIT2* ORF (to ensure correct homologous recombination into the genome). The deletion cassette fragment was transformed into yeast and nourseothricin (cloNat) resistant transformants were selected. Successful deletion of *CIT2* was validated by PCR analysis on genomic DNA: regions across (1), upstream (2) and downstream (3) of the *CIT2* loci were amplified (Fig 4.3A). The sizes of these PCR products were verified by gel electrophoresis and they matched the calculated expected sizes (Fig 4.3B). These results demonstrate that the *CIT2* gene has been successfully deleted in each of the four required strains.

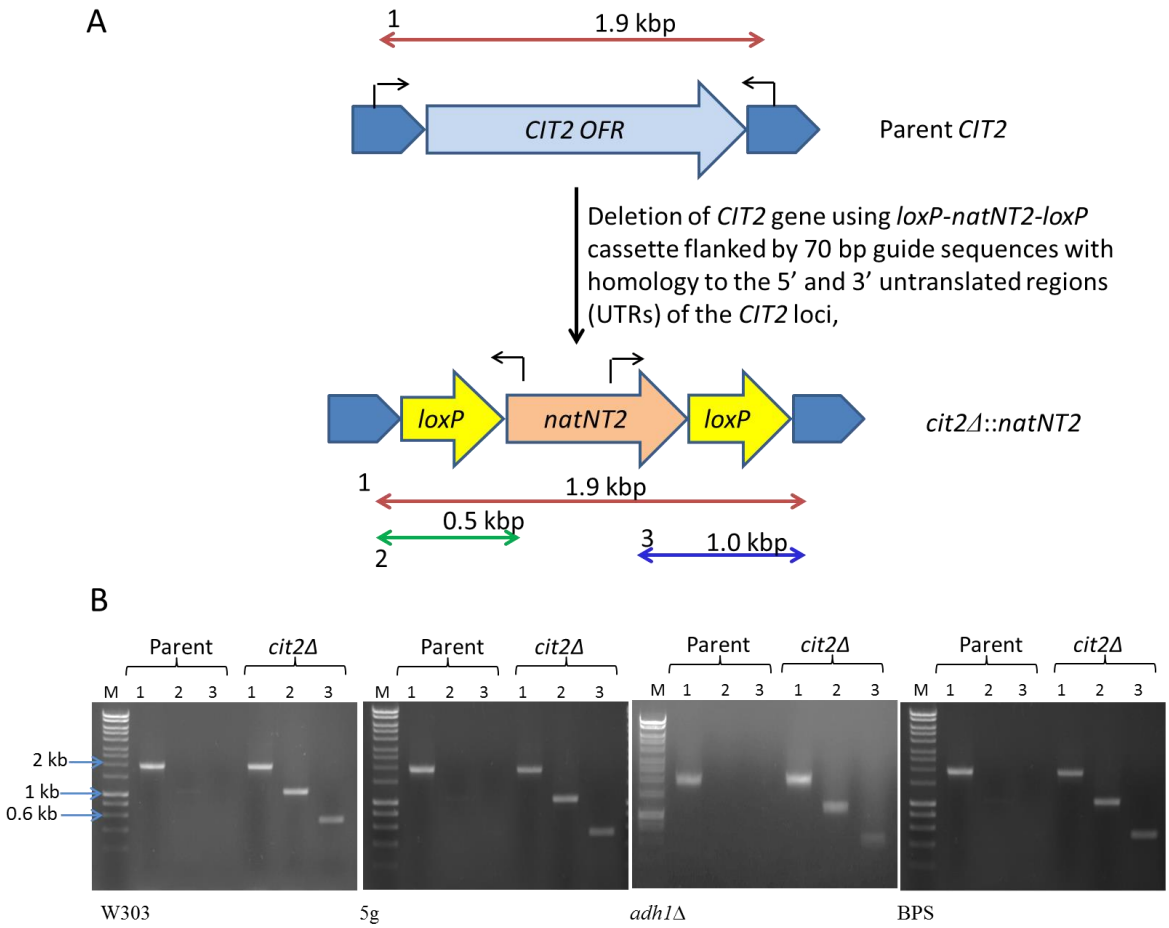

Figure 4.3 Deletion of CIT2 gene in yeast strains

Figure shows (A strategy for the deletion of *CIT2* using *loxP-natNT2-loxP* gene deletion cassette and the PCR-based verification for the confirmation of the *cit2Δ::natNT2* genotype using site specific primers. (B) Photographic images of 1% agarose gels showing the sizes of the verification PCR products separated by electrophoresis.

4.4.2 Construction of *mls1Δ* mutant strains

MLS1 encodes the cytosolic malate synthase (Fernandez *et al*, 1993) and it was deleted in the four strains described above using the same *loxP-natNT2-loxP* deletion cassette and overall strategy that was used for *CIT2*. Successful generation of *mls1Δ* across the four yeast strain backgrounds was confirmed by PCR analysis on genomic DNA prepared from transformants (Fig 4.4A) using site specific verification primers. Here appropriately sized PCR products were obtained (Fig 4.4B).

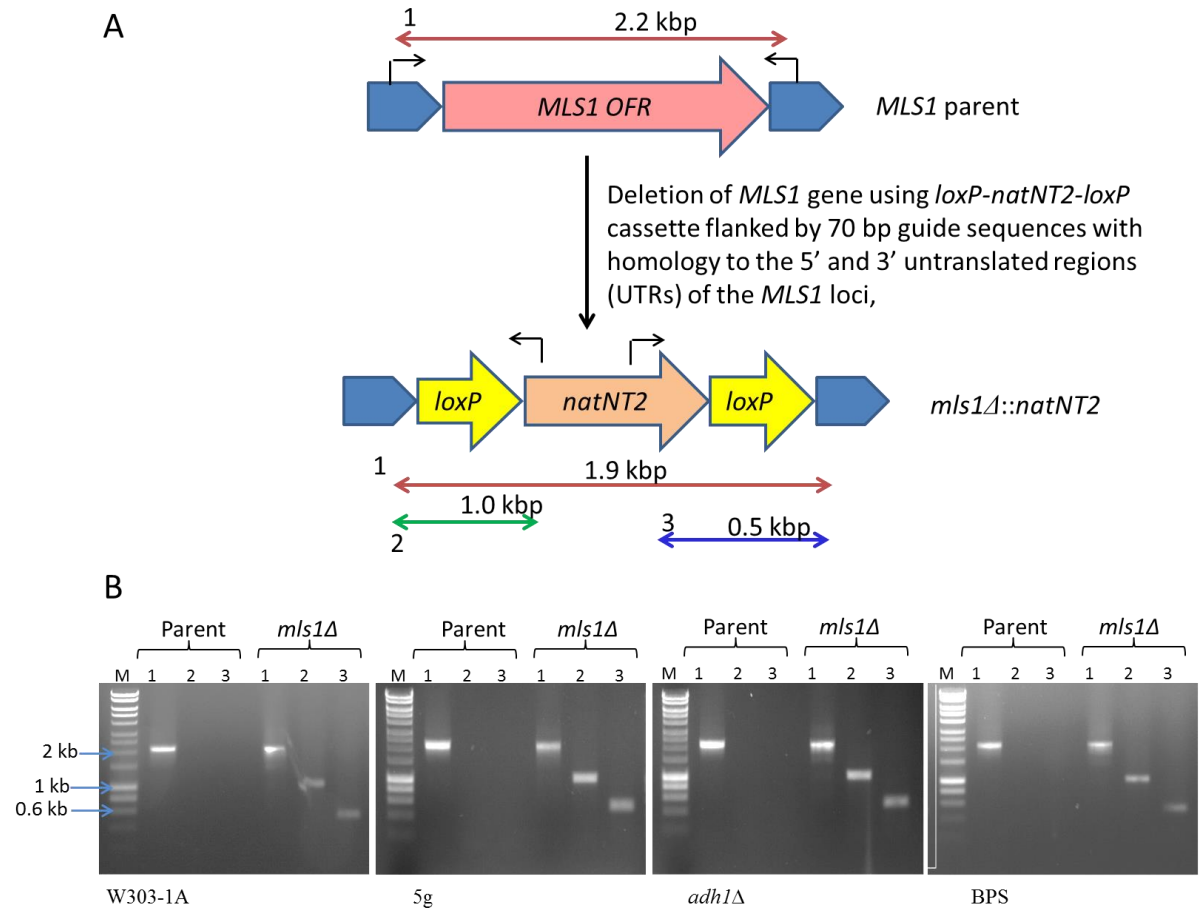

Figure 4.4 Deletion of MLS1gene in yeast strains

Figure shows (A) the strategy for deletion of *MLS1* and the PCR-based verification of the *mls1Δ::natNT2* genotype. The orientation of verification primers and expected product sizes are shown (B) Images of 1% agarose gels showing the sizes of the verification PCR products after their separation by electrophoresis.

4.4.3 *Cre*-recombinase excision of cloNat marker

Previous analysis has shown that deletion of genes encoding both of the cytosolic acetyl-CoA consuming enzymes steps in the glyoxylate cycle is important in increasing the level of acetyl-CoA available for biosynthetic reactions (Krivoruchko *et a*l., 2013). Therefore, in order to generate the double *CIT2 MLS1* deletion mutant across the four strain backgrounds to be tested, a first step was to remove the *natNT2* gene from one of the single mutants, to enable the use of cloNat selection for the next round of gene deletion (generation of the *cit2Δ mlsΔ1* mutants). Therefore, the cloNat marker gene was excised from the genome of the *cit2::natNT2* mutants by transformation with a plasmid carrying the Cre-loxP recombinase (Fig 4.5). Validation of the successful excision of *natNT2* gene from the genome in all four *cit2::natNT2* mutant strains was achieved by PCR analysis on genomic DNA prepared from candidate transformants (Fig 4.5B). Two sets of confirmation PCR amplifications were conducted (amplification of regions that are; 1-across and 2-upstream of the *loxP-natNT2-loxP* module at the endogenous *CIT2* gene loci (Fig 4.5A)). The sizes of these PCR products were verified by gel electrophoresis on 1% agarose to match the calculated expected sizes (Fig 4.5C). As a final step, strains where the *natNT2* marker gene had been removed were selected for loss of the plasmid pSH47 carrying the *Cre* recombinase. The presented results confirm that *natNT2* has been successfully excised from the four *cit2::natNT2* mutants to generate unmarked *CIT2* deletions.

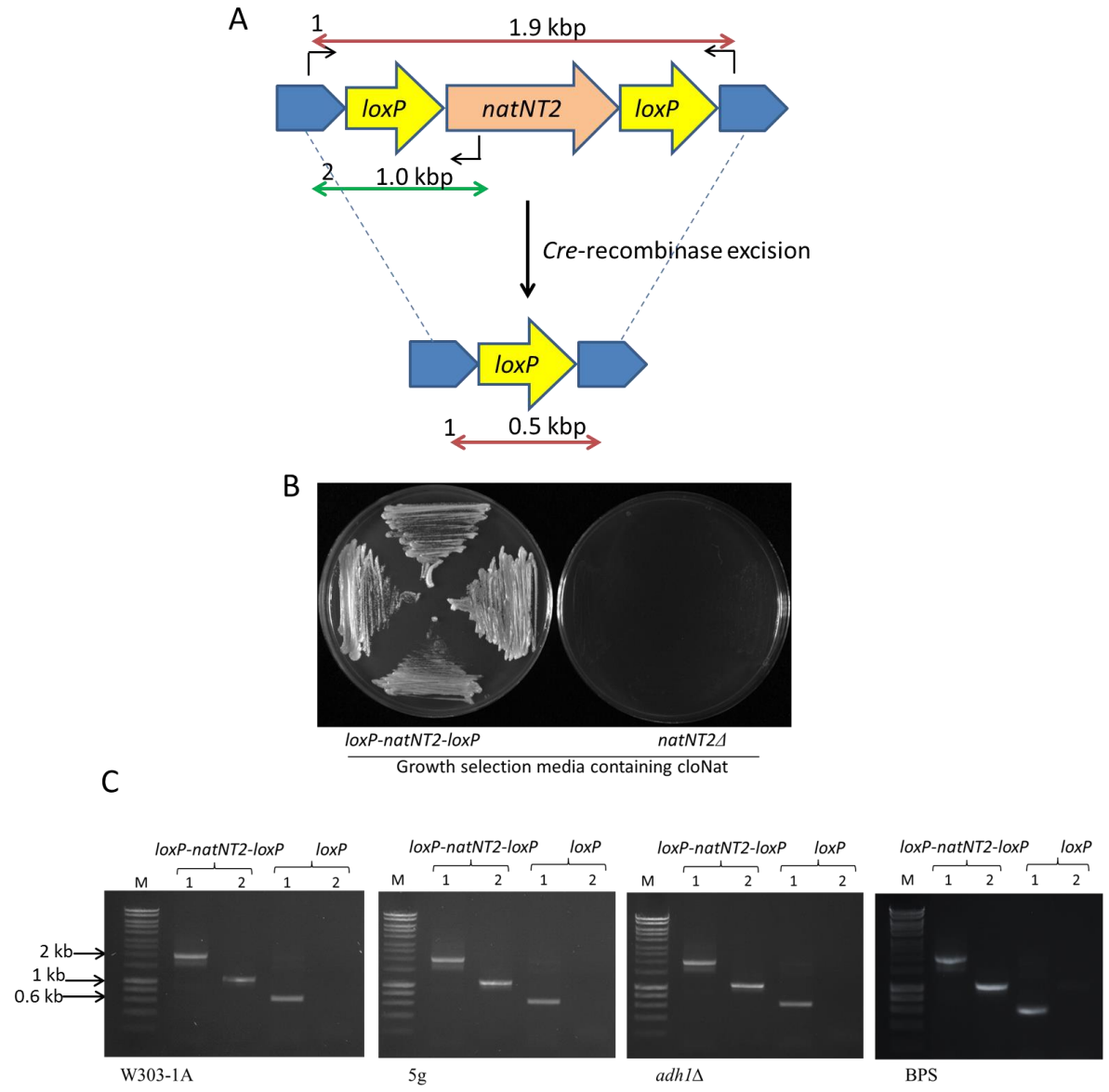

Figure 4.5 Cre-recombinase excision of loxP site from yeast strains

Figure shows; (A) strategy for the excision of *natNT2* gene using the *Cre*-recombinase excision system and verification by PCR amplification using site specific primers. (B) Images showing growth of the *natNT2* and *natNT2Δ* strains on media containing 100 µg/ml cloNat (C) Image of 1% agarose gels showing the sizes of the verification PCR products after their separation by electrophoresis. Name of strains are written under the gel pictures

4.4.4 Construction of *cit2Δ mls1Δ* strains.

As the final step in construction of the *cit2Δ mls1Δ* strains*, MLS1* was deleted in the unmarked *CIT2* deletion (*cit2::loxP*) strains, as described in section 4.4.2 above. Potential transformants were selected on media containing 100 µg/ml cloNat and genomic verification of transformants was done through PCR analysis as previously described (section 4.4.2). The sizes of the PCR products were verified by gel electrophoresis confirming that *MLS1* has been successfully deleted to generate *cit2Δ mls1Δ* mutant strains (Fig 4.6).

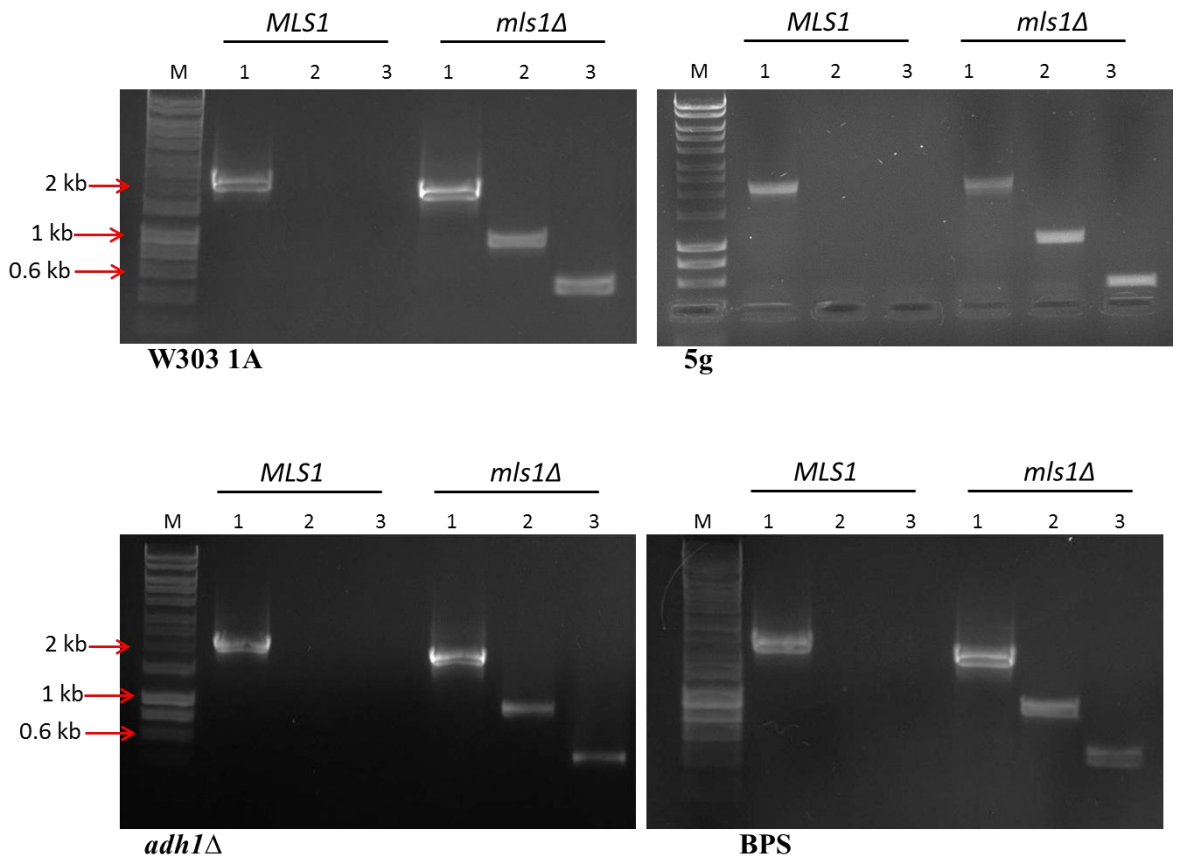

Figure 4.6 Verification of cit2Δ mls1Δ strains.

Figure is images of 1% agarose gel; showing the sizes of the verification PCR products (1, 2 and 3) similar to the verification of *mls1Δ* single deletion as shown in figure 4.4. The strain's name is written below each image.

4.5 Growth on ethanol, acetate and glycerol

The glyoxylate cycle enables yeast to utilise C2 compounds such as ethanol and acetate or fatty acids as a sole carbon source (Chen *et al*, 2012); therefore, the growth phenotypes of the mutant strains were characterized by a spot test assay on minimal media containing non fermentable carbons including: ethanol, acetate or glycerol (Fig 4.7). The result shows that *cit2Δ* strains were able to grow at a similar rate to their corresponding parent strains on all the media; this result is similar to Chen et al., (2012) whose results show that *cit2Δ* mutants grow on ethanol, acetate and glycerol containing media and they suggest a glyoxylate cycle bypass in the *cit2Δ* mutant as the possible explanation for their result. The *mls1Δ* and *mls1Δ cit2Δ* strains in the W303, 5g and *adh1Δ* backgrounds exhibit growth inhibition on all the media as previously reported (Chen *et al*, 2012; Kunze *et al*, 2006). However in the BPS strain background, the *mls1Δ* and *mls1Δ cit2Δ* mutants grows similar to the parent strain on all media. The ability of BPS *mls1Δ* and BPS *mls1Δ cit2Δ* strains to grow on acetate, ethanol and glycerol may be due to the uncharacterised glyoxylate cycle bypass suggested by Chen et al., (2012) and/or the overexpression of Acs2p enzyme (which catalyses the conversion of acetate to acetyl-CoA) It might be that the native Acs2p is not well expressed and overexpressing the synthetic Acs2p from a strong promoter rescues growth of the strains

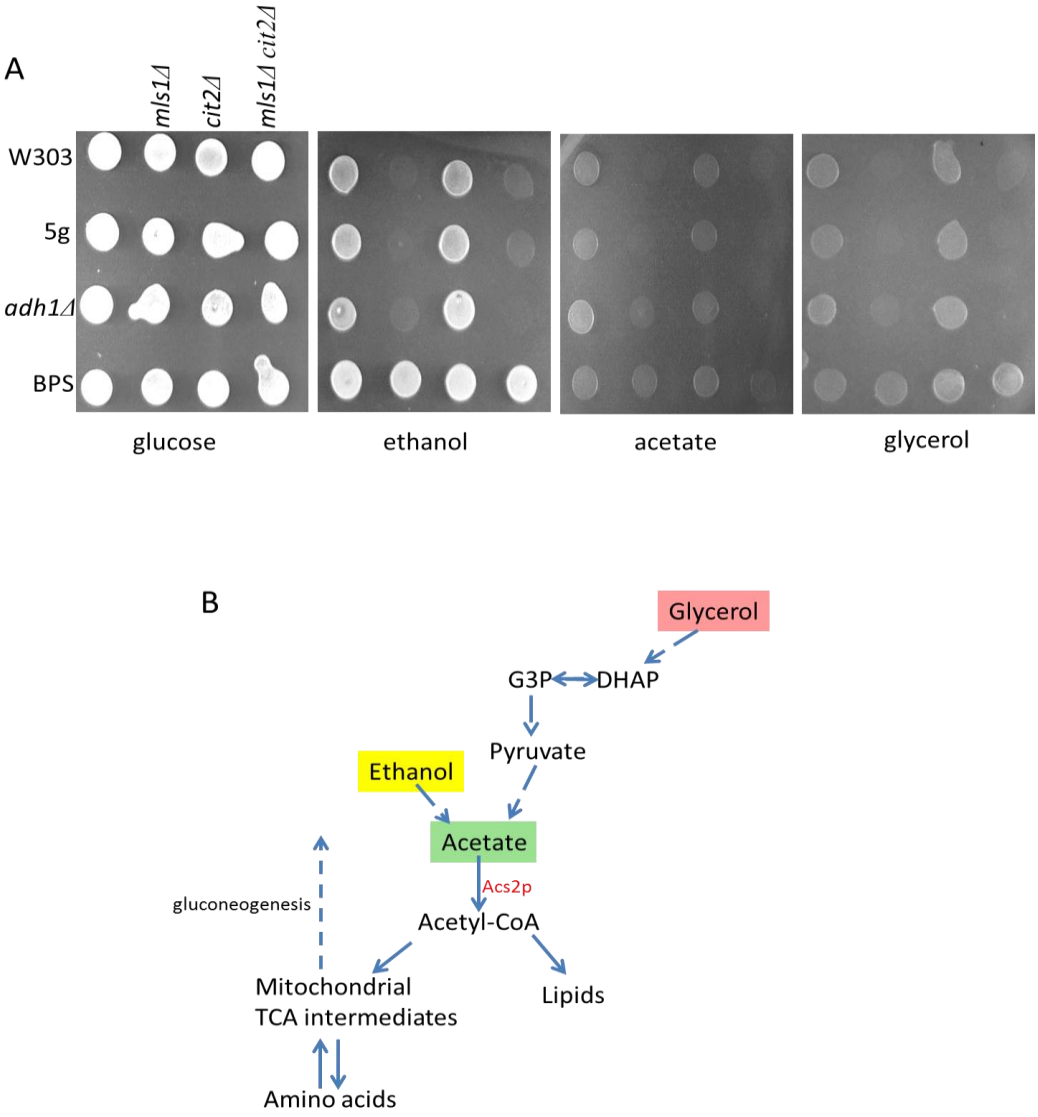

Figure 4.7 Growth of the strains on ethanol, acetate, and glycerol.

Figure is (A) photographic images of the growth medium showing the growth of the parent strains and the *mls1Δ*, *cit2Δ* and *mls1Δ cit2Δ* mutant strains after four days. (B) is summary of routes for ethanol, glycerol and acetate assimilation in *S. cerevisiae*. G3P and DHAP are acronyms for glyceraldehyde-3-phosphate and dihydroxyacetone phosphate respectively.

4.6 Measurement of intracellular acetyl-CoA abundance

Inhibiting the glyoxylate cycle (by deleting *CIT2* and/or *MLS1*) may lead to accumulation of acetyl-CoA and acetate in cells (Chen *et al*, 2012; Krivoruchko *et al*, 2013). However, how this would be affected by the various other genetic modifications made in the butanol producing strain and its derivatives is not known. Therefore, after constructing the various deletion mutant strains; their level of intracellular acetyl-CoA was measured (Fig 4.8). The strains were grown under the same semi-anaerobic growth conditions that favour butanol production and total cellular metabolites were extracted from the strains after which acetyl-coA levels were measured in the samples using an acetyl-CoA assay kit (Sigma-Aldrich) as described in materials and methods.

4.6.1 Intracellular acetyl-CoA in the parent strains

The results show that the BPS strain has higher intracellular acetyl-CoA concentrations than the three control strains (*adh1Δ*, 5g and W303-1A)(Fig 4.8). This increase is consistent with this strain containing an engineered overexpression pathway for acetyl-CoA synthesis (the overexpression of *ALD6* and *ACS2*). The *adh1Δ* strain has slightly higher acetyl-CoA compared to the W303-1A parent strain; this may be due to an accumulation of acetaldehyde (a cytotoxic intermediate), which is metabolised by endogenous levels of aldehyde dehydrogenase and acetyl-CoA synthase enzymes. Acetyl-CoA levels in the 5g strain are similar to the W303-1A parent.

4.6.2 Intracellular acetyl-CoA in *MLS1* and *CIT2* single deletion strains

The BPS *mls1Δ* mutant has higher acetyl-CoA levels than either the BPS or the other three *mls1Δ* mutant strains. In the 5g *mls1Δ* and W303-1A *mls1Δ* strains there are increases in acetyl-CoA compared to both the 5g and W303-1A parent strains respectively. These results are consistent with the conclusion that deletion of *MLS1* has disrupted the glyoxylate shunt and limited acetyl-CoA consumption. However, the levels of acetyl-CoA in the *adh1Δ mls1Δ* mutant are lower than in the *adh1Δ* mutant strain.

Similar to the effects of *MLS1* deletion; there is an increase in acetyl-CoA in the BPS *cit2Δ,* 5g *cit2Δ* and W303 *cit2Δ* strains compared to their respective parent strains. However, similar to the *adh1Δ mls1Δ* strain, the level of acetyl-CoA in the *adh1Δ cit2Δ* strain is lower than in the *adh1Δ* parent strain. The reason the deletions do not increase acetyl-CoA in the *adh1Δ* strain is unclear. However, strains lacking Adh1p may require an active glyoxylate shunt for the supply of reducing equivalent (via malate dehydrogenase) and essential intermediates (such as succinate, oxaloacetate and citrate) needed for metabolism and growth.

Overall, the results confirm that deletion of *CIT2* or *MLS1* individually lead to acetyl-CoA accumulation, except in *adh1Δ* strain background where the deletions cause decreases.

4.6.3 Intracellular acetyl-CoA in *CIT2 MLS1* double deletion strains

The most dramatic increase in acetyl-CoA levels observed across the strains was in the BPS *cit2Δ mls1Δ* mutant suggesting that combining the *MLS1* and *CIT2* mutations had an additive effect on acetyl-CoA concentrations. Again, decreased acetyl-CoA concentrations were observed when *MLS1* and *CIT2* were deleted in the *adh1Δ* mutant. In contrast, these deletions did not increase acetyl-CoA concentrations in the W303 or 5g strains.

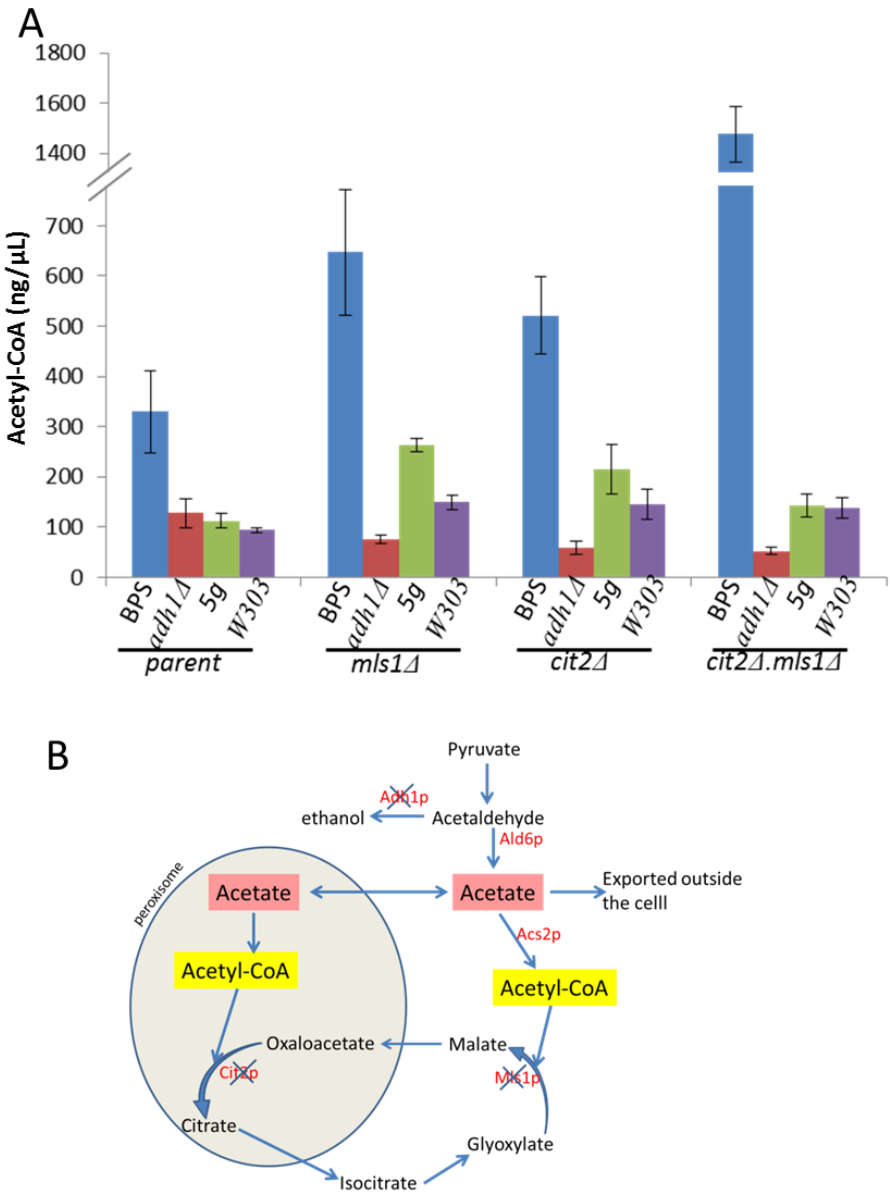

Figure 4.8 Comparison of intracellular acetyl-CoA in the parents and the mls1Δ, cit2Δ and mls1Δ cit2Δ mutant strains

Figure shows (A) graph of acetyl-CoA levels across the strains. Data represents the mean of three biological replicates with standard error bars. (B) Schematic showing the inhibition of the glyoxylate cycle in the BPS yeast strain.

4.7 Alcohol fermentation experiments in mls1Δ and cit2Δ mutant strains

After validating the construction of the *mls1Δ*, *cit2Δ* and *mls1Δ cit2Δ* mutant strains, fermentation studies were conducted to investigate yields of butanol. Cells

were grown under semi-anaerobic conditions in 50 ml sealed glass bottles for up to 18 days at 30^{o}C. Results of five biological repeats were recorded.

4.7.1 Fermentation with the W303-1A background strains

Growth analysis of the W303-1A wild-type strain and corresponding mutant strains revealed (Fig 4.9A) that the *cit2Δ* mutant has a similar growth profile to the parent strain, while there was a slight reduction in growth of the *mls1*Δ strain at day 9 compared to the parent. The *cit2Δ mls1Δ* mutant initially grew better than the parent (with a higher OD_{600}) at day 4 but then grew similar to the parent strain. There seem to be no appreciable difference in ethanol yield between the parent strains and any of the three mutant strains, and no butanol was detected for any of the strains (Fig 4.9B). Chen et al., (2012) reported similar growth and maximum ethanol yield among their *cit2Δ*, *mls1Δ* and parent strains. Overall, the results suggest that deleting *MLS1* and or *CIT2* in wild-type yeast strain W303 strain did not cause any major differences in fermentation and biomass accumulation.

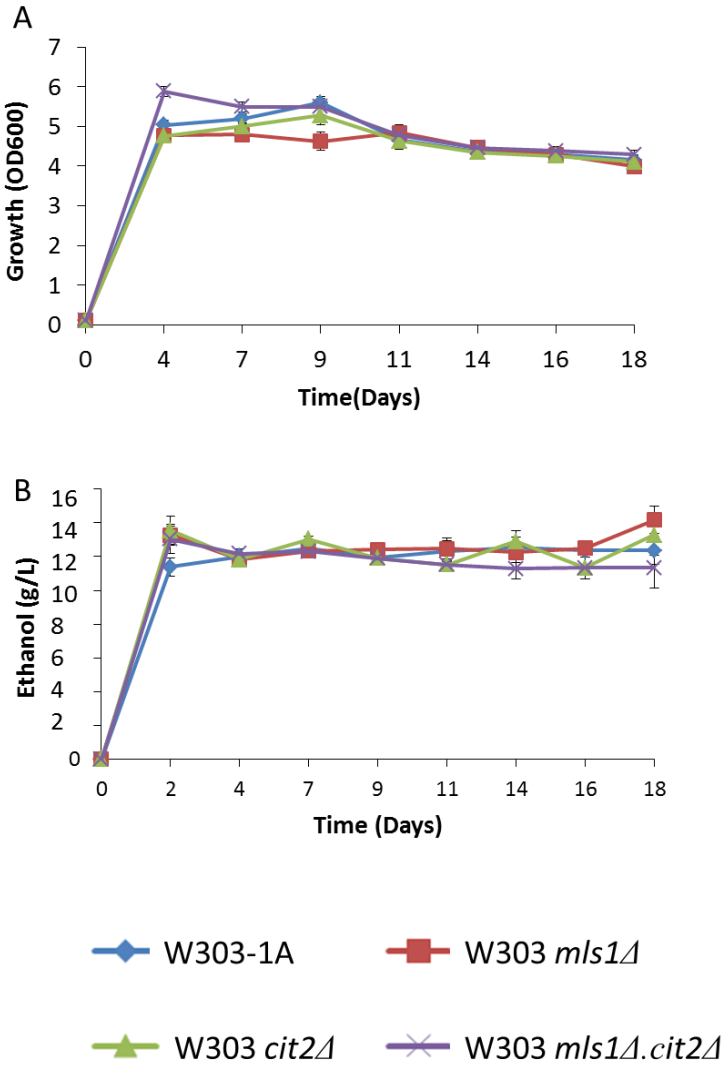

Figure 4.9 Fermentation yield in the W303-1A background strains

Figure shows (A) Growth and (B) ethanol levels in W303-1A strain and corresponding glyoxylate cycle mutants during fermentation. Data represents the mean of five biological replicates with standard error bars.

4.7.2 Fermentation with the 5g background strains

This result for the 5g strains is similar to the W303-1A strains. The *cit2Δ* and *mls1Δ* strains have similar growth profiles to the 5g parent strain (Fig 4.10A). The *mls1Δ cit2Δ* strain has a slightly higher cell density (OD_{600}) on day 4 compared to the 5g parent strain (Fig 4.10A). Ethanol production profile is similar across all the strains and butanol was not detected in any of the strains (Fig 4.10B). These results suggests that the *CIT2* and *MLS1* deletions did not cause any appreciable difference in the fermentation yield of the 5g strain which contains five heterologous butanol synthetic genes.

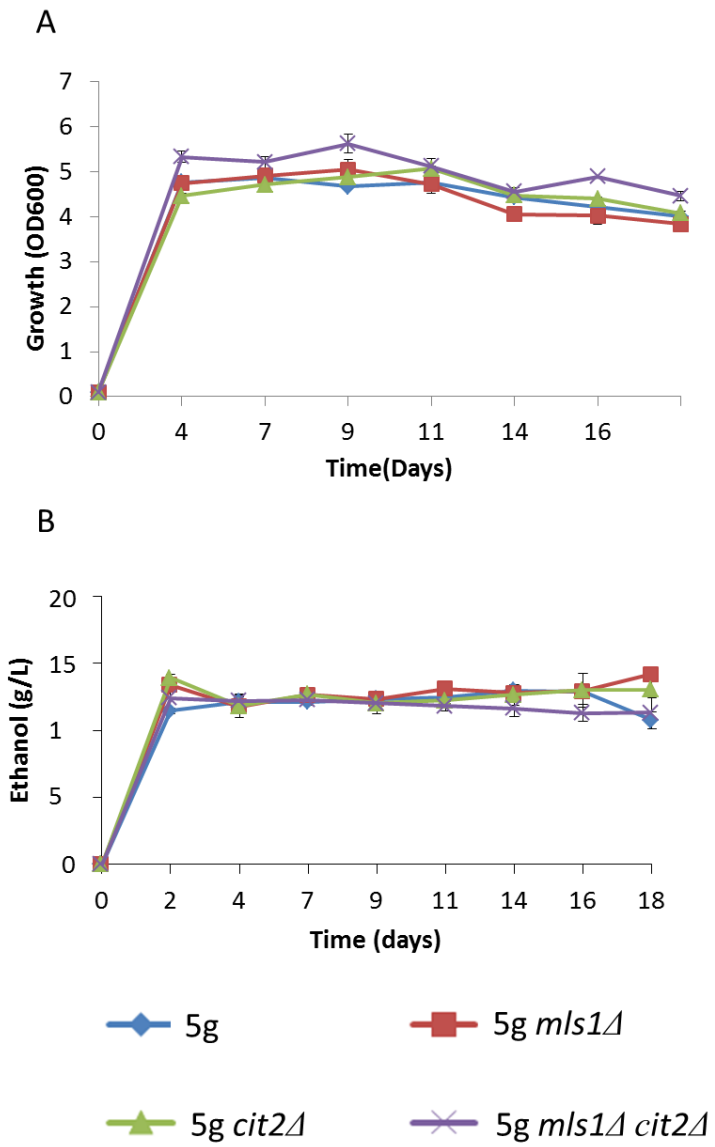

Figure 4.10 Fermentation yield in the 5g background strain

Figure shows (A) Growth and (B) ethanol levels in the 5g strain and corresponding glyoxylate cycle mutants during fermentation. Data represents the mean five biological replicates. Standard error bars are included

4.7.3 Fermentation with the *adh1Δ* background strain

Growth analysis showed that the *cit2Δ* mutant has significantly lower growth and biomass compared to *mls1Δ, mls1Δ cit2Δ* mutants and the *adh1Δ* parent strain. Kocharin et al., (2012) also reported lower biomass yield in their recombinant *cit2Δ* strain compared to *mls1Δ* strain, and both deletion strains have lower biomass compared to their non-deletion reference strains. Our result for, the *mls1Δ* mutant shows similar maximum cell density compared to the parent; however, there was initially a slight decrease in the growth rate compared to the parent strain. The growth rate of the *cit2Δ mls1Δ* mutant is lower compared to the parent strain (fig 4.11A). The ethanol yield profile shows a growth dependent trend (Fig 4.11B). In terms of butanol production (Fig 11C); the *cit2Δ* mutant has lower butanol yield compared to *mls1Δ*, *mls1Δ cit2Δ* and the parent, butanol yield for the *mls1Δ* mutant initially lagged behind that of parent strain but the strain got to similar maximum yield after day 11. The butanol of the *cit2Δ.mls1Δ* mutant shows an initial lag and slightly lower overall yield compared to the reference strain. Overall, none of the constructed mutants improve the butanol yield relative to the *adh1Δ* parent strain.

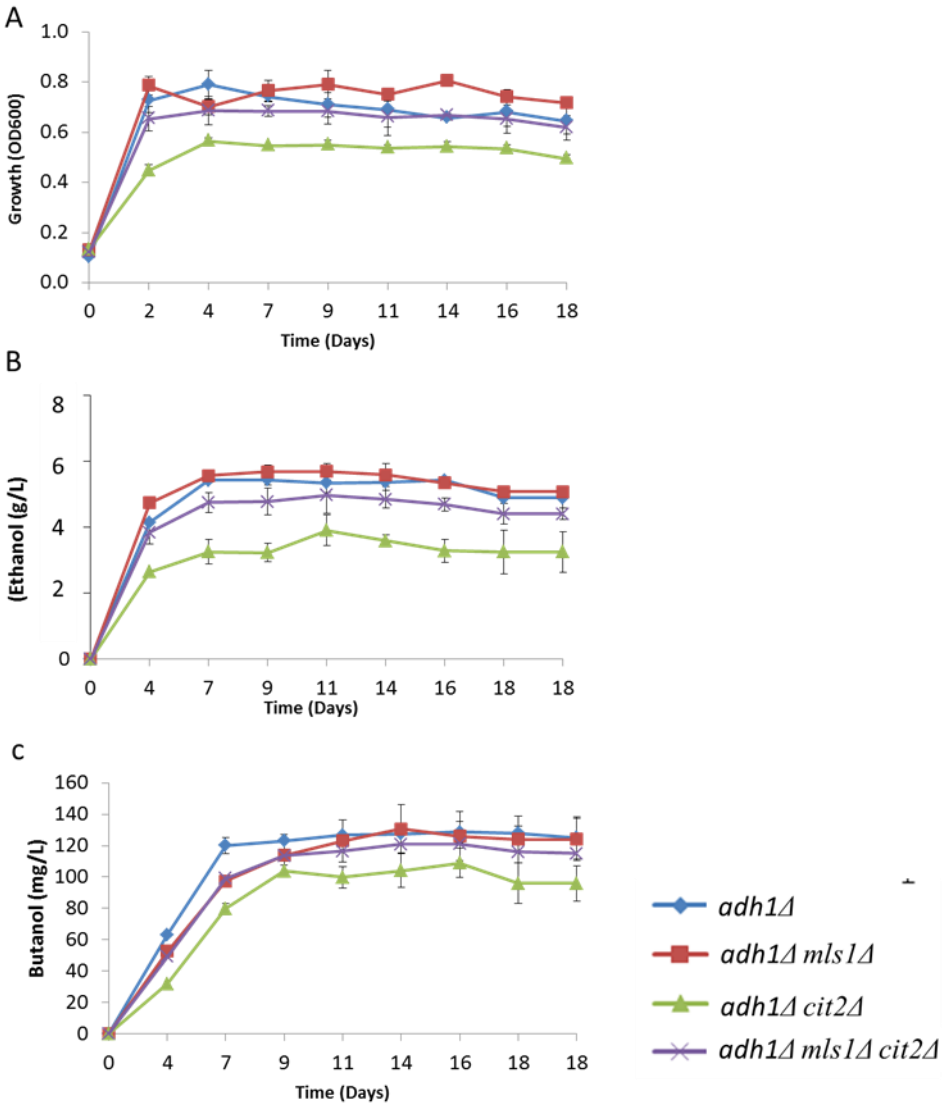

Figure 4.11 Fermentation in the adh1Δ background strains

Figure shows (A) growth curve, (B) butanol levelsd and (C) ethanol levels in the *adh1Δ* strain and corresponding glyoxylate cycle mutants during fermentation. Data represents the mean of five biological replicates with standard error bars included.

4.7.4 Fermentation with the BPS background strains

Our result on acetyl-CoA measurement shows increase in acetyl-CoA of the BPS upon deletion of *CIT2* and *MLS1*; we therefore anticipated that this might increase butanol production in the strain. However, the deletions led to severe decreases in butanol production in the mutants in a manner that seems dependent upon their growth (Fig 4.12A &C). Interestingly the amount of butanol produced in these strains is similar to the butanol yield of *adh1Δ* (~100mg/L) (Fig 4.11C); this suggests that the deletions may have obstructed the butanol synthetic pathway. Result shows that deleting *CIT2* and/or *MLS1* in the BPS leads to a severe decrease in growth rate and final cell yield of the mutants compared to the BPS parent strain (fig 4.12A); this result is similar to that of Kocharin *et al*., (2012) who reported a decrease in biomass of both their *cit2Δ* and *mls1Δ* mutants compared to their reference parent strains. Ethanol yield across the mutants is similar but lower compared to the parent strain.

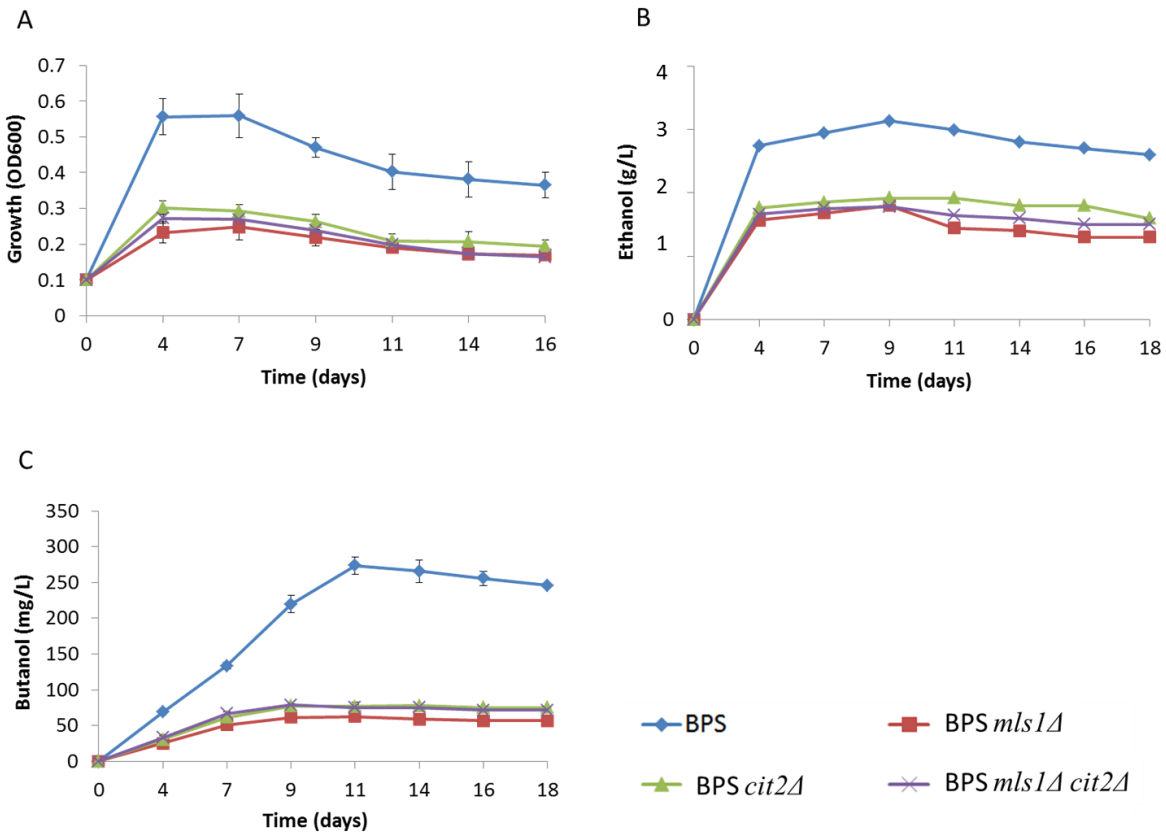

Figure 4.12 Fermentation in the BPS background strains

Figure shows (A) growth curve, (B) butanol levelsd and (C) ethanol levels in the BPS strain and corresponding glyoxylate cycle mutants during anaerobic culturing in rich media Data represents the mean of five biological replicates with standard error bars included.

Table 4.1 compares the peak fermentation yield across the mls1Δ, cit2Δ, mls1Δ cit2Δ and their respective parent strains. No butanol is produced across the W303 or 5g strain backgrounds and the ethanol titre is comparable across the W303 and 5g strains. In the *adh1⊿* strains, ethanol titre is lower compared to W303 however; the ethanol titre/OD_{600} values are higher compared to W303. Butanol production in the adh1Δ strain is unaffected by the deletions of *MLS1*, and/or *CIT2* genes. In the BPS strain, the deletions led to decrease in ethanol production, however, the ethanol titre/OD_{600} is comparable across the group. There is decrease in butanol production with deletions of *MLS1* and/or *CIT2* in the BPS strain.

Table 4.1 Summary of peak growth, ethanol and butanol across the strains with *mls1Δ, cit2Δ* and *mls1Δ cit2Δ* mutations

Strain	Max growth (OD_{600} unit)	Ethanol titre (g/L)	Ethanol titre/OD_{600} (g/L/OD_{600})	Butanol titre (mg/L)	Butanol titre/OD_{600} (mg/L/OD_{600})
W303 1A	5.76 ± 0.3	11.5 ± 0.55	2.0	-	-
W303 *mls1⊿*	4.84 ± 0.2	13.3 ± 0.63	2.75	-	-
W303 *cit2⊿*	5.28 ± 0.2	13.4 ± 0.98	2.54	-	-
W303 *cit2Δ mls1 Δ*	5.85 ± 0.2	13.0 ± 0.47	2.22	-	-
5g	4.85 ± 0.2	11.4 ± 0.37	2.35	-	-
5g *mls1⊿*	5.0 ± 0.3	13.6 ± 0.28	2.72	-	-
5g *cit2⊿*	4.87 ± 0.4	13.8 ± 0.25	2.83	-	-
5g *cit2Δ mls1Δ*	5.61 ± 0.3	12.7 ± 0.16	2.26	-	-
adh1⊿	0.76 ± 0.06	5.5 ± 0.4	7.24	122 ± 4.2	160.5
adh1⊿ mls1⊿	0.78 ± 0.04	5.6 ± 0.2	7.18	128 ± 18.5	164.1
adh1⊿ cit2⊿	0.45 ± 0.02	3.8 ± 0.3	8.44	98 ± 12.6	217.7
adh1Δ cit2Δ mls1Δ	0.64 ± 0.04	4.8 ± 0.6	7.5	120 ± 7.8	187.5
BPS	0.66 ± 0.05	3.1 ± 0.01	4.7	273 ± 14	413
BPS *mls1⊿*	0.4 ± 0.03*	1.8 ± 0.01*	4.5	62.6± 3.2*	156.5
BPS *cit2⊿*	0.43 ± 0.02*	1.9 ± 0.01*	4.42	76.8 ± 5.8*	178.6
BPS *cit2Δ mls1Δ*	0.41 ± 0.02*	1.8 ± 0.01*	4.39	75.3 ±4.5*	183.7

Standard errors of three biological replicates is indicates as (±). Student's t-test analysis was used for statistical analysis of the data for the BPS background strains in triplicates. Asterix sign (*) indicates a result that was significantly different compared to the reference BPS strain ($p < 0.05$).

4.8 Discussion

Acetyl-CoA is both a precursor and a building block for the biosynthesis of many interesting commodity products (Fig. 4.2). The exploitation of *S. cerevisiae* as a host organism for the production of these chemicals has valid biotechnological advantages. Therefore, the development and improvement of yeast cell factories for production of acetyl-CoA derived products represents an important strategy towards commercial commodity chemical and biofuel production. Increasing cytosolic acetyl-CoA abundance as a strategy to improve production of its derivable products has been reported in yeast (Chen *et al*, 2013; Kocharin *et al*, 2012; Krivoruchko *et al*, 2013).

The BPS yeast strain used in our studies was engineered for increased acetyl-CoA synthesis by a "block-pull" strategy. The 'block' strategy is designed to inhibit ethanol synthesis by deleting *ADH1*; this leads to accumulation of acetaldehyde. The 'pull' strategy involves overexpressing Ald6p and Acs2p for metabolizing acetaldehyde to acetyl-CoA. (Swidah *et al*, 2015). Our results suggest that the engineered acetyl-CoA synthetic pathway in the BPS strain is active, as demonstrated by the high levels of acetyl-CoA in the strain compared to control strains lacking this Ald6p/Acs2p overexpression. The result represents the total intracellular acetyl-CoA levels and not just cytosolic concentrations; however these may also report the relative cytosolic abundance. To further increase level of cytosolic acetyl-coA available for butanol synthesis in the strain, we deleted the *CIT2* and *MLS1* genes encoding citrate synthase 2 (Cit2p) and malate synthase 1 (Mls1p): these enzymes catalyse the two reactions of acetyl-CoA consumption in the glyoxylate cycle respectively. In our BPS yeast system, the singly and combined deletions of *CIT2* and *MLS1* led to increases in intracellular acetyl-CoA as expected however, these deletions caused unexpected decreases in

butanol production in the *cit2Δ* , *mls1Δ* and *mls1Δ cit2Δ* mutants. Since butanol is synthesized during the ethanol phase (after glucose is consumed in the growth media (Krivoruchko *et al*, 2013)); this suggests the involvement of mitochondrial metabolism and since the glyoxylate cycle is a source of intermediates for mitochondria metabolism and protein synthesis under certain conditions (Chen *et al*, 2012; Lee *et al*, 2011), its obstruction in the yeast BPS strain (lacking Adh1p) may prevent supply of metabolic intermediates needed for the marginal mitochondrial activities (which may be necessary for the cells to meet metabolic and physiological needs). This situation may present a 'survival' or 'butanol production' choice to the cell and may lead to inhibition of the butanol synthetic pathway in the mutants. Furthermore, since acetyl-CoA also serves as a signaling molecule which reports the energy status of the cell, its high abundance may signal the redirection of carbon flux away from central carbon energy metabolism on which the butanol synthetic pathway depends. Kocharin *et al*., (2012) similarly reported a decrease in biomass and poly-(R)-3-hydroxybutyrate (PHB) in their recombinant yeast after deleting *CIT2* or *MLS1* in the strain. Krivoruchko *et al*., (2013) reported an improvement in product yield (butanol) after deleting *CIT2* or *MLS1* in their recombinant yeast. Their result shows the importance of acetyl-CoA metabolism towards improving butanol production in yeast. Chen *et al. (2013)* also reported an improvement in α-santalene (an acetyl-CoA-derivable product) after deleting *CIT2* or *MLS1* in their engineered yeast. In both reports by Krivoruchko *et al*., (2013) and Chen *et al.* (2013); they used cells having active/intact Adh1p suggesting the importance of this enzyme for yeast robustness and bio-production.

4.9 Conclusion

The development of robust yeast platform cell factories for the production of fuels and chemicals has been the focus of much research. Here, we tested a strategy to increase acetyl-CoA abundance in the cytosol with a view to improving butanol production in our recombinant yeast BPS strain. Our results do show increased acetyl-CoA when the gyloxylate cycle is disrupted, which confirms the involvement of the glyoxylate cycle in acetyl-CoA utilization. However, the increased acetyl-CoA does not translate into improved butanol production especially in the BPS mutants. Interestingly, our result reveals that there is high level of intracellular acetyl-CoA in the parent BPS strain which suggests that its supply is not limiting; this however implies that the assimilation of acetyl-CoA through the butanol synthetic pathway may be limited probably due to low efficiency of the pathway's rate-limiting and committed reaction. The condensation of two acetyl-CoA molecules to form acetoacetyl-CoA is an important step committing acetyl-CoA towards butanol synthesis. However, under physiological condition the thiolase enzyme favours thiolytic cleavage in the reverse direction (Kim *et al*, 2015; Mann & Lutke-Eversloh, 2013); therefore, optimising this step may improve acetyl-CoA consumption through the pathway and increase butanol production.

5. Thiolase engineering for improved butanol production in yeast

5.1 Introduction

Biosynthetic thiolase (thiolase II) is a key enzyme responsible for carbon fixation in nature; this enzyme catalyses the reversible Claisen condensation of two molecules of acetyl-CoA to give acetoacetyl-CoA, which initiates the synthesis of high energy reduced compounds such as mevalonate (in eukaryotes), polyhydroxybutyrates and butanol (in bacteria) (Fox *et al*, 2014). The thiolase reaction mechanism involves thioester bond formation between the enzyme's cysteine catalytic residue and a carbonyl carbon on the CoA moiety (substrate). Thiolase II is highly conserved in nature and under stress conditions is thought to redirect metabolic flux for the production of antioxidants (hydroxybutyrates and isoprenoids) and reducing equivalents (NAD(P)H)(Fox *et al*, 2014). In *C. acetobutylicum*, thiolase II regulates the phase transition from acidogenesis to solventogenesis 'acetone-butanol-ethanol' production and its activity is regulated through a redox-switch mechanism via reversible formation of a disulphide bond between its catalytic cysteine residues. The enzyme is also competitively inhibited by its reaction by-product, coenzyme A (Kim *et al*, 2015).

Improved butanol yield was demonstrated after optimising thiolase activity in *Clostridium* (Kim *et al*, 2015). A 2-fold increase in butanol yield was described when overexpressing a non-redox-regulated mutant of *C. acetobutylicum* thiolase ($thlA^{red}$ - with three amino acids substitutions - V77Q/N153Y/A286K). The mutant is not able to form disulphide bonds using the catalytic cysteine residues, and it has higher activity than native *C. acetobutylicum* thiolase (*thlA*). Another thiolase optimising attempt identified a C*. acetobutylicum* mutant thiolase ($thlA^{CoA}$) from a random mutant library

screening method (Mann & Lutke-Eversloh, 2013). This mutant contains three amino acid substitutions (R133G/H156N/G222V) and has a reduced affinity for Coenzyme A (its physiological inhibitor) leading to an 18% increased butanol titre in *C. acetobutylicum*.

5.2 Acetyl-CoA accumulates in the BPS strain

In the butanol production yeast strain (BPS), there is high accumulation of acetyl-CoA compared to the control strains (Fig 5.1). This result confirms that over-expression of *ALD6* and *ACS2* (the acetyl-CoA synthetic pathway) in the strain is active. However, this accumulation of acetyl-CoA suggests that acetyl-CoA consumption by the ABE-butanol synthetic pathway is sub-optimal. The condensation of two acetyl-CoA to form acetoacetyl-CoA is the initiating commitment step of the acetyl-CoA dependent butanol synthetic pathway and this reaction step is thermodynamically unfavourable (Modis & Wierenga, 1999; Modis & Wierenga, 2000) and may therefore be limiting in a yeast system. Optimising this reaction step may prove important in improving acetyl-CoA utilisation and butanol production by yeast strains.

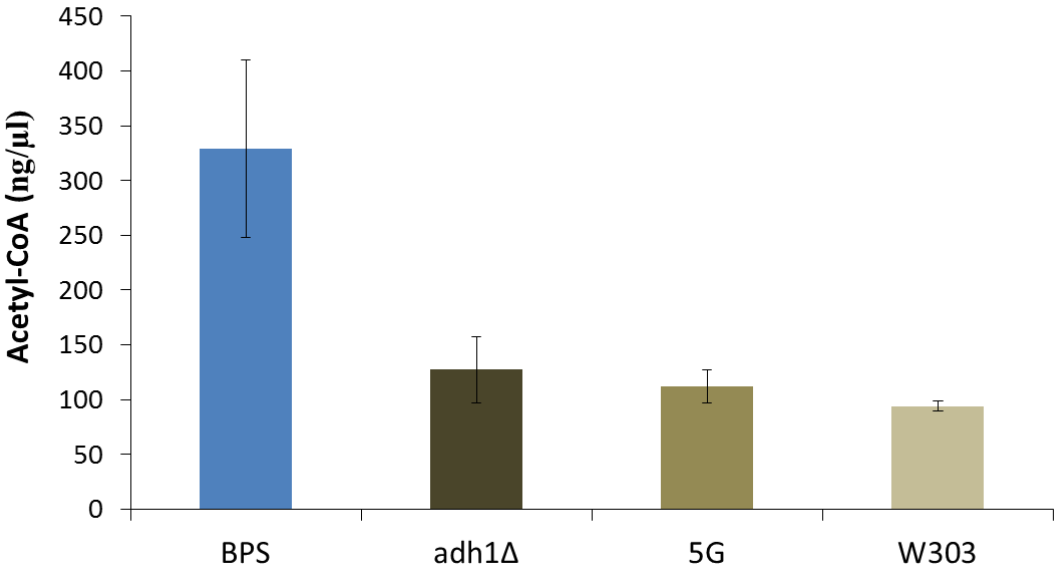

Figure 5.1 Comparison of intracellular concentrations of acetyl-CoA in the BPS and control yeast strains.

Graph shows the levels of acetyl-CoA in the BPS strain compared to levels in *adh1Δ*, 5g and W303-1A control strains. Data represents the mean of three biological repeats with standard error bars.

5.3 Optimising thiolase function in BPS yeast strain

Four bacterial thiolases were selected for analysis in the BPS yeast strain. These thiolases were selected based on their predisposition towards high product yield in their native hosts. *Zoogloea ramigera* thiolase II (PhaA) participates in the production of high levels of polyhydroxybutyrate, while *C. acetobutylicum* thiolase II (ThlA) is naturally involved in butanol synthesis. In addition, two mutant forms of the ThlA thiolase; $ThlA^{red}$ and $ThlA^{CoA}$ were selected as having higher activities than the native type ThlA thiolase (Kim *et al*, 2015; Mann & Lutke-Eversloh, 2013). The $ThlA^{red}$ thiolase mutant has three amino acids substituted (V77Q/N153Y/A286K) and is unable to form a disulphide bond between two catalytic cysteine residues (Cys88 and Cys378) thus preventing its switch to an inactive (oxidized) form (Kim *et al*, 2015). Under oxidized conditions, Cys378 rotates 180^{o} towards Cys88 via rotation of the peptide bond between Leu377 and Cys378 leading to disulfide bond formation between the two catalytic cysteine residues. These changes cause a large conformational alteration in the catalytic cysteine loop (residues 378–384) which in turn moves away from the active site (as illustrated in Fig 5.2), making the oxidized ThlA thiolase inactive (Kim *et al*, 2015). The $ThlA^{CoA}$ thiolase has lower affinity for Coenzyme A (its physiological inhibitor) than ThlA; this mutant has three amino acid changes (R133G, H156N, G222V) within the enzyme's loop domain (Mann & Lutke-Eversloh, 2013) which interacts with the CoA moiety during catalysis (Modis & Wierenga, 1999; Modis & Wierenga, 2000).

Each of the four bacterial thiolase genes were codon optimized for yeast expression and transformed into the yeast BPS* strain (the BPS strain lacking the exogenous *ERG10* gene) to generate four new strains:

1. BPS*_thlA :_* Strain expressing native *C. acetobutylicum thlA* thiolase

2. BPS*$thlA^{red}$:* Strain expressing *C. acetobutylicum* $thlA^{red}$ mutant thiolase

3. BPS*$thlA^{CoA}$:* Strain expressing *C. acetobutylicum* $thlA^{CoA}$ mutant thiolase

4. BPS*_phaA :_* Strain expressing native *Z. ramigera phaA* thiolase

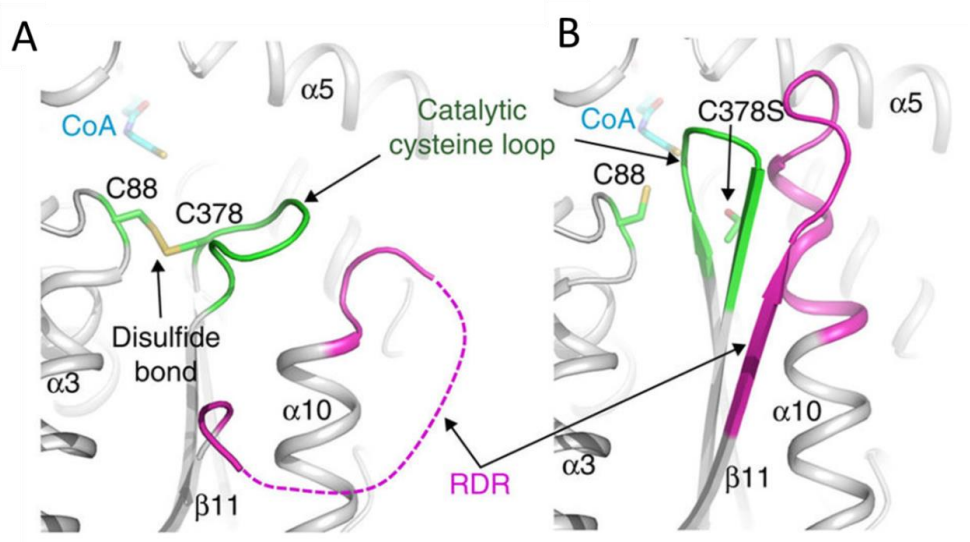

Figure 5.2 Ribbon diagram of C. acetobutylicum ThlA thiolase (active site)(Kim *et al*, 2015).

Figure shows structural changes of catalytic cysteine loop (green) and the regulatory determinant region (RDR) (magenta) of the oxidized inactive (**A**) and reduced active (**B**) form (Kim *et al*, 2015). The two catalytic cysteine residues and the CoA molecule are shown in green and cyan, respectively. The secondary structure elements are labelled as α and β (Kim *et al*, 2015).

5.4 Establishing sequence homology of thiolase II

Thiolases are known to share high sequence and structural similarity across eukaryotes and prokaryotes. Though much is reported about biosynthetic thiolases of *C. acetobutylicum* and *Z. ramigera*, little is reported about the catalytic structure of thiolase II of *S. cerevisiae*. Therefore, the sequence of the biosynthetic thiolases from *S. cerevisiae*, *C. acetobutylicum* and *Z. ramigera* were aligned in order to determine similarities: particularly in the catalytic and substrate binding domains. The thiolase sequences were obtained from Uniprot® (http://www.uniprot.org/) and were submitted to Clustal Omega® http://www.ebi.ac.uk/Tools/msa/clustalo/ for sequence alignment. The result (Fig 5.3) shows that the yeast thiolase (Erg10) has 45% and 40% sequence identity to *Z. ramigera* thiolase (PhaA) and *C. acetobutylicum* thiolase (ThlA), respectively, and there is 100% identity in the catalytic subunit residues across the three proteins.

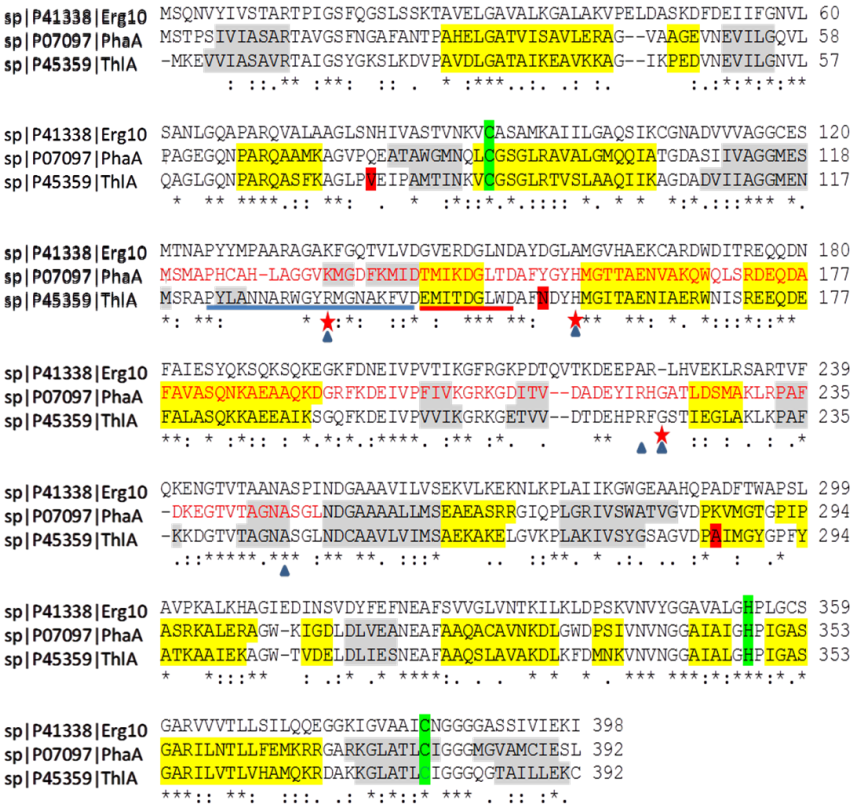

	1	2	3
1: sp|P41338|Erg10	100.00	45.52	40.15
2: sp|P07097|PhaA	40.15	57.29	100.00
3: sp|P45359|ThlA	45.52	100.00	57.29

Figure 5.3 Multi-sequence alignments for biosynthetic thiolases.

Figure shows alignment of thiolase sequences from *S. cerevisiae* (Erg10*), Z. ramegira* (PhaA) and *C. acetabutylicum* (ThlA). The secondary structure elements of PhaA and ThlA are indicated; β and α strands are grey and yellow respectively. The loop domain of PhaA is indicated by red text. Residues conserved among the three sequences are indicated with an asterix. Residues involved in CoA binding in both PhaA and ThlA (are indicated with a blue triangle (Kim *et al*, 2015). Residues belonging to the tetramerization motif of PhaA are indicated by a blue line. Residues belonging to the specificity loop, which is responsible for determining the substrate specificity of the PhaA enzymes, are indicated by the red line (Kim *et al*, 2015; Modis & Wierenga, 1999). The locations of point mutations in the ThlA redox switch mutant are coloured red (Kim *et al*, 2015), while mutations in the optimised ThlA with reduced CoA sensitivity are indicated with a red star.

5.5 Optimising bacterial thiolase sequences for expression in yeast

The protein sequences of ThlA and PhaA thiolases of *C. acetobutylicum* and Z*. ramigera* were obtained from UniProt (http://www.uniprot.org/). The *thlA* gene sequence was then adjusted to generate the two mutant versions; $thlA^{red}$ and $thlA^{CoA}$ by making mutations to give amino acid substitutions (V77Q/N153Y/A286K and R133G/H156N/G222V respectively) in the *thlA* sequence (Kim *et al*, 2015; Mann & Lutke-Eversloh, 2013). The four thiolase sequences (*thlA*, $thlA^{red}$ $thlA^{CoA}$ and *phaA*) were submitted to IDT (https://www.idtdna.com/CodonOpt) codon optimisation tool for optimization in *S. cerevisiae.* Each codon optimised sequence was then updated to match the *S. cerevisiae* codon usage table (http://downloads.yeastgenome.org /unpublished_data /codon/ysc.gene.cod). After making the appropriate codon usage update in the thiolase sequences, they were submitted to ExPASY® (http://web.expasy.org/translate/) and SWISS MODEL® (https://swissmodel.expasy.org /interactive/bPVnQS/templates/) online tools for verification and protein modeling respectively. Results produced a homotetramer protein model with up to 99% identity to Acetyl-CoA acetyltransferase (biosynthetic thiolase II) (Fig 5.4), confirming that the optimized thiolase sequences have both secondary and tertiary structure elements of acetyl-CoA acetyltransferase biosynthetic thiolase II.

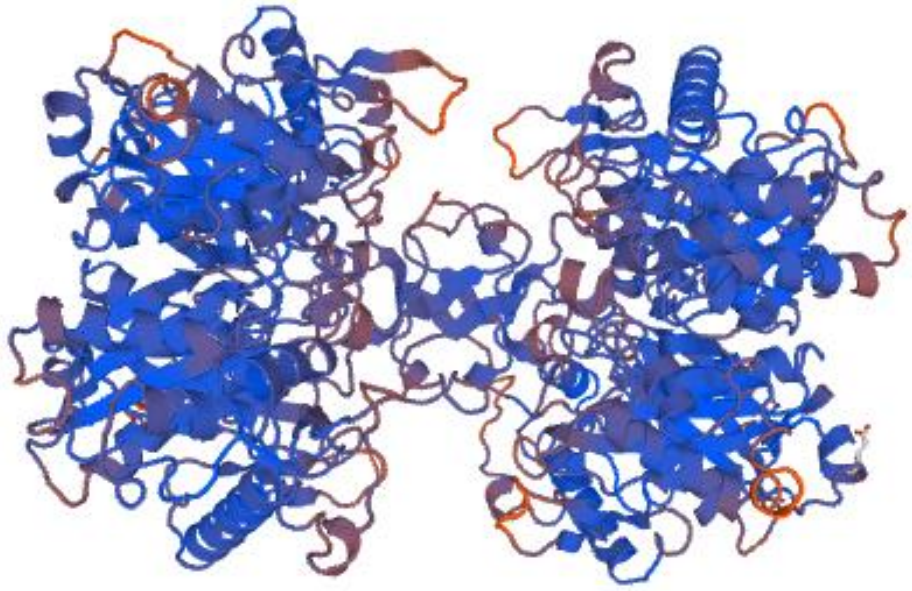

Figure 5.4 Protein model of optimised thiolase.

Figure shows the protein model of optimized thiolase sequence submitted to (https://swissmodel.expasy.org/interactive/bPVnQS/templates/). The model represents a homotetrameric protein structure.

5.6 Designing thiolase gene modules.

To enable their expression in yeast, the bacterial thiolase sequences were arranged into gene modules with the necessary gene expression control regions. More specifically, the codon-optimised thiolase sequence was placed downstream of the *TDH3* promoter sequence and upstream of a *CYC1* terminator sequence. The thiolase open reading frames were also placed in-frame with a C-terminal 3x myc protein epitope tag to allow detection. This tag sequence was flanked with *Mlu*I restriction sites to allow easy removal if necessary. The entire module was also designed with flanking *Bam*HI restriction sites to allow sub-cloning (Fig 5.5).

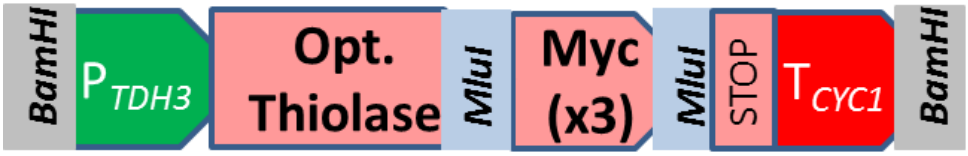

Figure 5.5 Layout of the thiolase gene module.

Diagram represents the arrangement of components in the thiolase gene module. The optimised thiolase (Opt. thiolase) is arranged with the necessary gene expression regulator units: *TDH3* promoter (P_{TDH3}) and *CYC1* terminator (T_{CYC1}). Three myc protein sequence (surrounded by *Mlu*I sites) is places in-frame to the Opt thiolase at its C-terminal. The module is surrounded by *BamHI* sites.

5.7 Synthesis of thiolase gene modules

Two of the thiolase gene modules, *thlA*^{red} and *phaA* were commercially produced by GeneArt^{TM} (Thermofischer scientific); the *thlA*^{red} gene was produced as string DNA (uncloned, linear dsDNA) fragments while *phaA* was cloned in a plasmid pMK-*phaA* having a *KanMX4* marker gene. The two other thiolase gene modules (*thlA* and *thlA*^{CoA}) could not be produced commercially as string DNA due to the complexity in their sequences and because of the constraint of our limited finances in producing them as cloned plasmid constructs, we decided to construct the two gene modules via step-wise site-directed mutagenesis of *thlA*^{red}. First *thlA* was synthesised from *thlA*^{red} by mutating three amino acid codons and then a further three amino acid codon changes were introduced to give *thlA*^{CoA}. Figure 5.6 shows a summary of the DNA cloning and mutagenesis strategies used.

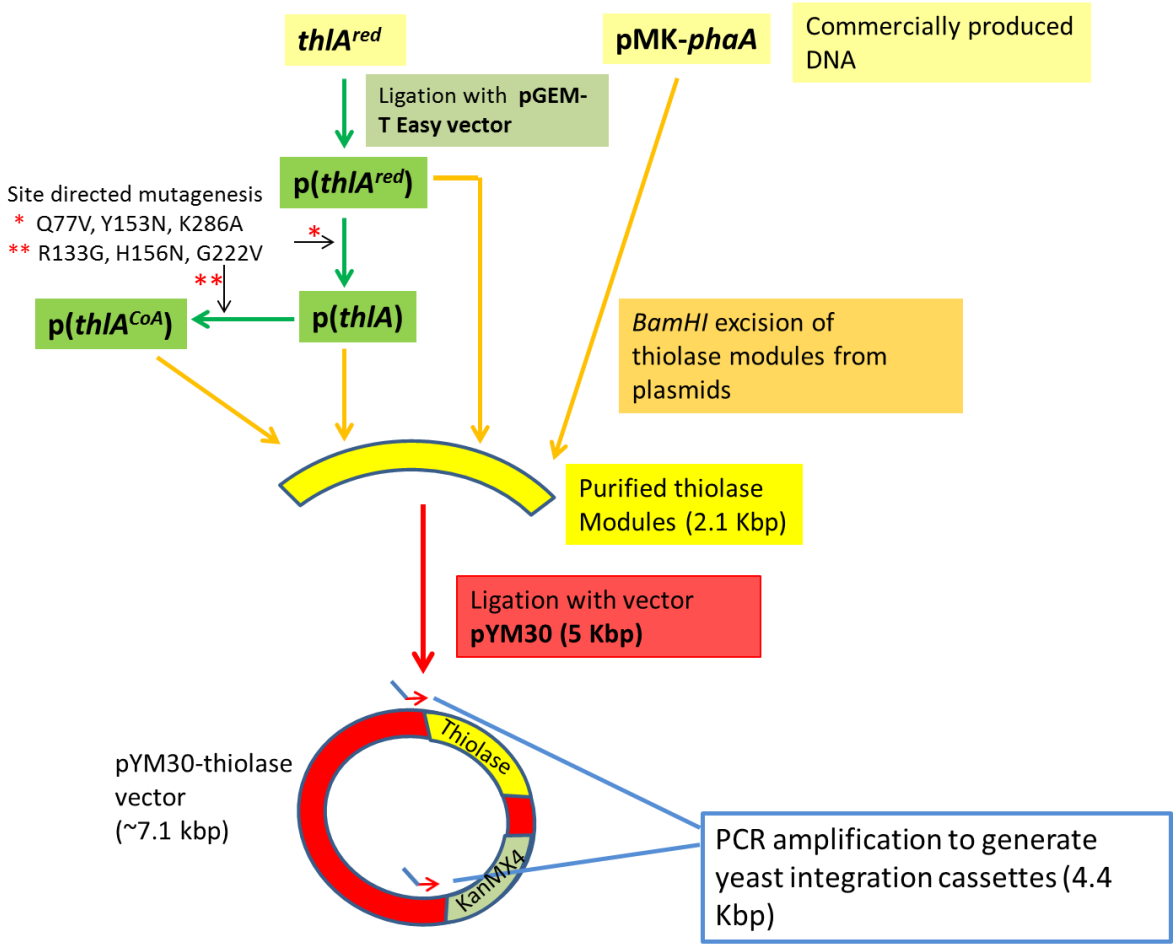

Figure 5.6 Summary of DNA cloning strategies.

Figure shows various stages involved in the construction and purification of the thiolase gene modules. ThlA^{red} is first subcloned into pGEMT-Easy. ThlA and ThlA^{CoA} were synthesised via site directed mutagenesis. Purified gene modules were finally subcloned into pYM30 plasmids and PCR is used to amplify yeast integration cassettes from the pYM30-thiolase vectors using integration primers.

5.8 Subcloning and site-directed mutagenesis of thlA^{red} gene module

The *thlA*^{red} gene module (produced as string DNA) was sub-cloned into the pGEM-T Easy vector to create a construct for easy manipulation (Fig 5.7A and 5.7B). The DNA sequence of the *thlA*^{red} gene region (2.1 Kbp) in the plasmid was verified by DNA sequencing analysis using site specific primers and was confirmed to be unaltered during the cloning procedure.

The pGEM-*thlA*^{red} construct was then used to generate the *thlA* sequence via three successive rounds of site directed mutagenesis using the Qiagen QuikChange® system. The amino acids substitutions: glutamine 77 to valine, tyrosine 153 to asparagine and lysine 286 to alanine (Q77V/Y153N/K286A) were generated. DNA sequence analysis confirmed construction of the *thlA* mutant thiolase (Fig 5.8).

The *thlA*^{CoA} module was then synthesised from *thlA* using the same strategy as above. Again three different amino acid substitutions were generated: arginine 133 to glycine, histidine 156 to asparagine and glycine 222 to valine (R133G/H156N/G222V). The DNA sequence of the altered thiolase sequence was verified to confirm that the three substitutions were successfully made in *thlA* to generate *thlA*^{CoA} (Fig 5.9).

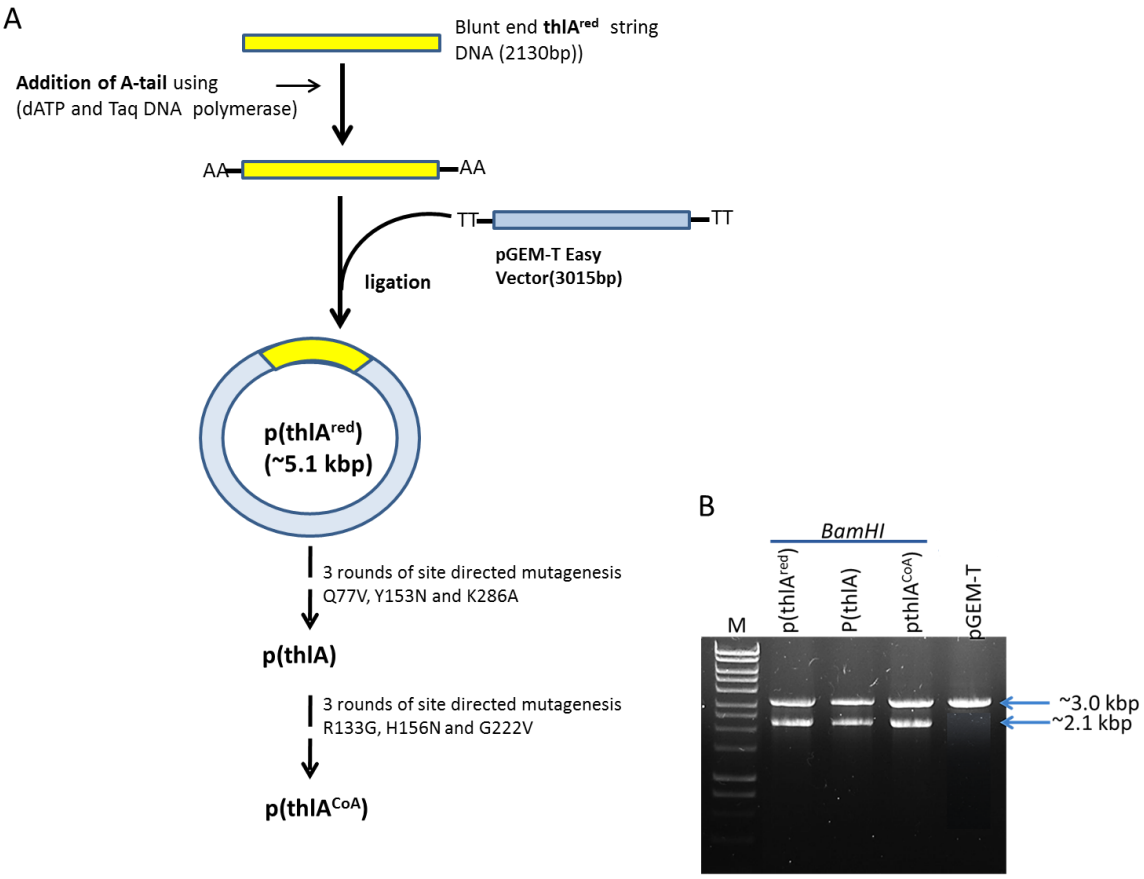

Figure 5.7 Summary of subcloning and site directed mutagenesis of *thlA*^{red}

Figure shows (A) Scheme for subcloning thlA^{red} into pGEMT vector and the synthesis of thlA and thlA^{CoA} by amino acid changes. (B) Image of agarose gel showing sizes of the *BamH*I restriction fragments of p(thlAred), p(thlA) p(thlACoA) and pGEMT plasmids after electrophoresis.

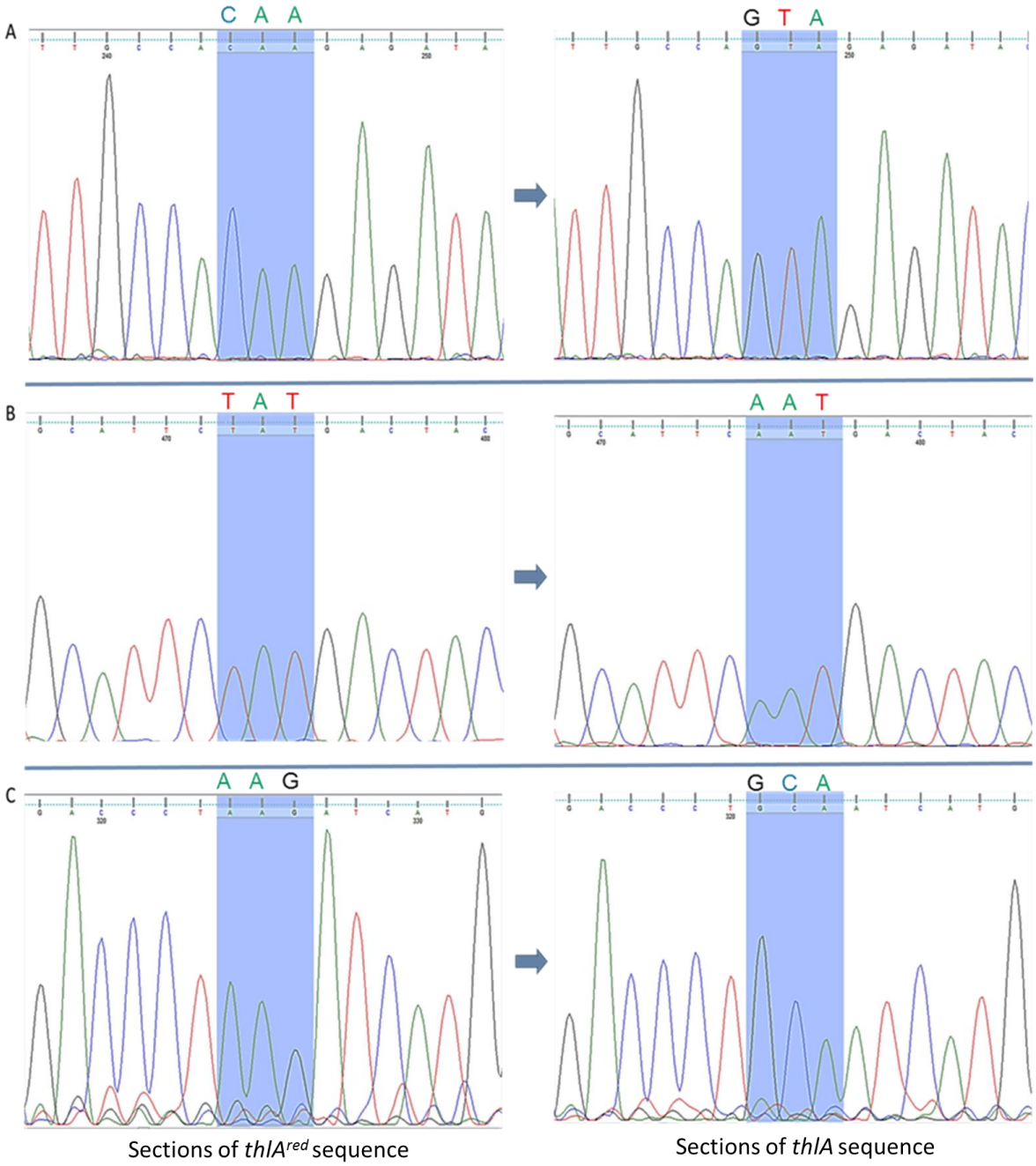

Figure 5.8 Verification of the thlA sequence.

Images of sections of DNA sequence chromatograph showing the three amino acid substitutions made to create *thlA* sequence from *thlA*^{red}. Substituted amino acid codons (nucleotides) are highlighted. (A) Glutamine changed to valine. (B) Tyrosine changed to asparagine. (C) Lysine changed to alanine.

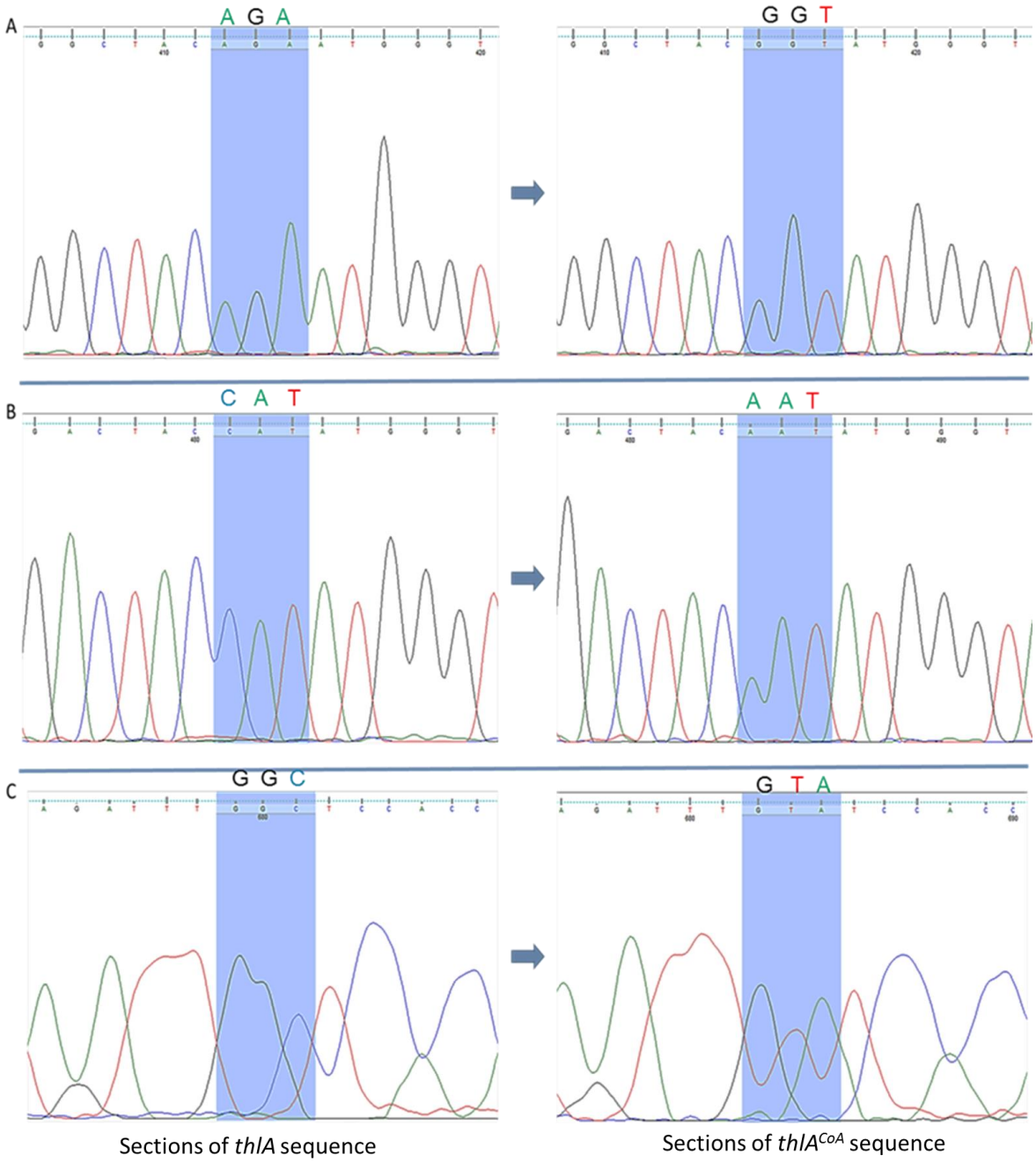

Figure 5.9 Verification of thlACoA sequence.

Images of section of DNA sequence chromatograph showing the three amino acid substitutions made to create *thlA*^{CoA} from *thlA* sequence Substituted amino acid codons (nucleotides) are highlighted. (A) Glutamine changed to valine. (B) Tyrosine changed to asparagine. (C) Lysine changed to alanine.

5.9 Sub-cloning into the pYM30 vector

To enable yeast selection after transformation, it was necessary to generate yeast integration cassettes that have an adjacent selectable marker gene. The vector pYM30 has a *KanMX4* gene downstream of a *Bam*HI restriction site. Therefore, the thiolase modules were inserted into the pYM30 vector at the *Bam*HI site using standard DNA sub-cloning techniques (Fig 5.10A). DNA restriction enzyme analysis (Fig 5.10B) confirmed the validity of the constructs.

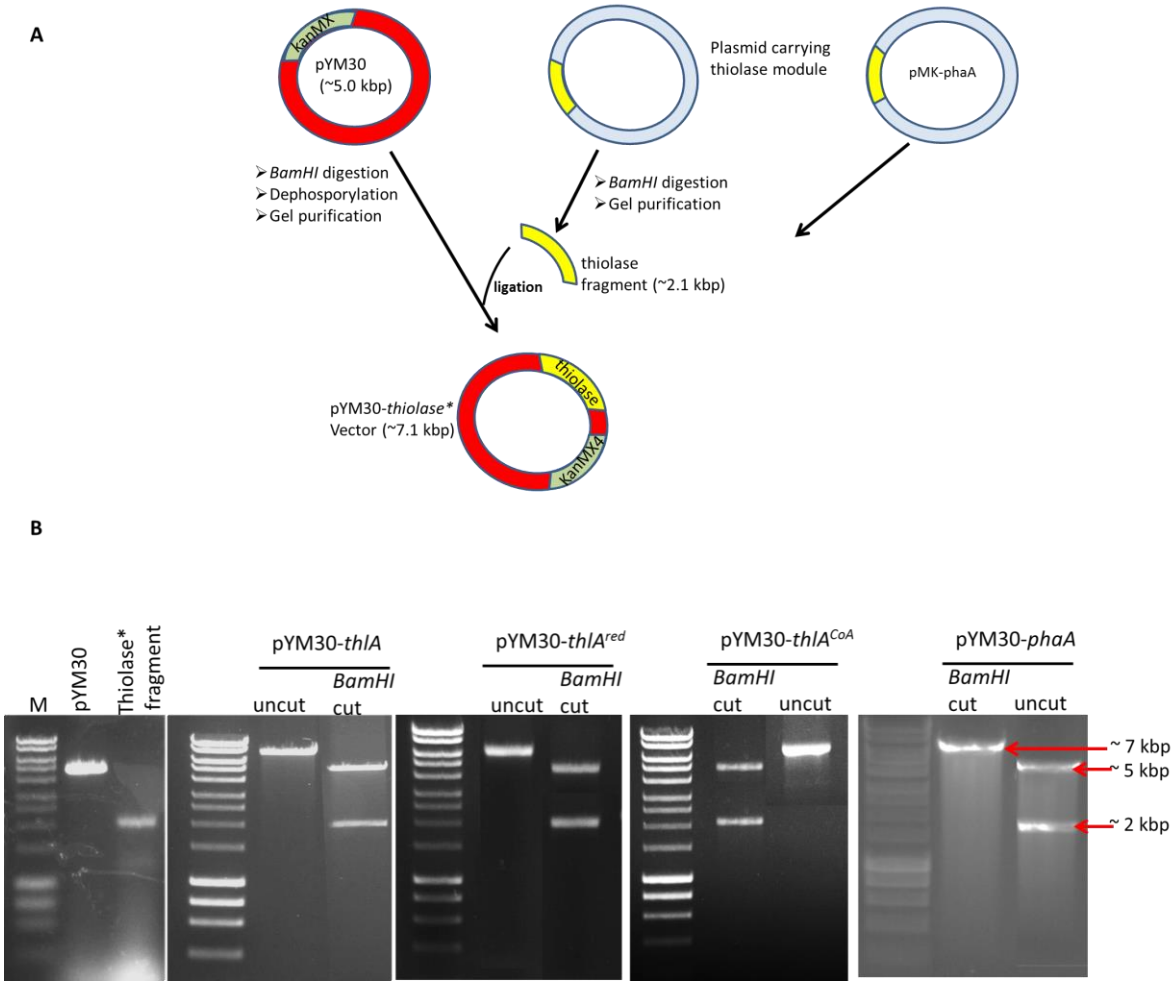

Figure 5.10 Sub-cloning of thiolase gene modules into pYM30 vectors.

Figure shows; (A) Scheme for sub-cloning thiolase gene modules into pYM30 vectors. (B) Images of agarose gels showing the fragment sizes of each pYM30-thiolase construct digested with *Bam*HI and separated by electrophoresis. The extreme left image shows the size of vector (pYM30) and thiolase insert respectively as separated by electrophoresis.

5.10 Amplification of integration cassettes by PCR

The four thiolase integration cassettes (*thlA-KanMX4*, *thlA*^{red}*-KanMX4*, *thlA*^{CoA}*-KanMX4* and *phaA-KanMX4*) were amplified from the relevant pYM30 derived vectors

by PCR using primers that surround the thiolase-*KanMX4* region within the plasmid (Fig 5.11A). The primers have 70bp guiding sequences homologous to regions within yeast chromosome XIV 727312 loci. The PCR products were verified by electrophoresis and they all produced bands corresponding to the calculated sizes (4.4 kbp) of the integration cassettes (Fig 5.11B)

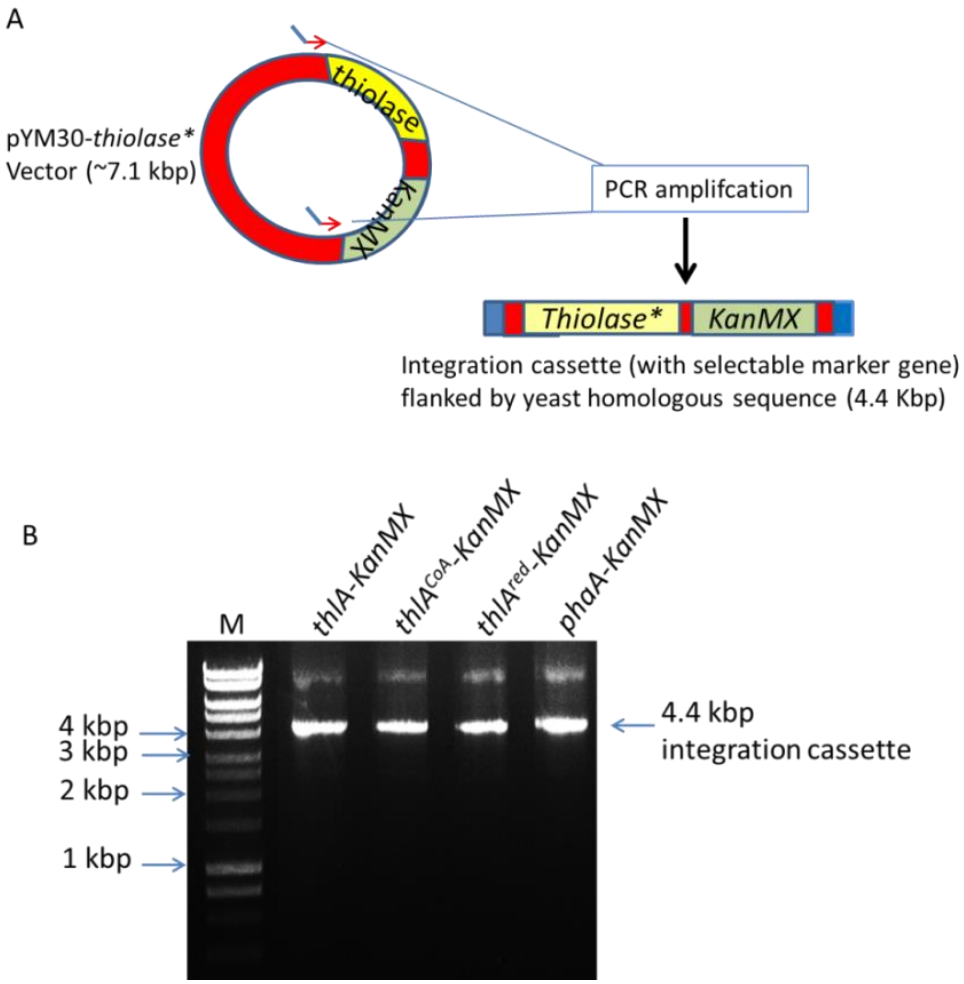

Figure 5.11 Amplification of thiolase integration cassettes.

Figure shows (A) scheme for the amplification of integration cassettes from pYM30-thiolase by PCR. Positions of the pair of amplification primers (surrounding the thiolase and *KanMX4* region) are shown. (B) Image of agarose gel showing the sizes of the four integration cassettes (generated by PCR) after electrophoretic separation.

5.11 Transformation of yeast

The BPS* strain, that is deleted for *ADH1*, expresses Ald6p/Acs2p to allow acetyl CoA production and expresses four butanol production genes *ccr*, *hbd*, *crt* and *adhe2*, was transformed with the thiolase integration cassettes (4.4 Kbp) using the lithium acetate protocol (Gietz & Woods, 2002). Homologous recombination with each cassette is expected at chromosome XIV 727312 loci. Four new strains, BPS**thlA*, BPS**thlA*^{red}, BPS**thlA*^{CoA} and BPS**phaA* (Fig 5.12A) that grow on plates with 300 µg/ml G418 were generated. Genomic DNA was obtained from each strain and PCR amplification of regions upstream and downstream of the thiolase integration site was conducted using site specific primers. The BPS**thlA*^{red} genome produced PCR products of the correct sizes (Fig 5.12B; U is 1.1 Kbp and D is 0.5 Kbp) confirming that integration occurred at the expected locus in the genome. No PCR product was obtained (after several attempts) for the other constructs (BPS**thlA*, BPS**thlA*^{CoA} and BPS**phaA*), indicating that integration in these strains might have occurred at unexpected locus within the genome.

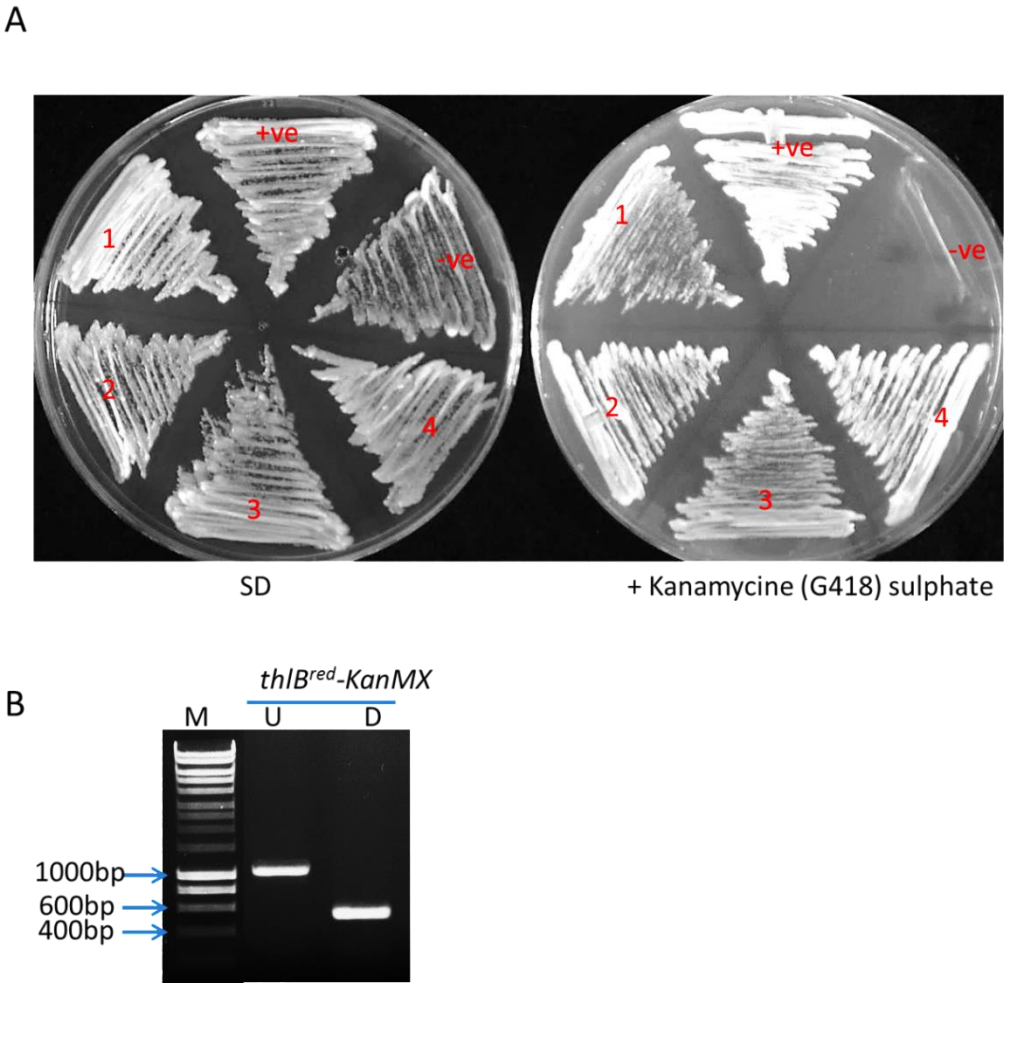

Figure 5.12 Verification of yeast transformation.

Figure shows; (A) growth of strains on SD and SD+G418 agar mediium (1. BPS**thlA* 2. BPS**thlA*^{red} 3. BPS**thlA*^{CoA} and 4. BPS**phaA*). BPS and BPS* strains are includes as +ve and -ve controls respectively. (B) Image of 1% agarose gel showing sizes of the upstream (U) and downstream (D) verification PCR products of BPS**thlA*^{red} genome.

5.12 Immuno detection of Myc-tagged thiolase protein

Concomitant with the PCR analysis above, Western blotting was performed to asses any expression of the thiolase genes in potential transformants. The thiolase genes were designed with a C-terminal 3x Myc epitope tag to allow their expression to be analysed. The expression of each Myc-tagged bacterial thiolase gene and other heterologous Flag-tagged genes (butanol synthesis) in the four strains was detected immunological by western blot assay using anti-Myc and anti-Flag antibodies, respectively. The results showed that even though three out of the four strains did not contain the thiolase cassette at the designated locus, protein extracts from all four strains contained myc-reactive bands of ~54 Kda (size of thiolase), while the BPS and BPS* strains have no bands on the blot (Fig 5.13A). The anti-Flag immunoblot for all the strains show bands corresponding to the sizes of six Flag-tagged heterologous proteins (overexpressed in the strains) and the BPS strain has an extra band corresponding to the size of Erg10p (Fig 5.13B). The results confirm the absence of exogenous *ERG10* gene in the BPS* strain series and the expression of the bacterial thiolases in these yeast strains. Results also confirm the expression of six heterologous butanol synthetic proteins in the strains including expression of Erg10p in the BPS strain.

Given that the four strains all produced the desired thiolase proteins and the relative levels appeared similar (Fig. 5.13B), a decision was made in the interest of expediency towards the end of the PhD experimental period to continue with these strains. If time had permitted the four strains with the thiolase genes integrated at the same genetic loci would have been generated.

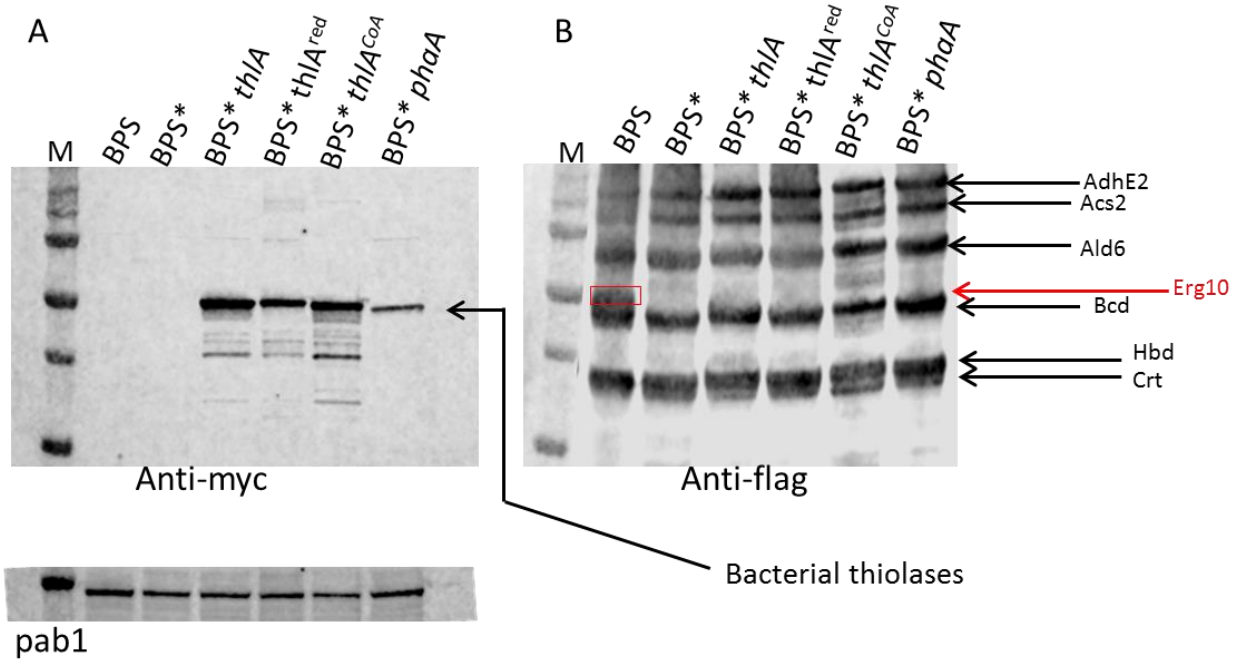

Figure 5.13 Immuno-detection of Myc-tagged thiolases and Flag-tagged proteins

(A) Image of anti-Myc immunoblot showing protein bands corresponding to the myc-tagged bacterial thiolases. (B) Image of anti-Flag immunoblot showing protein bands corresponding to the flag-tagged proteins. The position of Erg10 protein band is labelled in red letters for emphasis. The band corresponding to pab1 (selected as loading control) is shown.

5.13 Initial test fermentations to measure intracellular acetyl-CoA.

The intracellular concentrations of acetyl-CoA in the strains were determined in initial fermentations to investigate the impact of expressing the bacterial thiolases. If the thiolase genes were highly active a reduction in acetyl-CoA might have been expected. Strains were cultured under semi-anaerobic conditions for butanol production and samples were taken on day 4. The samples were used to measure the intracellular concentration of acetyl-CoA, the butanol concentration and the cell density of the culture.

Results (Fig 5.14) show that; for the BPS* strain, the level of acetyl-CoA is similar to the BPS strain while butanol and cell densities are lower. The lack of effect on acetyl-CoA levels is perhaps surprising, as the BPS* strain lacks overexpression of the yeast thiolase Erg10p. If this were active its removal should affect acetyl-CoA levels. It is possible, however, that endogenous Erg10p levels somehow compensate leading to little overall alteration in acetyl-CoA levels.

For the BPS**thlA* strain, the level of acetyl-CoA is higher while butanol is lower compared to the parent BPS* strain. The high acetyl-CoA and low butanol suggests that the ThlA enzyme in this strain is not particularly active in the direction of acetoacetyl-CoA production.

The BPS**thlA*^{CoA} strain when compared to the BPS strain exhibits lower acetyl-CoA, and similar butanol levels. These data suggest that ThlA^{CoA} has greater activity than the ThlA enzyme, however, it is unclear why the reduction in acetyl-CoA isn't accompanied with improved levels of butanol. It is possible that improved growth for

this strain somehow relates to this discrepancy, given that generally butanol is produced in the yeast strains after cell densities have reached a maximum.

The BPS**phaA* strain has high acetyl-CoA and no butanol suggesting that expression of the PhaA thiolase negates any impact the endogenous Erg10p yeast thiolase has in the strain. One possible explanation is that PhaA favours the reverse reaction when expressed in yeast and therefore would act to increase acetyl-CoA and prevent accumulation of butanol by consuming acetoacetyl-CoA.

Thus far none of the expressed thiolases appear to reduce acetyl-CoA levels or increase butanol production (Fig 5.14). However, for the BPS**thlA*^{red} strain, lower acetyl-CoA was detected and about 1.5-fold higher butanol levels were observed compared with the parent BPS* strain. It is therefore plausible that the presence of the ThlA^{red} thiolase generates a minor improvement in butanol levels and that expression of this thiolase holds promise in terms of improving butanol production in yeast.

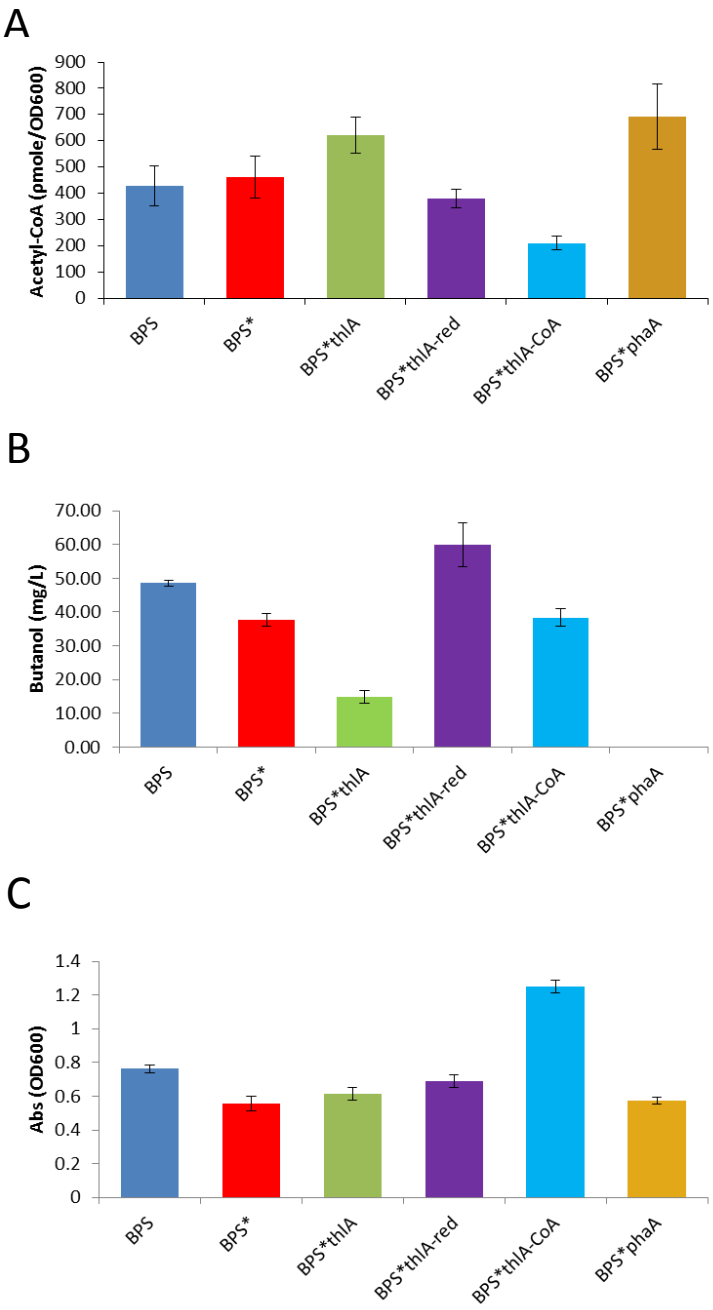

Figure 5.14 Comparison of acetyl-CoA, butanol and growth levels in the strains.

Figure shows (A) acetyl-CoA, (B) butanol and (C) growth levels in the strains after 4 days fermentation. Data represents the mean of three biological repeats with standard error bars.

5.14 Fermentation with various thiolase altered strains

After the initial promising fermentation analysis of butanol production, at least for the BPS* *thlA*^{red} strain*, a* full three week fermentation analysis was undertaken for the strains under semi-anaerobic conditions. The yeast BPS and BPS* strains were also tested as control strains.

In the BPS* strain, the results (Fig 5.15) show that growth, ethanol and butanol yield are lower compared to the BPS strain. Up until day 7, the strain has similar butanol levels to the BPS strain however this level did not increase subsequently. This result suggests that the overexpression of yeast Erg10p in the BPS strain contributes significantly to the level of butanol obtained. However, the impact of this Erg10p over-expression is only really apparent after prolonged fermentation.

Similar to the initial fermentation results above, the strains with *thlA*, *thlA*^{CoA} or *phaA* exhibit lower butanol levels, whereas the BPS**thlA*^{red} strain generates about 2-fold higher butanol levels than the BPS* parent strain. The butanol levels are also slightly higher (significant ($p<0.05$) on days 9, 11 and 14) for the BPS**thlA*^{red} strain relative to the *ERG10*-containing BPS strain.

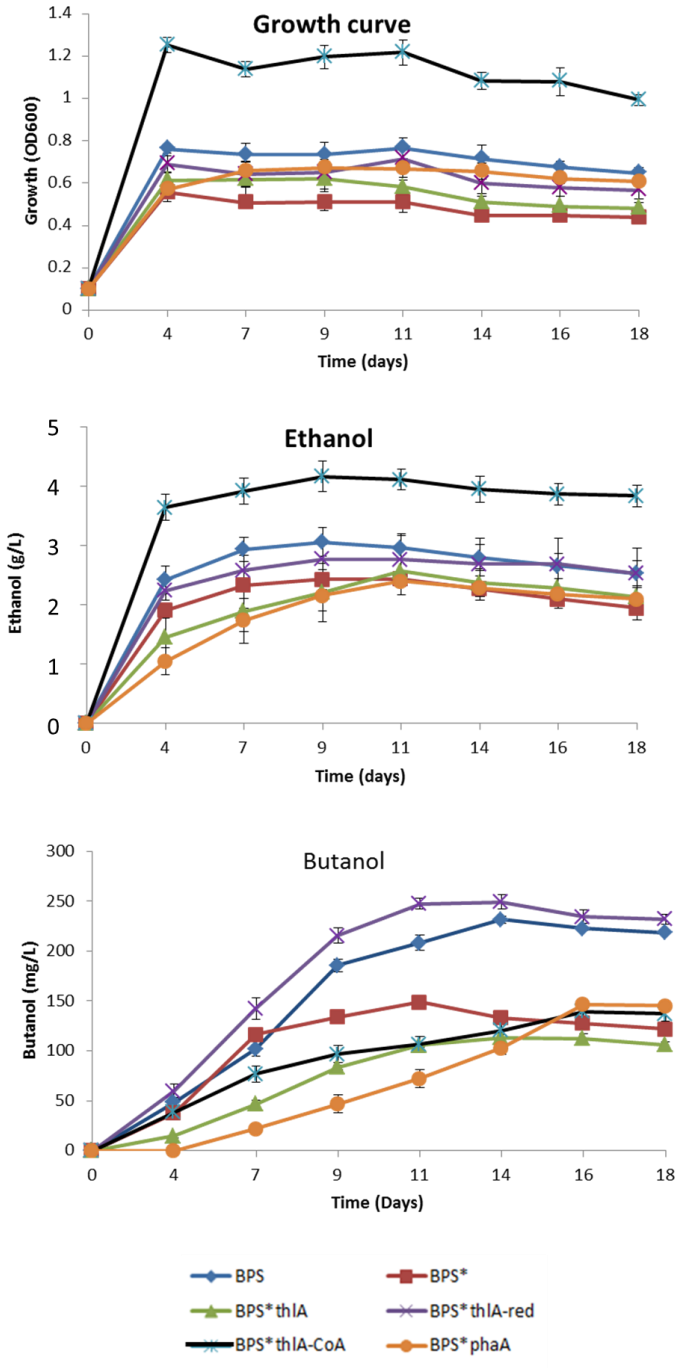

Figure 5.15 Fermentation with the thiolase altered strain

Graphs showing; (A) growth, (B) ethanol and (C) butanol yield in thiolase altered strains during fermentation. Data represents the mean of three biological repeats with standard error bars.

Table 5.1 compares the peak fermentation yield across all the BPS strain versions. Growth is significantly reduced in the BPS* strain while the BPS *thlA*^{CoA} has significantly higher growth cell density compared with the standard BPS strain. Butanol is significantly reduced in all the experimental strains except the BPS*thlA^{red} which has significantly higher butanol compared to the reference BPS strain

Table 5.1 Summary of peak growth, ethanol and butanol across the thiolase engineered strains

Strain	**Max growth (OD_{600} unit)**	**Ethanol titre (g/L)**	**Ethanol titre/OD_{600} (g/L/OD_{600})**	**Butanol titre (mg/L)**	**Butanol titre/OD_{600} (mg/L/OD_{600})**
BPS	0.73 ± 0.05	3.9 ± 0.02	5.34	231 ± 4	316
BPS*	0.51 ± 0.03*	3.1 ± 0.02	6.07	148 ± 2*	290
BPS*_thlA_	0.62 ± 0.09	2.8 ± 0.05	4.52	113 ± 3*	182
BPS*_thlA_^{red}	0.65 ± 0.06	3.5 ± 0.02	5.38	249 ± 7*	383
BPS*_thlA_^{CoA}	1.20 ± 0.04*	5.3 ± 0.08	4.41	139 ± 7*	115
BPS*_phaA_	0.67 ± 0.07	2.7 ± 0.03	4.02	102 ± 7*	152

Standard errors of three biological replicates is indicates as (±). Student's t-test analysis was used for statistical analysis of the growth and butanol titre in triplicates. Asterix sign (*) on data indicates a result that was significantly different compared to the reference BPS strain ($p < 0.05$).

5.15 Discussion

In yeast, biosynthetic thiolase initiates the production of mevalonate, which is required for the biosynthesis of sterols (e.g. ergosterol) and non-sterol isoprenoids, such as farnesol (Nielsen, 2014) Having established the Clostridial ABE-butanol pathway in the yeast *S. cerevisiae* (BPS strain), we show that there is an accumulation of acetyl-CoA in the strain; suggesting that the initiating thiolase enzyme is potentially sub-optimal. New strains were then developed where the overexpressed exogenous

ERG10 thiolase was substituted with four forms of bacterial thiolase - *phaA* from *Zoogloea ramigera*, *thlA* from *Clostridium acetobutylicum,* and two mutant forms of *thlA*: $thlA^{red}$ and $thlA^{CoA}$, which express mutant enzymes with higher activities than *thlA*.

In the BPS* strain relative to the BPS strain, the absence of the exogenous Erg10p thiolase may limit acetyl-CoA consumption resulting in lower butanol production particularly during prolonged fermentation. The reason that Erg10p over-expression only impacts on butanol production at late stages of a fermentation is currently unclear but could include the cell's attention to the butanol pathway for redox balance after glucose is exhausted in the media. Also, since yeast naturally expresses Erg10 activities during the ethanol-growth phase (late fermentation)(Kornblatt & Rudney, 1971); the activity of over-expressed Erg10p enzyme could equally be subject to modulation by the native Erg10 control elements thereby delaying it to the later stages of fermentation (after Day 4).

The thlA thiolase is redox switch regulated (oscillating between active and inactive forms depending on the cell's redox state) (Kim *et al*, 2015) the yeast cytosol may favour formation of oxidised (inactive) thlA enzyme therefore limiting butanol production in the BPS**thlA* strain. Also, overexpression of the *thlA* thiolase may have negative impact on the native Erg10p enzyme activity in the strain. The $thlA^{red}$ mutant thiolase is not affected by redox-switch modulation , and it is reported to have higher activity than the native thlA thiolase (Kim *et al*, 2015); overexpression of the $thlA^{red}$ thiolase may therefore lead to improved butanol production as observed for the BPS*$thlA^{red}$ strain. The $thlA^{CoA}$ thiolase has low affinity for Co-enzyme A (physiological

inhibitor of biosynthetic thiolases)(Mann & Lutke-Eversloh, 2013) and is therefore expected to show higher activity (acetyl-CoA condensation) compared to native thiolases including thlA, phaA and Erg10 thiolases. The thlA^{CoA} thiolase containing strain shows lower butanol yield compared to thlA, phaA and Erg10 -containing strain and surprisingly, the strain shows improved growth rate compared to the other strains. The reason for these apparently contradictory results is not known, but, thiolase plays a role in regulating energy metabolism and a role in regulating gluconeogenesis has been suggested (Kornblatt & Rudney, 1971). Studies have shown that phaA thiolase is debilitated under oxidation conditions thus limiting its activity; the intracellular conditions in the BPS*phaA strain may be oxidative, thereby inactivating the phaA thiolase and limiting butanol production in the strain compared to the BPS* strain. Butanol production in the strains expressing heterologous thiolases may be dependent on these thiolases and not on the native Erg10p activity which is tightly regulated. It could also be that, constitutive expression of the heterologous thiolases in yeast may signal the repression of the native Erg10 to prevent any translation burden in cells.

5.16 Conclusion

Overall, results seem to suggest that butanol production in the strains is affected by the activity of the heterologous thiolase and that expression of appropriate bacterial thiolases can result in minor improvements in these strains. Therefore, thiolase engineering presents a valid strategy to improve acetyl-CoA consumption for biosynthetic pathways that rely upon acetyl-CoA assimilation via thiolase function, particularly, for ABE-butanol production. One option is to generate the thlA^{red}

mutations in yeast Erg10p enzyme, which may improve its activity by favouring the acetyl-CoA condensation reaction and improve butanol production in the strain. In addition, since Erg10p is part of the yeast circuitry that regulates energy homeostasis (by regulating acetyl-CoA and CoA concentrations in the cell), the activities of this circuitry via native Erg10p activity may impair the butanol synthetic pathway, perhaps, deleting the *ERG10* gene in the BPS strain may optimise butanol production in the strain. Furthermore, increases in cytosolic acetyl-CoA level may increase acetyl-CoA carboxylase activity for fatty acid synthesis; a drain of substrate away from butanol synthesis. Modulating fatty acid synthesis may limit this drain and optimise butanol production in yeast BPS strain.

6. General Discussion

6.1 Introduction

Many microbes can feasibly be utilised as biotechnology platforms for sustainable production of either biofuels or commodity chemicals. The yeast *S. cerevisiae* is an amenable host for such strategies having many advantages as a cell factory (Buijs *et al*, 2013; Gonzalez-Ramos *et al*, 2013; Hong & Nielsen, 2012; Si *et al*, 2014a). Butanol production and optimisation in *S. cerevisiae* has been attempted via a number of molecular strategies including the importation of heterologous pathways, elimination of host competing pathways, redirecting metabolic fluxes, controlling redox and cofactor balance, metabolite synthesis and engineering of alternative enzymes. However, butanol production in *S. cerevisiae* is still very low compared to ethanol production. In this study, three strategies were explored with a view to optimising butanol production in a butanol production yeast strain (BPS strain) that was previously developed (Swidah *et al*, 2015).

6.2 Modulation of glucose repression.

Since heterologous metabolic pathways draw from their host's central carbon network; it is expected that constitutive de-repression of glucose repressed genes in yeast may improve carbon fluxes towards the heterologous butanol pathway and enhance butanol synthesis in butanol production strains. The *REG1* gene was deleted to allow the derepression of glucose repressed genes (about 1/3 of yeast genome) and the *snf1Δ* opposite mutation with constitutive glucose repression was constructed largely as a control strain; although formally this mutation might also improve butanol

production by channelling glucose for fermentation. The resulting strains were tested in terms of growth on non-fermentable carbon sources, tolerance to butanol and butanol production. The pattern of results obtained did not show any improvement in fermentation, butanol tolerance or growth on non-fermentable sugars in the strains. The disablement of the glucose repression pathway in the *reg1Δ* strain may create a burden on the cell as many proteins are expressed that are unnecessary. This wholesale expression of up to a third of the genome that would normally be silent could have a host of negative interactions by antagonising other genes and proteins. As a result, the cells may likely readjust their metabolism in order to balance the needs for growth and other physiological requirements. Unpicking both the initial alterations and subsequent adaptations would represent an enormous challenge. For instance, it is possible that a detailed 'omics' (including transcriptomics, proteomics and metabolomics) analysis of the strains would provide insight into the complex pattern of molecular readjustments arising from the deletion of these important regulator genes; but given the lack of effect on butanol production, such analysis was not deemed to represent an astute use of resources.

6.3 Disabling Glyoxylate cycle

The heterologous ABE-butanol synthetic pathway is dependent on cytosolic acetyl-CoA, therefore we took an approach to disable the competitive acetyl-CoA consuming glyoxylate cycle by deleting *CIT2* and *MLS1* genes in the strains. The strategy whereby competitive pathways are disabled to facilitate improved product yield has been reported previously in a number of studies. As expected, the single and

combined deletions of *MLS1* and *CIT2* genes in the butanol production strain caused increases in acetyl-CoA levels across the strains but disappointingly, the deletions did not increase butanol levels. This increase in intracellular acetyl-CoA does confirm the involvement of Cit2p and Mls1p proteins in cytosolic acetyl-CoA utilisation; however, the reason(s) for the unexpected decrease in butanol level in the *mls1Δ* BPS, *cit2Δ* BPS and *cit2Δ mls1Δ* BPS strains despite increases in acetyl-CoA is unclear. One possibility is that since four of the intermediates in the ABE-butanol synthesis pathway are CoA-bound (acetoacetyl-CoA, 3-hydroxylbutyryl-CoA, crotonyl-CoA and butyryl-CoA), high levels of acetyl-CoA may competitively or allosterically inhibit some of the enzymes in the pathway. Another plausible explanation is that the inhibition of the glyoxylate cycle may impair important succinate-dependent anaplerotic reactions needed for metabolic fitness. A further possibility could be that the accumulated acetyl-CoA is somehow unavailable for butanol synthesis. Since acetyl-CoA metabolism is compartmentalised in yeast, the intracellular acetyl-CoA concentration measurement may reflect the concentration in other organelles such as the peroxisome. So the inhibition of the glyoxylate cycle may cause acetate accumulation in the cytosol, which is transported to the peroxisome for the synthesis of peroxisomal acetyl-CoA. A final possible reason that increased acetyl-CoA does not improve butanol production, could relate to the fact that two pathways are thought to contribute to butanol production in the BPS strain – an endogenous (yet to be characterised) pathway and the heterologous ABE-butanol synthetic pathway (Swidah *et al*, 2015). Endogenous pathways in yeast for butanol synthesis have been reported; a pathway via threonine degradation triggered by *adh1Δ* deletion (Si *et al*, 2014a) and a glycine dependent pathway (Branduardi *et al*, 2013b). It seems likely that these novel endogenous

butanol pathways are functional in our strain and they might require an active glyoxylate cycle. Under this scenario, a limitation to the glyoxylate cycle might debilitate the putative endogenous butanol pathways to decrease butanol production in the BPS yeast strain.

6.4 Optimising pathway enzymes

Expression of heterologous proteins in cells is fraught with potential pitfalls in terms of expression levels, solubility, enzymatic activity and unwanted regulation; so, suboptimal pathway enzyme(s) can lead to poor utilisation of precursors and intermediates. For the ABE-butanol synthetic pathway, the condensation of two molecules of acetyl-CoA by a thiolase enzyme is the initiating reaction, and this reaction is tightly regulated by micromolar concentrations of CoASH, by ATP and by butyryl-CoA. The reaction is also thermodynamically unfavourable except in the presence of excess substrate and prompt product clearance (Mann & Lutke-Eversloh, 2013). To address the possibility of sub-optimal thiolase activity; especially given that there is an accumulation of acetyl-CoA in the BPS strain, four bacterial thiolases were selected to replace the synthetic Erg10 thiolase in the BPS strain.

Our result shows that the redox switch mutant thiolase $ThlA^{red}$ of *C. acetobutylicum* (Kim *et al*, 2015) improved butanol yield by about two-fold compared to the wild-type ThlA thiolase in the BPS strain. This result provides a proof of principle that optimising pathway reactions via enzyme engineering is a viable strategy and detailed study of the butanol pathway's stoichiometry and catalysis could further identify potential reaction bottlenecks.

Another potential bottleneck is the butyry-CoA dehydrogenase reaction. Naturally, in *C. acetobutylicum*, the reduction of butyryl-CoA by butyry-CoA dehydrogenase (Bcd) requires the participation of electron transfer flavoproteins EtfA and EtfB. The synthetic ABE-butanol pathway in the BPS does not include the *etfA* and *etfB* genes giving concern that the Bcd enzyme in the BPS strain may be sub-optimal. However, since the strain produces butanol in a manner reliant upon expression of the Clostridiidal ABE pathway enzymes, it could be that a yeast flavoprotein homologue is active in the strain. Equally, pro-mitochondrial flavoproteins may be available to provide needed electron transfer function for the Bcd enzyme in the strain.

Another reaction that could be optimised is the NADPH dependent hydroxybutyraldehyde dehydrogenase (Hbd) reaction. The activity of this enzyme may become limiting because $NADP^+$/NADPH use is restricted to the pentose phosphate pathway in yeast and there are no transhydrogenases to shuttle electrons between NAD^+/NADH and $NADP^+$/NADPH (van Dijken & Scheffers, 1986). However, if this is a problem the overexpression of $NADP^+$ dependent acetaldehyde dehydrogenase Ald6p in the BPS strain, should serve as a coupling reaction to regenerate NADPH.

6.5 Loss of metabolic intermediates may impair butanol production

The loss of reaction intermediates to competitive pathways is a factor that may reduce metabolic fluxes for product synthesis. For example, glyceraldehyde-3-phosphate is used for glycerol synthesis, acetyl-CoA is converted to malonyl-CoA for fatty acid synthesis, acetoacetyl-CoA is converted to mevalonate for the synthesis of steroids and isoprenoids and acetate can be transported into other organelles or

extracellularly. Minimising these drains might represent another means to improve yeast butanol synthesis.

6.6 Maintaining Redox Balance is important for butanol production

Redox balance is also an important factor affecting butanol synthesis (Schadeweg & Boles, 2016a). The sequential reduction of acetoacetyl-CoA to butanol via the ABE-butnol pathway requires four molecules of reducing cofactors (NADH and NADPH). In the BPS yeast, *ADH1* gene is deleted as a strategy to create a driving force (accumulation of NADH) for butanol synthesis. Adh1p is the major yeast alcohol dehydrogenase for regenerating NAD^+ needed for glycolysis, its deletion may signal metabolic recalibration such as reduction in glycolytic flux and activation of other native pathways for regeneration of NAD^+ (such as glycerol synthesis); these may reduce carbon flux to the downstream butanol pathway.

To create an additional driving force for reductive ABE-butanol synthesis in the BPS strain; the Adh2p enzyme (catalysing the oxidation of ethanol to acetaldehyde) can be overexpressed to generate more NADH, and the glycerol-3-phosphate dehydrogenases (Gpd1 and Gpd2) genes can be deleted to stop the drain of glycolytic intermediates to glycerol. Combining these alterations in the BPS yeast strain may increase the cytosolic NADH pool, reduce ethanol contamination and increase carbon flux, for improved butanol synthesis in the strain.

6.7 Conclusions

Metabolic pathway engineering in microbes has led to the production of many commodity compounds, such as butanol in the yeast *S. cerevisiae*. Many factors have the potential to limit butanol synthesis in yeast, some of these are: lack of cofactor availability, redox imbalance, metabolic network restrictions, loss of intermediates, tightly regulated and strict protein synthesis and by-product (ethanol and glycerol) contamination. Optimising the ABE-butanol pathway in yeast has therefore been the focus of many research projects and strategies including: the generation of pathway precursors and metabolic driving forces and, the elimination of competitive pathways, energy-dependent reactions and pathway by-products. Yet yeast butanol production is still below a level for commercialisation. The establishment of multi-enzyme pathways in foreign host organisms such as yeast requires a delicate balance between growth, redox, protein expression and metabolic flux. To achieve high production of butanol in yeast, there must be adequate metabolic flow towards the product pathway and a balance of the afore stated factors. However, because of the complexity and compartmentalisation of yeast metabolic networks, the range of metabolic flux distributions is limited (Matsuda *et al*, 2011) causing several imbalances. Therefore, to make yeast butanol production as robust and commercially sustainable as ethanol production, the application of whole synthetic biology; the Design, Build, Test and Know - approach for the revision of current metabolic engineering strategies and the development of more compatible pathways seems ideal (Bokinsky *et al*, 2013; Peralta-Yahya *et al*, 2012). Synthetic biology provides the means to construct novel and functional biological pathways or redesign natural pathways around a host's central metabolic network for the synthesis of new products (Ferry *et al*, 2012). By sourcing

biological pieces from different species, new functionalities can be achieved around a host's metabolic networks to minimise/eliminate metabolic imbalances that inhibit the current approach of importing whole heterologous pathways into a host organism. The availability of yeast molecular tools for its improvements gives future hope for the production of butanol in yeast towards its commercial competitiveness to supplement current fuel demands.

Bibliography

Algae for biofuel production. (2014, January 31). Retrieved from http://articles.extension.org/pages/26600/algae-for-biofuel-production#Production_challenges

Ashe MP, De Long SK, Sachs AB (2000) Glucose Depletion Rapidly Inhibits Translation Initiation in Yeast. *Molecular Biology of the Cell* **11**(3)**:** 833-848

Ashe MP, Slaven JW, De Long SK, Ibrahimo S, Sachs AB (2001) A novel eIF2B-dependent mechanism of translational control in yeast as a response to fusel alcohols. *Embo j* **20**(22)**:** 6464-74

Atsumi S (2007) Metabolic engineering of Escherichia coli for 1-butanol production. In *Metab Eng*.

Atsumi S, Cann AF, Connor MR, Shen CR, Smith KM, Brynildsen MP, Chou KJ, Hanai T, Liao JC (2008) Metabolic engineering of Escherichia coli for 1-butanol production. *Metab Eng* **10**(6)**:** 305-11

Bokinsky G, Groff D, Keasling J (2013) Chapter 11 - Synthetic Biology of Microbial Biofuel Production: From Enzymes to Pathways to Organisms A2 - Zhao, Huimin. In *Synthetic Biology*, pp 207-223. Boston: Academic Press

Bond-Watts BB, Bellerose RJ, Chang MCY (2011) Enzyme mechanism as a kinetic control element for designing synthetic biofuel pathways. *Nat Chem Biol* **7**(4)**:** 222-227

Boucher MB, Unker SA, Hawley KR, Wilhite BA, Stuart JD, Parnas RS (2008) Variables affecting homogeneous acid catalyst recoverability and reuse after esterification of concentrated omega-9 polyunsaturated fatty acids in vegetable oil triglycerides. *Green Chemistry* **10**(12)**:** 1331-1336

Bradford MM (1976) A rapid and sensitive method for the quantitation of microgram quantities of protein utilizing the principle of protein-dye binding. *Analytical Biochemistry* **72**(1–2)**:** 248-254

Branduardi P, Longo V, Berterame NM, Rossi G, Porro D (2013a) A novel pathway to produce butanol and isobutanol in Saccharomyces cerevisiae. *Biotechnology for Biofuels* **6**(1)**:** 68

Branduardi P, Longo V, Berterame NM, Rossi G, Porro D (2013b) A novel pathway to produce butanol and isobutanol in Saccharomyces cerevisiae. *Biotechnology for Biofuels* **6:** 68-68

Buijs NA, Siewers V, Nielsen J (2013) Advanced biofuel production by the yeast Saccharomyces cerevisiae. *Curr Opin Chem Biol* **17**(3)**:** 480-8

Busti S, Coccetti P, Alberghina L, Vanoni M (2010) Glucose signaling-mediated coordination of cell growth and cell cycle in Saccharomyces cerevisiae. *Sensors (Basel)* **10**(6)**:** 6195-240

Cai L, Sutter BM, Li B, Tu BP (2011) Acetyl-CoA induces cell growth and proliferation by promoting the acetylation of histones at growth genes. *Mol Cell* **42**(4)**:** 426-37

Cannon JF (2010) Function of protein phosphatase-1, Glc7, in Saccharomyces cerevisiae. *Adv Appl Microbiol* **73:** 27-59

Carlson M (1998) Regulation of glucose utilization in yeast. *Current Opinion in Genetics & Development* **8**(5)**:** 560-564

Carlson M (1999) Glucose repression in yeast. *Curr Opin Microbiol* **2**(2)**:** 202-7

Carter Z, Delneri D (2010) New generation of loxP-mutated deletion cassettes for the genetic manipulation of yeast natural isolates. *Yeast* **27**(9)**:** 765-75

Celenza JL, Carlson M (1986) A yeast gene that is essential for release from glucose repression encodes a protein kinase. *Science* **233**(4769)**:** 1175-1180

Chen Y, Daviet L, Schalk M, Siewers V, Nielsen J (2013) Establishing a platform cell factory through engineering of yeast acetyl-CoA metabolism. *Metabolic Engineering* **15:** 48-54

Chen Y, Siewers V, Nielsen J (2012) Profiling of cytosolic and peroxisomal acetyl-CoA metabolism in Saccharomyces cerevisiae. *PLoS One* **7**(8)**:** e42475

De Vit MJ, Waddle JA, Johnston M (1997) Regulated nuclear translocation of the Mig1 glucose repressor. *Molecular Biology of the Cell* **8**(8)**:** 1603-1618

Dombek KM, Voronkova V, Raney A, Young ET (1999) Functional analysis of the yeast Glc7-binding protein Reg1 identifies a protein phosphatase type 1-binding motif as essential for repression of ADH2 expression. *Mol Cell Biol* **19**(9)**:** 6029-40

Dowhan DH (2008) Purification and Concentration of Nucleic Acids. In *Current Protocols Essential Laboratory Techniques*. John Wiley & Sons, Inc.

Dürre P (2007) Biobutanol: An attractive biofuel. *Biotechnology Journal* **2**(12)**:** 1525-1534

Fernandez E, Fernandez M, Rodicio R (1993) Two structural genes are encoding malate synthase isoenzymes in Saccharomyces cerevisiae. *FEBS Lett* **320**(3)**:** 271-5

Ferry MS, Hasty J, Cookson NA (2012) Synthetic biology approaches to biofuel production. *Biofuels* **3**(1)**:** 9-12

Fischer CR, Klein-Marcuschamer D, Stephanopoulos G (2008a) Selection and optimization of microbial hosts for biofuels production. *Metab Eng* **10**(6)**:** 295-304

Fischer CR, Klein-Marcuschamer D, Stephanopoulos G (2008b) Selection and optimization of microbial hosts for biofuels production. In *Metab Eng*.

Fortman JL, Chhabra S, Mukhopadhyay A, Chou H, Lee TS, Steen E, Keasling JD (2008) Biofuel alternatives to ethanol: pumping the microbial well. *Trends Biotechnol* **26**(7)**:** 375-81

Fox AR, Soto G, Mozzicafreddo M, Garcia AN, Cuccioloni M, Angeletti M, Salerno JC, Ayub ND (2014) Understanding the function of bacterial and eukaryotic thiolases II by integrating evolutionary and functional approaches. *Gene* **533**(1)**:** 5-10

Gancedo JM (1998) Yeast carbon catabolite repression. *Microbiol Mol Biol Rev* **62**(2)**:** 334-61

García V, Päkkilä J, Ojamo H, Muurinen E, Keiski RL (2011) Challenges in biobutanol production: How to improve the efficiency? *Renewable and Sustainable Energy Reviews* **15**(2)**:** 964-980

Generoso WC, Schadeweg V, Oreb M, Boles E (2015) Metabolic engineering of Saccharomyces cerevisiae for production of butanol isomers. *Curr Opin Biotechnol* **33:** 1-7

Gheshlaghi R, Scharer JM, Moo-Young M, Chou CP (2009) Metabolic pathways of clostridia for producing butanol. *Biotechnol Adv* **27**(6)**:** 764-81

Gietz RD, Woods RA (2002) Transformation of yeast by lithium acetate/single-stranded carrier DNA/polyethylene glycol method. *Methods Enzymol* **350:** 87-96

Gonzalez B, Francois J, Renaud M (1997) A rapid and reliable method for metabolite extraction in yeast using boiling buffered ethanol. *Yeast* **13**(14)**:** 1347-55

Gonzalez-Ramos D, van den Broek M, van Maris AJ, Pronk JT, Daran JM (2013) Genome-scale analyses of butanol tolerance in Saccharomyces cerevisiae reveal an essential role of protein degradation. *Biotechnol Biofuels* **6**(1)**:** 48

Gueldener U, Heinisch J, Koehler GJ, Voss D, Hegemann JH (2002) A second set of loxP marker cassettes for Cre-mediated multiple gene knockouts in budding yeast. *Nucleic Acids Research* **30**(6)**:** e23-e23

Hedbacker K, Carlson M (2008) SNF1/AMPK pathways in yeast. *Front Biosci* **13:** 2408-20

Hiser L, Basson ME, Rine J (1994) ERG10 from Saccharomyces cerevisiae encodes acetoacetyl-CoA thiolase. *J Biol Chem* **269**(50)**:** 31383-9

Hong KK, Nielsen J (2012) Metabolic engineering of Saccharomyces cerevisiae: a key cell factory platform for future biorefineries. *Cell Mol Life Sci* **69**(16)**:** 2671-90

Ithayaraja M, Janardan N, Wierenga RK, Savithri HS, Murthy MR (2016) Crystal structure of a thiolase from Escherichia coli at 1.8 A resolution. *Acta Crystallogr F Struct Biol Commun* **72**(Pt 7)**:** 534-44

Jiang R, Carlson M (1996) Glucose regulates protein interactions within the yeast SNF1 protein kinase complex. *Genes & Development* **10**(24)**:** 3105-3115

Jin C, Yao M, Liu H, Lee C-fF, Ji J (2011) Progress in the production and application of n-butanol as a biofuel. *Renewable and Sustainable Energy Reviews* **15**(8)**:** 4080-4106

Johnston M (1999) Feasting, fasting and fermenting: glucose sensing in yeast and other cells. *Trends in Genetics* **15**(1)**:** 29-33

Kenny P, Flynn KJ (2017) Physiology limits commercially viable photoautotrophic production of microalgal biofuels. *Journal of Applied Phycology* **29**(6)**:** 2713-2727

Kim JH, Roy A, Jouandot D, 2nd, Cho KH (2013) The glucose signaling network in yeast. *Biochim Biophys Acta* **1830**(11)**:** 5204-10

Kim S, Jang YS, Ha SC, Ahn JW, Kim EJ, Lim JH, Cho C, Ryu YS, Lee SK, Lee SY, Kim KJ (2015) Redox-switch regulatory mechanism of thiolase from Clostridium acetobutylicum. *Nat Commun* **6:** 8410

Ko CH, Liang H, Gaber RF (1993) Roles of multiple glucose transporters in Saccharomyces cerevisiae. *Mol Cell Biol* **13**(1)**:** 638-48

Kocharin K, Chen Y, Siewers V, Nielsen J (2012) Engineering of acetyl-CoA metabolism for the improved production of polyhydroxybutyrate in Saccharomyces cerevisiae. *AMB Express* **2:** 52-52

Kornblatt JA, Rudney H (1971) Two Forms of Acetoacetyl Coenzyme A Thiolase in Yeast: II. INTRACELLULAR LOCATION AND RELATIONSHIP TO GROWTH. *Journal of Biological Chemistry* **246**(14)**:** 4424-4430

Krivoruchko A, Serrano-Amatriain C, Chen Y, Siewers V, Nielsen J (2013) Improving biobutanol production in engineered Saccharomyces cerevisiae by manipulation of acetyl-CoA metabolism. *J Ind Microbiol Biotechnol* **40**(9)**:** 1051-6

Kuchin S, Vyas VK, Carlson M (2003) Role of the yeast Snf1 protein kinase in invasive growth. *Biochem Soc Trans* **31**(Pt 1)**:** 175-7

Kumar R, Singh S, Singh OV (2008) Bioconversion of lignocellulosic biomass: biochemical and molecular perspectives. *J Ind Microbiol Biotechnol* **35**(5)**:** 377-91

Kunze M, Pracharoenwattana I, Smith SM, Hartig A (2006) A central role for the peroxisomal membrane in glyoxylate cycle function. *Biochimica et Biophysica Acta (BBA) - Molecular Cell Research* **1763**(12)**:** 1441-1452

Kursula P, Ojala J, Lambeir A-M, Wierenga RK (2002) The Catalytic Cycle of Biosynthetic Thiolase: A Conformational Journey of an Acetyl Group through Four Binding Modes and Two Oxyanion Holes. *Biochemistry* **41**(52)**:** 15543-15556

Lagunas R (1993) Sugar transport in Saccharomyces cerevisiae. *FEMS Microbiol Rev* **10**(3-4)**:** 229-42

Lamsen EN, Atsumi S (2012) Recent progress in synthetic biology for microbial production of C3–C10 alcohols. *Frontiers in Microbiology* **3:** 196

Lee S-H, Eom M-H, Kim S, Kwon M-A, Choi J-D-R, Kim J, Shin Y-A, Kim KH (2015) Ex situ product recovery and strain engineering of Clostridium acetobutylicum for enhanced production of butanol. *Process Biochemistry* **50**(11)**:** 1683-1691

Lee SK, Chou H, Ham TS, Lee TS, Keasling JD (2008a) Metabolic engineering of microorganisms for biofuels production: from bugs to synthetic biology to fuels. *Curr Opin Biotechnol* **19**(6)**:** 556-63

Lee SY, Park JH, Jang SH, Nielsen LK, Kim J, Jung KS (2008b) Fermentative butanol production by clostridia. *Biotechnology and Bioengineering* **101**(2)**:** 209-228

Lee WH, Seo SO, Bae YH, Nan H, Jin YS, Seo JH (2012) Isobutanol production in engineered Saccharomyces cerevisiae by overexpression of 2-ketoisovalerate decarboxylase and valine biosynthetic enzymes. *Bioprocess Biosyst Eng* **35**(9)**:** 1467-75

Lee YJ, Jang JW, Kim KJ, Maeng PJ (2011) TCA cycle-independent acetate metabolism via the glyoxylate cycle in Saccharomyces cerevisiae. *Yeast* **28**(2)**:** 153-66

Lewin AS, Hines V, Small GM (1990) Citrate synthase encoded by the CIT2 gene of Saccharomyces cerevisiae is peroxisomal. *Mol Cell Biol* **10**(4)**:** 1399-405

Lian J, Si T, Nair NU, Zhao H (2014) Design and construction of acetyl-CoA overproducing Saccharomyces cerevisiae strains. *Metab Eng* **24:** 139-49

Lian J, Zhao H (2015) Reversal of the β-Oxidation Cycle in Saccharomyces cerevisiae for Production of Fuels and Chemicals. *ACS Synthetic Biology* **4**(3)**:** 332-341

Luque R, Herrero-Davila L, Campelo JM, Clark JH, Hidalgo JM, Luna D, Marinas JM, Romero AA (2008) Biofuels: a technological perspective. *Energy & Environmental Science* **1**(5)**:** 542-564

Luthe DS (1983) A simple technique for the preparation and storage of sucrose gradients. *Analytical Biochemistry* **135**(1)**:** 230-232

Mann MS, Lutke-Eversloh T (2013) Thiolase engineering for enhanced butanol production in Clostridium acetobutylicum. *Biotechnol Bioeng* **110**(3)**:** 887-97

Marisco G, Saito ST, Ganda IS, Brendel M, Pungartnik C (2011) Low ergosterol content in yeast adh1 mutant enhances chitin maldistribution and sensitivity to paraquat-induced oxidative stress. *Yeast* **28**(5)**:** 363-73

Mark J, Marian C (1992) 5 Regulation of Carbon and Phosphate Utilization. *Cold Spring Harbor Monograph Archive; Volume 21B (1992): Volume II: The Molecular and Cellular Biology of the Yeast Saccharomyces: Gene Expression*

Matsuda F, Furusawa C, Kondo T, Ishii J, Shimizu H, Kondo A (2011) Engineering strategy of yeast metabolism for higher alcohol production. *Microb Cell Fact* **10:** 70

Merilainen G, Poikela V, Kursula P, Wierenga RK (2009) The thiolase reaction mechanism: the importance of Asn316 and His348 for stabilizing the enolate intermediate of the Claisen condensation. *Biochemistry* **48**(46)**:** 11011-25

Modis Y, Wierenga RK (1999) A biosynthetic thiolase in complex with a reaction intermediate: the crystal structure provides new insights into the catalytic mechanism. *Structure* **7**(10)**:** 1279-1290

Modis Y, Wierenga RK (2000) Crystallographic analysis of the reaction pathway of Zoogloea ramigera biosynthetic thiolase1. *Journal of Molecular Biology* **297**(5)**:** 1171-1182

Momcilovic M, Hong S-P, Carlson M (2006) Mammalian TAK1 Activates Snf1 Protein Kinase in Yeast and Phosphorylates AMP-activated Protein Kinase in Vitro. *Journal of Biological Chemistry* **281**(35)**:** 25336-25343

Nielsen DR, Leonard E, Yoon SH, Tseng HC, Yuan C, Prather KL (2009) Engineering alternative butanol production platforms in heterologous bacteria. *Metab Eng* **11**(4-5)**:** 262-73

Nielsen J (2014) Synthetic Biology for Engineering Acetyl Coenzyme A Metabolism in Yeast. *mBio* **5**(6)**:** e02153-14

Nielsen J, Larsson C, van Maris A, Pronk J (2013) Metabolic engineering of yeast for production of fuels and chemicals. *Current Opinion in Biotechnology* **24**(3)**:** 398-404

Nigam PS, Singh A (2011) Production of liquid biofuels from renewable resources. *Progress in Energy and Combustion Science* **37**(1)**:** 52-68

Ocampo A, Barrientos A (2011) Quick and reliable assessment of chronological life span in yeast cell populations by flow cytometry. *Mech Ageing Dev* **132**(6-7)**:** 315-23

Ozcan S, Johnston M (1995) Three different regulatory mechanisms enable yeast hexose transporter (HXT) genes to be induced by different levels of glucose. *Molecular and Cellular Biology* **15**(3)**:** 1564-1572

Peralta-Yahya PP, Zhang F, del Cardayre SB, Keasling JD (2012) Microbial engineering for the production of advanced biofuels. *Nature* **488**(7411)**:** 320-8

Pietrocola F, Galluzzi L, Bravo-San Pedro JM, Madeo F, Kroemer G (2015) Acetyl coenzyme A: a central metabolite and second messenger. *Cell Metab* **21**(6)**:** 805-21

Pittman JK, Dean AP, Osundeko O (2011) The potential of sustainable algal biofuel production using wastewater resources. *Bioresource Technology* **102**(1)**:** 17-25

Regenberg B, Grotkjær T, Winther O, Fausbøll A, Åkesson M, Bro C, Hansen LK, Brunak S, Nielsen J (2006) Growth-rate regulated genes have profound impact on interpretation of transcriptome profiling in Saccharomyces cerevisiae. *Genome Biology* **7**(11)**:** R107

Rolland F, Winderickx J, Thevelein JM (2002a) Glucose-sensing and -signalling mechanisms in yeast. *FEMS Yeast Res* **2**(2)**:** 183-201

Rolland F, Winderickx J, Thevelein JM (2002b) Glucose-sensing and -signalling mechanisms in yeast. *FEMS Yeast Research* **2**(2)**:** 183-201

Sakuragi H, Morisaka H, Kuroda K, Ueda M (2015) Enhanced butanol production by eukaryotic Saccharomyces cerevisiae engineered to contain an improved pathway. *Bioscience, Biotechnology, and Biochemistry* **79**(2)**:** 314-320

Sanz P, Alms GR, Haystead TA, Carlson M (2000) Regulatory interactions between the Reg1-Glc7 protein phosphatase and the Snf1 protein kinase. *Mol Cell Biol* **20**(4)**:** 1321-8

Saxena RC, Adhikari DK, Goyal HB (2009) Biomass-based energy fuel through biochemical routes: A review. *Renewable and Sustainable Energy Reviews* **13**(1)**:** 167-178

Schadeweg V, Boles E (2016a) Increasing n-butanol production with Saccharomyces cerevisiae by optimizing acetyl-CoA synthesis, NADH levels and trans-2-enoyl-CoA reductase expression. *Biotechnol Biofuels* **9:** 257

Schadeweg V, Boles E (2016b) n-Butanol production in Saccharomyces cerevisiae is limited by the availability of coenzyme A and cytosolic acetyl-CoA. *Biotechnology for Biofuels* **9**(1)**:** 1-12

Shen CR, Lan EI, Dekishima Y, Baez A, Cho KM, Liao JC (2011) Driving Forces Enable High-Titer Anaerobic 1-Butanol Synthesis in Escherichia coli. *Applied and Environmental Microbiology* **77**(9)**:** 2905-2915

Shi S, Si T, Liu Z, Zhang H, Ang EL, Zhao H (2016) Metabolic engineering of a synergistic pathway for n-butanol production in Saccharomyces cerevisiae. **6:** 25675

Shiba Y, Paradise EM, Kirby J, Ro D-K, Keasling JD (2007) Engineering of the pyruvate dehydrogenase bypass in Saccharomyces cerevisiae for high-level production of isoprenoids. *Metabolic Engineering* **9**(2)**:** 160-168

Shirra MK, McCartney RR, Zhang C, Shokat KM, Schmidt MC, Arndt KM (2008) A Chemical Genomics Study Identifies Snf1 as a Repressor of GCN4 Translation. *The Journal of Biological Chemistry* **283**(51)**:** 35889-35898

Si T, Luo Y, Xiao H, Zhao H (2014a) Utilizing an endogenous pathway for 1-butanol production in Saccharomyces cerevisiae. *Metabolic Engineering* **22**(0)**:** 60-68

Si T, Luo Y, Xiao H, Zhao H (2014b) Utilizing an endogenous pathway for 1-butanol production in Saccharomyces cerevisiae. *Metabolic Engineering* **22:** 60-68

Simpson CE, Ashe MP (2012) Adaptation to stress in yeast: to translate or not? *Biochem Soc Trans* **40**(4)**:** 794-9

Steen EJ, Chan R, Prasad N, Myers S, Petzold CJ, Redding A, Ouellet M, Keasling JD (2008) Metabolic engineering of Saccharomyces cerevisiae for the production of n-butanol. *Microb Cell Fact* **7:** 36

Swidah R, Wang H, Reid PJ, Ahmed HZ, Pisanelli AM, Persaud KC, Grant CM, Ashe MP (2015) Butanol production in S. cerevisiae via a synthetic ABE pathway is enhanced by specific metabolic engineering and butanol resistance. *Biotechnology for Biofuels* **8:** 97

Tamaki H (2007) Glucose-stimulated cAMP-protein kinase A pathway in yeast Saccharomyces cerevisiae. *J Biosci Bioeng* **104**(4)**:** 245-50

Thevelein JM, de Winde JH (1999) Novel sensing mechanisms and targets for the cAMP-protein kinase A pathway in the yeast Saccharomyces cerevisiae. *Mol Microbiol* **33**(5)**:** 904-18

Trumbly RJ (1992) Glucose repression in the yeast Saccharomyces cerevisiae. *Mol Microbiol* **6**(1)**:** 15-21

Tu J, Carlson M (1995) REG1 binds to protein phosphatase type 1 and regulates glucose repression in Saccharomyces cerevisiae. *Embo j* **14**(23)**:** 5939-46

van Dijken JP, Scheffers WA (1986) Redox balances in the metabolism of sugars by yeasts. *FEMS Microbiology Reviews* **1**(3-4)**:** 199-224

Zheng YN, Li LZ, Xian M, Ma YJ, Yang JM, Xu X, He DZ (2009) Problems with the microbial production of butanol. *J Ind Microbiol Biotechnol* **36**(9)**:** 1127-38

Özcan S, Johnston M (1999) Function and regulation of yeast hexose transporters. *Microbiology and Molecular Biology Reviews* **63**(3)**:** 554-569